Sara Peres de Morais

Licenciatura em Biologia

Juvenile Parkinson disease caused by parkin mutations: large deletions and pathogenic mechanisms

Dissertação para obtenção do Grau de Mestre em
Genética Molecular e Biomedicina

Orientadora: Doutora Isabel Alonso, Investigadora Auxiliar, IBMC

Júri:

Presidente: Prof. Doutor José Paulo Sampaio
Arguente: Prof. Doutora Ana Sofia Almeida Oliveira
Vogal: Doutora Isabel da Conceição Moreira Pereira Alonso

FCt FACULDADE DE
CIÊNCIAS E TECNOLOGIA
UNIVERSIDADE NOVA DE LISBOA

Novembro, 2011

Juvenile Parkinson disease caused by parkin mutations: characterization of large genomic deletions and pathogenic mechanisms

À Profª Doutora Margarida Castro Caldas Braga pela sua supervisão ao longo deste ano.

À minha família porque são o meu suporte e estão sempre presentes para o que for preciso. Aos meus pais que me apoiam desde sempre em todas as minhas decisões e que juntamente com os meus avós e o meu irmão me dão todo o amor que só a família é capaz.

Ao Ricardo, o meu mais que tudo, tenho o dever de dar um agradecimento muito especial, porque mais ninguém teve de aturar tanto as minhas crises existenciais este ano como ele. Esteve sempre ao meu lado, acompanhando-me, apoiando-me, ajudando-me e dando-me todo o amor e carinho que eu precisava.

Às minhas espanholitas, Inês Simões e Liliana Carvalho, por mesmo estando tão longe, estarem sempre presentes a acompanhar-me e dar-me uma mãozinha importante a arranjar aqueles artigos mais teimosos.

Ao meu grupo de amigos karatecas que demonstrou ser um grupo fantástico, muito animado e sempre presente com pessoas espectaculares sempre prontas a aturar-me e a animar as minhas noites dos fins-de-semana entre outras ocasiões especiais.

Contents

Index of Figures

Index of Tables

Abbreviations

aa – Amino acid

ACTB – β-actin

AD – Alzheimer disease

ALS – Amyotrophic lateral sclerosis

AR-JP – Autosomal recessive juvenile Parkinsonism

CNS – Central nervous system

CP – Core particle of the 26S proteasome

CT – Threshold cycle

ddNTPs – Dideoxynucleotide triphosphates

DMEM – Dulbecco's modified eagle medium

DMSO – Dimethyl sulfoxide

DNA – Deoxyribonucleic acid

DUBs – Deubiquitinating enzymes

E1 – Ubiquitin-activating enzyme

E2 – Ubiquitin-conjugating enzyme

E3 – Ubiquitin protein ligase

E4 – Ubiquitin chain elongation factors

EOP – Early onset Parkinsonism

ExoSAP – Exonuclease and shrimp alkaline phosphatase mix

FBS – Fetal bovine serum

GFP – Green fluorescent protein

GPi – Globus pallidus interna

GWAS – Genome wide association study

HD – Huntington's disease

HSP – Heat shock protein

IBR – In-between-RING domain

LB – Lewy body

LB in "Material and Methods" – Luria bertani medium

MAF – Minor allele frequency

MLPA – Multiplex dependent ligation probe amplification

MPTP – 1-methyl-4-phenyl-1,2,3,6-tetrahydropyridine

MS – Multiple sclerosis

mtDNA – Mitochondrial DNA

NHEJ – Non-homologous end joining

PACRG – Parkin co-regulated gene

Pael-R – Parkin-associated endothelin receptor-like

PARK2 – Parkin gene

PBS – Phosphate-buffered saline

PBS-T – Phosphate-buffered saline with tween-20

PCR – Polymerase chain reaction

PD – Parkinson disease

pDNA – Plasmid deoxyribonucleic acid

Pu – Putamen

PVDF – Polyvinylidene fluoride

RBR – Ring between ring fingers

r.f.u. – Relative fluorescence units

RING – ''Really interesting new gene''

RIPA – Radio-immunoprecipitation assay buffer

RNA – Ribonucleic acid

RPs - Regulatory particles of the 26S proteasome

SAP – Shrimp alkaline phosphatase mix

SBE – Single-base extension

SDS-PAGE – Sodium dodecyl sulfate-polyacrylamide gel electrophoresis

SE – Standard error

SNc – *Substantia nigra* pars compacta

SNP – Single nucleotide polymorphism

Th – Thalamus

Ub – Ubiquitin

UBL – Ubiquitin-like domain

UCH-L1 – Ubiquitin C-terminal hydrolase L1

UPS – Ubiquitin proteasome system

WT – Wild type

Abstract

Autosomal recessive juvenile Parkinson disease (AR-JP) is mainly caused by mutations in *PARK2*. AR-JP presents with rigidity, bradykinesia and resting tremor, usually before age 40 years. Large *PARK2* deletions account for 50% of the mutations identified in patients with AR-JP of Portuguese origin. The *PARK2* gene encodes parkin, an E3 ubiquitin ligase, an important part of the cellular machinery that covalently tags target proteins with ubiquitin for degradation by the ubiquitin-proteasome system (UPS), the main cellular protein degradation system responsible for targeted degradation of damaged and misfolded proteins.

This project aims were: determine the breakpoints of the deletion found in Portuguese patients in order to identify the genomic mechanisms underlying these gene rearrangements and to explore the pathogenic mechanisms of parkin mutations by assessing the dynamics of formation and degradation of aggregates by UPS and also by determining its effects in the UPS degradation capacity and its relation with neuronal death.

A successful approach was developed to narrow the deletion breakpoint intronic position. Cellular models expressing wild-type and mutant parkin were developed and characterized regarding mRNA and protein expression, as well as, aggregate formation, cell viability and proteasome activity.

Our data show that the different studied mutations do not have an impact on cell viability, although resulted in differences in the number of cell with aggregates for the cells expressing N52MfsX29, L358RfsX77 and R275W mutants as well as in the number of aggregates present in each cell. We were also able to show that proteasome inhibition has as impact both in cell viability and in aggregate formation, resulting in decreased viability and increased aggregate formation.

The study of the cellular mechanisms resulting in neuronal dysfunction is crucial for the identification of potential therapeutic targets for Parkinson disease.

Keywords: AR-JP; Parkin; Ubiquitin-proteasome system; protein aggregation; neuronal death.

Sumário

A doença de Parkinson juvenil com transmissão autossómica recessiva é maioritariamente causada por mutações no gene *PARK2*. Esta doença caracteriza-se pela presença de rigidez, bradicinésia e tremor de repouso, geralmente antes dos 40 anos.

Grandes deleções no gene *PARK2* são responsáveis por 50% das mutações identificadas em doentes com Parkinson juvenil na população portuguesa. Este gene codifica a proteína parkina, uma E3 ubiquitina ligase, que faz parte da maquinaria celular que adiciona ubiquitinas às proteínas-alvo para degradação pelo sistema ubiquitina-proteossoma (UPS), o mais importante sistema de degradação de proteínas responsável pela degradação de proteínas danificadas ou com uma conformação errada.

Os objectivos deste trabalho foram: determinar os *breakpoints* das deleções encontradas em doentes portugueses de modo a identificar os mecanismos genómicos subjacentes aos rearranjos génicos, explorar os mecanismos patogénicos das mutações da parkina, avaliando a dinâmica de formação e degradação de agregados pelo UPS e determinar os efeitos das mutações na capacidade de degradação do UPS e sua relação com a morte neuronal.

Foi desenvolvida com sucesso uma abordagem para delimitar a posição intrónica dos *breakpoints* das deleções. Foram criados modelos celulares que expressam a proteína *wild-type* e mutante e foi realizada a sua caracterização ao nível do mRNA e da proteína, assim como, a formação de agregados, viabilidade celular e actividade do proteossoma.

Os nossos resultados demonstram que as diferentes mutações estudadas não afectam a viabilidade celular, resultando no entanto, em diferenças no número de células com agregados nos mutantes N52MfsX29, L358RfsX77 e R275W, assim como, no número de agregados em cada célula. Demonstramos também que a inibição do proteossoma tem efeito tanto na diminuição da viabilidade celular como no aumento da formação de agregados.

O estudo dos mecanismos celulares que resultam na disfunção neuronal é crucial para a identificação de potenciais alvos terapêuticos para a doença de Parkinson.

Termos-chave: Doença de Parkinson juvenil com transmissão autossómica recessiva; parkina; sistema ubiquitina-proteossoma; agregação de proteínas; morte neuronal.

1. Introduction

Neurodegenerative diseases are a large group of heterogeneous disorders characterized by slowly progressive loss of neurons in the central nervous system (CNS), which leads to deficits in specific brain functions (e.g. memory, movement, cognition) and results in heterogeneous clinical and pathological expression (Przedborski et al., 2003). Neurodegenerative diseases are a major cause of morbidity, disability and mortality, being a fundamental issue for both medical care and research for the 21st century. These disorders are becoming more common, largely as a result of increased life expectancy and changing in population demographics (Skovronsky et al., 2006). Neurodegeneration may precede clinical manifestations by many years and the mechanism that drives chronic progression of neurodegenerative diseases remains largely elusive. The major pathological lesion and a common hallmark of neurodegenerative disorders is protein misfolding and subsequent aggregate and inclusion formation in patients' affected tissues. Most cases of neurodegenerative disorders are sporadic, although some genetic forms have also been described. This group of neurodegenerative diseases includes, among others, Alzheimer's disease (AD), Parkinson's disease (PD), amyotrophic lateral sclerosis (ALS), multiple sclerosis (MS) and Huntington's disease (HD) (Ross and Poirier, 2004).

1.1 Parkinson disease

Parkinson disease (PD) is the most common neurodegenerative movement disorder and the second most common neurodegenerative disease after AD, with a prevalence that increases with age from approximately 1% in population older than 65 years to about 4% over 85 years-old (de Lau and Breteler, 2006).

The aetiology of the disease is an interaction of genetic susceptibility factors and environmental risk factors. Among the environmental risk factors, ageing is the most important factor associated with others like being a male, having European ancestry, exposition to pesticides or drugs like methyl-phenyl-tetrahydropyridine (MPTP). Cigarette smoking and coffee consumption have been shown to reduce the risk of PD (de Lau and Breteler, 2006; Gasser, 2009). The importance of the role of genetic factors in PD development has only been recognized with the identification of genes responsible for monogenic forms of the disease. Until now, sixteen Parkinson disease *loci* have been identified and, at least, six disease-causing genes together with numerous putative genetic risk factors (Crosiers et al., 2011; Gasser, 2009) were already found; this numbers continue to grow with the increase of linkage analysis studies and genome-wide association studies (GWAS). The familial forms of PD account for about 10% of all PD patients while idiopathic PD corresponds to 80% of the PD cases. Several genes

were by now identified as responsible for autosomal dominant and recessive PD forms. Among the autosomal-dominant forms of PD there are two major genes - *SNCA* (PARK1) and *LRRK2* (PARK8), and for the recessive forms four genes were identified – *PARK2* (PARK2), *PINK1* (PARK6), *DJ-1* (PARK7) and *ATP13A2* (PARK9) (Crosiers et al., 2011; Gasser, 2009). The mutations on *PARK2* and *PINK1* are the most frequent causes for autosomal recessive juvenile Parkinsonism (AR-JP). This thesis focuses in this form of Parkinsonism caused by *PARK2* mutations.

1.2 Autosomal recessive juvenile Parkinsonism

1.2.1   Pathophysiology

Autosomal recessive juvenile Parkinsonism (AR-JP) is an early-onset form of Parkinsonism that is usually clinically indistinguishable from idiopathic PD forms. The main clinical manifestations include bradykinesia (slowed movements), rigidity, resting tremor, postural instability and gait impairment. Other clinical manifestations are sensory symptoms like pain and tingling, hyposmia (impaired olfaction), abnormal executive and working memory-related functions and neuropsychiatric symptoms (being the most common sleep alterations, depression and anxiety) (Rodriguez-Oroz et al., 2009; Shulman et al., 2011). However, AR-JP is defined has a distinct clinical entity because diverges from idiopathic PD in the early age-at-onset, mostly in parkin-associated AR-JP. Some authors divide early-onset forms of the disease in AR-JP when age-at-onset is inferior to 20 years and early-onset parkinsonism (EOP) when age-at-onset occurs between 20 and 45 years (Cookson et al., 2003). Other authors classify all the cases with age-at-onset below 40 years as EOP (Hedrich et al., 2001). Nevertheless, most of the early-onset cases with age-at-onset inferior to 40 years are denominated AR-JP (von Coelln et al., 2004). In the context of this thesis, we will use the latter terminology. This disease is also characterized for a very good response to levodopa, however treatment side-effects include the development of early and severe levodopa–induced motor-fluctuations and dyskinesias. AR-JP patients show PD atypical clinical features as early prominent dystonia, symmetric onset of motor symptoms, diurnal fluctuations of symptoms and reflex changes. Also, the disease seems to progress slowly and loss of olfaction or late cognitive decline and dementia, that are characteristic non-motor manifestations of PD, are not found. Another feature is the absence, with a few exceptions, of Lewy bodies (LB), the pathological hallmark of PD, on the neuropathological analysis of AR-JP patients' brains (Gasser, 2009; Shulman et al., 2011).

These motor manifestations present in PD are attributable to the progressive loss of dopaminergic neurons in the *substantia nigra* pars compacta (SNc). As shown in figure 1.1, the reduction of dopaminergic input to the putamen (Pu), which corresponds to the motor region of the *striatum*, leads to a decrease in the excitation of the direct pathway that functions to facilitate movements. In this

direct pathway, the Pu inhibits the *globus pallidus* interna (GPi), which inhibits the thalamus (Th). Thalamus is responsible for the excitatory input to the motor cortex. Also, the indirect pathway that functions to repress movements and is inhibited by the dopaminergic input is enhanced in PD patients.
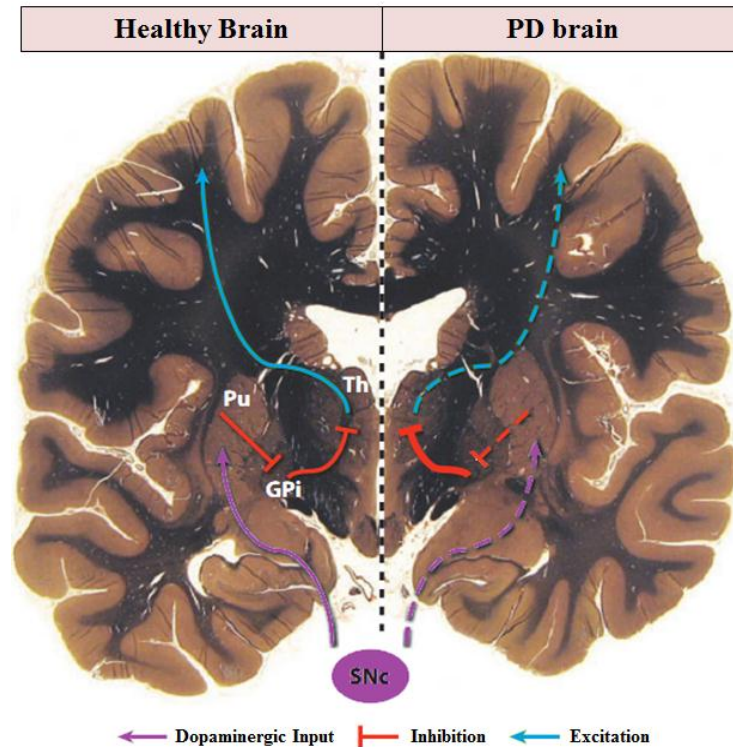
Figure 1.1: Schematic representation of the neurodegenerative processes affected in PD. Adapted from (Shulman et al., 2011).

When PD motor symptoms are clinically recognized, already 60% of dopaminergic neurons are lost, which results in an 80% depletion of striatal dopamine. This explains why motor symptoms respond well to dopamine replacement therapy and to the direct modulation of basal ganglia activity via the implantation of deep brain stimulators in the subthalamic nucleus. These PD therapies are only effective in controlling the symptoms, delaying disability and extending life expectancy. The non-motor symptoms, however, are not responsive or show a weak response to dopamine replacement, thus contributing to overall patients' disability. Currently, the impact of PD neurodegeneration in other brain systems is still unclear (Shulman et al., 2011).

1.2.2   Genetics

1.2.2.1 *PARK2* gene

The Park2 locus was mapped in 1997 to chromosome 6q25.2-q27 (Matsumine et al., 1997). Later, the gene was identified by positional cloning and its encoded protein was named parkin. Parkin encoding gene has only 12 exons but these are surrounded by large intronic regions spanning more than 500 kilobases. The coding sequence with a 1,395-base-pair open reading frame is deposited in the GenBank database (accession number AB009973) (Kitada et al., 1998; von Coelln et al., 2004).

1.2.2.2 Parkin

The *PARK2* gene encodes a 465-amino-acid protein with a molecular weight of 51,652 daltons, named parkin. This protein is ubiquitously expressed, with abundant expression in various brain regions, including the *substantia nigra*. In a cell, the majority of parkin protein is localized in the cytosol and Golgi fractions and a small amount in the microsomal fraction (Kitada et al., 1998; Shimura et al., 1999).

Parkin belongs to the RBR (ring between ring) protein family, characterized by the presence of two RING (really interesting new gene) domains, RING1 and RING2, that flank an IBR (in-between RINGs) domain (Marin et al., 2004). Besides these domains, parkin contains an Ubiquitin-like (UBL) domain in the protein N-terminal, from the residues 1 to 76 (figure 1.2). This UBL domain shares 62% homology with ubiquitin (Ub) and may be involved in substrate recognition (Dev et al., 2003). Also, structural information reveals that it binds to the Rpn10 subunit of the 19S regulatory subcomplex in the 26S proteasome. The central domain of the parkin, from residue 145 to 232, has an yet unknown function, however in this region, and additional RING domain was recently recognized, from residue 150 to 215, and named RING0 as it is located upstream of RING1. This RING0 was identified by classic proteolytic biochemistry and apparently has two parts separated by a 26 amino acid linker region. RING0, like the other RINGs present in the RBR domain (residues 238 to 449) and located in protein C-terminal, are cysteine-rich zinc fingers implicated in substrate recognition and binding to E2 enzymes. Parkin also contains a PDZ binding motif that is responsible for interaction with proteins containing PDZ domains like CASK (calcium/calmodulin-dependent serine protein kinase) (Rankin et al., 2011). The parkin promoter has been found to be a bidirectional promoter, also regulating the transcription of parkin co-regulated gene (*PACRG*) that is upstream of *PARK2* and in an antisense direction (von Coelln et al., 2004).
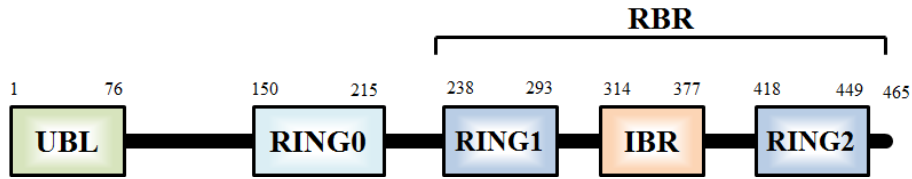
Figure 1.2: Schematic representation of the most relevant parkin domains.

Similar to other RING finger proteins, parkin is an E3 ubiquitin ligase (Shimura et al., 2000). E3 ligases are an important part of the cellular machinery that covalently tags target proteins with ubiquitin for degradation by the ubiquitin-proteasome system (UPS). E3 ligases usually confer substrate specificity to the ubiquitination process (which will be further explored in the next section) by bringing the substrate protein into juxtaposition for direct ubiquitination by an E2 Ub-conjugating enzyme (Dev et al., 2003; Moore et al., 2005).

An impaired E3 ligase function may lead to an accumulation of parkin substrates because these proteins cannot be properly degraded and this accumulation contributes to neurotoxicity. This is the reason why, the identification of parkin substrates on the basis of *in vitro* and cell culture experiments, has been highly relevant (von Coelln et al., 2004). The first parkin substrate identified was CDCrel-1 (cell division control related protein) which interacts with RING2 domain. CDCrel-1 is a synaptic vesicle-enriched septin GTPase, predominantly expressed in the nervous system and implicated in regulating neurotransmitter release through the inhibition of exocytosis by interacting with syntaxin. Overexpression of CDCrel-1 in SNc neurons of rats by virus-mediated gene transfer induces dopamine-dependent neurodegeneration. Other substrate is Synphilin-1, a protein with unknown function that interacts with α-synuclein (mutations in which are responsible for a dominant form of PD). Synphilin-1 is a component of LBs in PD and in related synucleinopathies. This protein interacts with RING2 domain of parkin and when overexpressed in cultured cells, results in protein inclusions. These protein inclusions also occur when α-synuclein, the major component of LBs, is overexpressed. An O-glycosylated form of α-synuclein (αSp22) is ubiquitinated by parkin and seems to accumulate in AR-JP patients brains; however its relevance for the pathogenesis needs further elucidation. Parkin-associated endothelin receptor-like (Pael-R), p38 and Synaptotagmin XI are other parkin substrates. Pael-R is a putative G-protein-coupled transmembrane protein that plays a role in dopaminergic signaling and interacts with parkin by the C-terminal region (residues 217 to 465). This protein is ubiquitously expressed throughout the brain and its overexpression in *Drosophila* has been shown to cause a selective loss in dopaminergic neurons. Moreover, overexpression of Pael-R produced insoluble, ubiquitinated proteins and leads to an increase in cell death. The protein p38 is a subunit of the aminoacyl-tRNA synthetase complex involved in protein biosynthesis that is present in LBs. Overexpression of this protein results in aggresome-like inclusion body formation and/or cell death, depending on the cell type. Synaptotagmin XI is a protein involved in the maintenance of synaptic function, which is present in the core of LBs in PD. Other parkin putative substrates are cyclin E, a

regulatory subunit of cyclin-dependent kinase 2 protein, SIM2 that is a transcription factor present in the nucleus, and others like α/β tubulin and poly-(Q)-expanded huntingtin. Parkin substrates are diverse, widely distributed and appear to have little in common. Moreover, none of the putative parkin substrates have been reported to accumulate in the brains of parkin knockout mice. These results have questioned the authenticity of these substrates as well as the contribution of parkin to their degradation by the UPS (Moore et al., 2005; Rankin et al., 2011; von Coelln et al., 2004).

In addition to substrate binding, parkin also interacts with E2 enzymes and other proteins, which indicate that parkin may function as a part of a multi-protein complex. Parkin interacts with E2 enzymes through its RING domains. Generally, one RING finger is sufficient for E2 binding, however, the two parkin RING fingers may work in combination and provide a molecular mechanism that allows for the close association of E2 enzymes and the substrate. The ubiquitin-conjugating enzymes interacting with parkin are UbcH7, UbcH8 and the UbcH13/Uev1a E2 heterodimer that is thought to be responsible for the catalysis of K63-linked ubiquitin chains as well as with the endoplasmic reticulum-associated E2s, Ubc6 and Ubc7. AR-JP mutations in parkin gene impair the interaction with E2 enzymes, reducing or abolishing its ubiquitin ligase activity (Chaugule et al., 2011; Dev et al., 2003).

Parkin can be auto-ubiquitinated and in cell–free *in vitro* assays has been shown to be capable of multiple mono-ubiquitination. Also, it is capable of K48-linked poly-ubiquitination and K63-linked poly-ubiquitination (Rankin et al., 2011). Recently, it was discovered that the Ubl domain of parkin may function to inhibit its intrinsic auto-ubiquitination activity being the mutations located in this domain responsible for relieving auto-inhibition and leading to a rapid degradation of these proteins by the proteasome (Chaugule et al., 2011). Parkin is degraded by the proteasomal complex (Choi et al., 2000) and has been shown that is a substrate of Nrdp1, also an E3 ubiquitin ligase. Nrdp1 interacts with the N-terminus (first 76 amino acids) of parkin and is responsible for its ubiquitination, thus promoting parkin degradation. This interaction influences the production of reactive oxygen species (ROS), what suggest a potential involvement of Nrdp1 in PD pathogenesis, being a possible new candidate causative factor (Yu and Zhou, 2008). However, a study in a Chinese population did not found any sequence variation in this gene, although further research is necessary (Mo et al., 2010).

1.2.2.3 Parkin mutations and juvenile Parkinson disease

Mutations in *PARK2* are the most common cause of Parkinsonism with early-onset. In a European study, parkin mutations were identified in about 50% of the familial cases and in approximately 10% of sporadic early-onset PD patients. The frequency is much higher (around 77%) if only patients with disease onset at 20 years or younger were considered (Lucking et al., 2000).

All type of mutations have been described in PD patients, from point mutations resulting in amino acid exchanges (missense mutations) and premature stop codons (nonsense mutations) to deletions and insertions of nucleotides, often resulting in frameshift mutations. Splice site mutations and gene rearrangements involving the deletion of multiple exons, duplications or triplications were also found (von Coelln et al., 2004). Moreover, mutations are found throughout the entire gene including changes in each of its twelve exons. Regardless of their heterogeneity, there are no discernable differences in the clinical manifestations among patients carrying different parkin mutations, although differences in age-at-onset were described for patients with R275W mutation (Lohmann et al., 2003). Gene rearrangements represent 50% of the identified mutations and, when present in the heterozygous state, are not detectable by conventional screening methods like sequencing (Hedrich et al., 2001).

AR-JP caused by mutations in *parkin* gene is an autosomal-recessive disorder with high penetrance and with patients showing either homozygous or compound heterozygous mutations that result in parkin loss of function (Gasser, 2009). However, in Parkinsonism the distinction between dominant and recessive forms is unclear. There are several descriptions of families in which parkin mutations and disease segregation are incompatible with a recessive inheritance mode. The role of heterozygous parkin mutations is still not clear: it is a matter of debate if they may cause or increase the susceptibility to late-onset PD. This could be mediated by three mechanisms. One is haploinsufficiency, if half of the wild-type (WT) protein dosage is not enough to preserve normal function. In this case, because it is thought that parkin has a neuroprotective effect, it is possible that this 50% reduction can increase the susceptibility of neurons to toxicity such as oxidative stress. Other possibility is a dominant-negative effect, if the mutant variant reduces the function of the WT protein, for example, if the mutant protein forms a heteromeric complex with the normal molecule, knocking out the activity of the entire complex. The third mechanism is the acquisition of a dominant toxic gain-of-function effect, if the mutant protein acquires a novel and different function (Bossy-Wetzel et al., 2004). Some arguments are in favor for a pathogenic role of the heterozygous parkin mutations: these mutations are more common in patients than in controls, although the frequency of heterozygous mutations in healthy individuals is still unknown and the case-control studies, so far, have variable results; also, the heterozygous mutations are more common in patients than mathematically expected and the mean age-at-onset in heterozygous carriers is between that of patients with homozygous or compounds heterozygous mutations and that of patients without mutations. Also, neuroimaging studies show preclinical changes in heterozygous mutations carriers. On the contrary, the arguments against this theory are that heterozygous mutations are found in controls, however they have not all been neurological examined and there is no clinical follow-up. Moreover, not all heterozygous relatives in affected families show signs of parkinsonism (Klein et al., 2007).

The heterozygous mutations might have different effects depending on the sequence variation within the gene. If the alteration causes more severe consequences on structure and function of the protein, this mutation might show a more pathogenic effect. For example, mutations like the R275W

substitution in the RING1 domain and mutations that cause the formation of aggresome-like inclusions upon overexpression have been pointed out as possibly having a dominant-negative effect. However, this hypothesis has not yet been supported by parkinsonism mouse models and further studies are required (Klein et al., 2007).

1.2.3 The ubiquitin proteasome system

The ubiquitin proteasome system (UPS) is the main cellular protein degradation system and is capable of targeted degradation of mutant, damaged, toxic or misfolded intracellular proteins, as well as short-lived key regulatory proteins that mediate a number of cellular events such as cell cycling, signal transduction, transcription, neurotransmission, receptor endocytosis, metabolism and the immune response. (Moore et al., 2003) The UPS is responsible for the rapid degradation of 30% or more of newly produced proteins within the cell. This process requests the ligation of ubiquitin, a small covalent modifier that forms a poly-ubiquitin chain on the target protein, becoming a signal for degradation by the 26S proteasome (Tanaka et al., 2004).

Poly-ubiquitination of substrates is the priming event for proteasome-mediated degradation. In this process, the small and highly conserved protein tag, ubiquitin, consisting of 76 amino acid residues, is covalently attached to the target protein through an ATP-dependent enzymatic pathway that occurs by sequential steps catalyzed by three enzymes. First, the ubiquitin is activated by an ubiquitin-activating enzyme (E1), which forms a thiol ester bond between a cysteine residue and a carboxy-terminal glycine of ubiquitin in an ATP-dependent manner. Then, the activated ubiquitin is transferred to one of the several ubiquitin-conjugating enzymes (E2) through the formation of another thiol bond. In the last step, ubiquitin is ligated to the substrate by an interaction of C-terminal glycine residue of ubiquitin with ε-amino groups on side chains of lysine residues of the target protein that is bound to an E3 ligase, like parkin. The E3 ubiquitin ligases bind both the E2 and a specific protein target to which the ubiquitin is covalently attached, transferring the ubiquitin from the E2 to the substrate. Each step of this process becomes more restricted in its substrate, being the E3 ligases determinants to confer specificity to substrate recognition (Betarbet et al., 2005; Moore et al., 2003). It is the successive repetition of this process that links additional ubiquitin molecules into the previously attached ubiquitin resulting in the formation of poly-ubiquitin chain that is the degradation signal recognized by the proteasome, requiring a chain of, at least, four ubiquitin molecules (Berke and Paulson, 2003). In 1999, Koegl *et al*. identified and described one protein that could be a novel ubiquitination factor, named E4 (Koegl et al., 1999). These E4 ubiquitin ligases, also known as U-box E3, can be described as ubiquitin chain elongation factors, possibly being responsible for adding ubiquitin molecules to form these poly-ubiquitin chains. This process is common to all known ubiquitination reactions,

independently of whether the substrate-bound ubiquitin will signal for proteasomal proteolysis, endocytosis or other fate. So, additional factors are necessary, like the subcellular localization of the substrate or the number and topology of the substrate-conjugated ubiquitins. There are a total of seven lysine residues on ubiquitin (at positions 6, 11, 27, 29, 33, 48 and 63) and the poly-ubiquitination could occur through alternative lysine residues (Dawson, 2006). There are at least three ways to ubiquitinate a protein: if substrates are destined for the proteasome, they generally are conjugated to a poly-ubiquitin chain in which successive ubiquitins are linked through an internal lysine residue (K48) to the terminal residue (G76) of a new ubiquitin monomer by isopeptide bonds forming a K48-G76-linked poly-ubiquitination chain. However, when this ubiquitin molecules chain is linked through lysine 63 by K63-G76 bonds, the destination could be probably non-proteolytic, like clearance by autophagy (Tan et al., 2008). Other ubiquitination process is multi-mono-ubiquitination, where occurs the attachment of multiple molecules per protein but only one ubiquitin per lysine residue, being responsible for regulating transcription, translation, protein trafficking, DNA repair and other cellular functions. The specificity in signaling is mediated by the ubiquitination process. The recognition of substrates for ubiquitination is governed by the presence and accessibility of primary sequence or structural motifs in the substrate, known as ubiquitination signals, recognized by the E3s (Pickart, 2001). The E3s are central determinants of specificity because they play an important role in the selection of target proteins for degradation by binding the substrate with a degree of selectivity for ubiquitination in a temporally and spatially regulated fashion (Tanaka et al., 2004). The E3s are classified in several groups: one share the HECT domain that harbors a 350-residue region with a strictly conserved cysteine residue forming an essential thio-ester bond for binding ubiquitin (Pickart, 2001). The major group of E3s, designed RING-type E3, share a RING finger domain capable of binding Zn^{2+} of approximately 70 residues consisting in a cysteine-rich consensus sequence flanked by one or two histidine residues. There are typical and atypical forms of this RING-finger motif, dividing the typical in three classes with small differences in their structure: RING-HC (C3HC4), RING-H2 (C3H2C3) and RING-IBR-RING where parkin belongs. The third group of E3s shares a U-box domain whose tertiary structures are similar of the RING-finger domain but do not show a binding potency to Zn^{2+} that is probably necessary for keep the domain structure in RING-type E3s. The last group consists of very unique E3s that have no sequence homology to known E3 enzymes (Tanaka et al., 2004).

After the labeling of unwanted/damaged proteins with chains of activated ubiquitin molecules, the ubiquitinated proteins are transported to the proteasome by chaperone molecules like heat shock proteins (HSP) and then are recognized and unfolded by proteasome regulators, followed by an ATP-dependent degradation of unwanted proteins by the proteasome (Olanow and McNaught, 2006).

The 26S proteasome is a eukaryotic ATP-dependent protease of over 2.5 megadaltons. This multi-subunit proteolytic complex is composed by a 700-kilodaltons central catalytic core particle (CP), the 20S proteasome and two terminal regulatory particles (RPs) also designated PA700 or 19S complex

(Finley, 2009). CP is a barrel-like structure made up of 28 subunits arranged into four hetero-heptameric rings, two inner rings and two outer rings, each one made up of seven structurally similar α- and β-subunits associated in the following order, αββα (Betarbet et al., 2005; Tanaka et al., 2004). Each inner ring is formed by β-type subunits, three of which have catalytically active threonine residues at their N-terminus being proteolytic active sites (β1, β2 and β5) that can cleave a broad range of peptide sequences. β1 prefer to cleave on the C-terminal side of acidic residues, β2 after tryptic residues and β5 after hydrophobic residues, being the site specificities generally classified as caspase-like, trypsin-like and chymotrypsin-like activities. These three different catalytic sites of the proteasome reside on the inner surface of the inner rings, thus preventing unselective degradation of proteins (Finley, 2009). The two outer rings containing the α-subunits serve to anchor the two RPs (Moore et al., 2003) which are attached to both ends of the central core in opposite orientations to form the enzymatically active 26 proteasomal complex (Tanaka et al., 2004). It is in this hollow cylindrical structure with an interior space whose largest dimensions are approximately 100Å axially and 60Å along the orthogonal symmetry axis that proteolysis occurs. The 19S regulatory complex consists of two sub-complexes known as the base and the lid which correspond to the portions proximal and distal to 20S proteasome. The base is composed by six paralogous ATPases (Rpt 1 - 6), which are critical for the 19S-20S complex formation, and four non-ATP subunits, the scaffolding proteins Rpn1 and Rpn2 and the ubiquitin receptors Rpn10 and Rpn13. The base of the 19S complex has three ATP-dependent functions: recognize the poly-ubiquitin chain, which is removed and cleaved into monomers by deubiquitinating enzymes (DUBs), unfolds the target proteins and translocates them through the opened channel of the 20S proteasome. The lid of the 19S is a 400-kDa complex made up of multiple non-ATPases subunits like Rpn3 that can be released from the proteasome or rebind under certain conditions. The role of the lid is still unclear but it is necessary for proper degradation of the target proteins (Glickman and Ciechanover, 2002). Considering the nine lid subunits, only Rpn11 has a known function, being a DUB. Besides the 19S complex, the most studied proteasome activator of the 20S core is the 11S regulator (PA28), a heteromeric complex of 28-kDa subunits. PA28 activator is a complex of two alternating subunits, PA28α and PA28β, which associate with the α-subunits of 20S proteasome at both or either ends and opens the channel of the 20S core but via an ATP-independent process. Beyond the lack of ATPase activity, PA28 also lacks the ability to bind ubiquitin conjugates. The 11S-20S proteasomal complex has been suggested to mediate the degradation of non-ubiquitinated short peptides including oxidized proteins. PA28 is also known to modulate proteasome-catalyzed production of antigenic peptides presented to the immune system on MHC class I molecules (Betarbet et al., 2005; Finley, 2009).

The degradation products of proteasomal catalysis are short peptides that are released to the cytosol, and once there, are processed by other cytoplasmatic peptidases to generate single amino acids, which are then recycled to produce new proteins. The same happens to the poly-ubiquitin chains that, after the release from the target proteins, are recycled back into the ubiquitin pathway. Prior to

entry into the proteasome, ubiquitin chains are detached from proteins and cleaved into monomers by deubiquitinating enzymes such as ubiquitin C-terminal hydrolase L1 (UCH-L1) that has also been associated with familial PD. When this deubiquitination process is blocked, degradation is inhibited and ubiquitinated substrates accumulate leading to cell death (Betarbet et al., 2005; Finley, 2009). A simplified scheme of the sequential steps needed for the targeted degradation of proteins by the UPS is presented in figure 1.3.
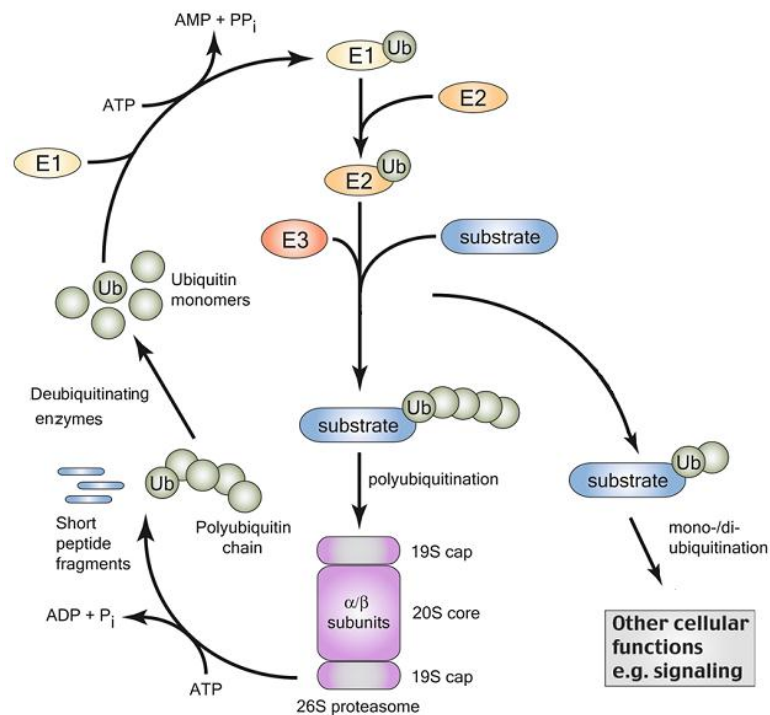
Figure 1.3: Schematic representation of the steps involved in the targeted degradation of proteins by the UPS. Adapted from (von Coelln et al., 2004).

Since proteasomes are present in the cytoplasm (associated with centrosomes, cytoskeletal networks and the outer surface of the endoplasmatic reticulum), in perinuclear regions and nuclei of all eukaryotic cells (Betarbet et al., 2005), these are the locations where aggregates of proteasomes accumulate when the proteolytic pathway is impaired.

1.3 Molecular pathways of neurodegeneration in PD

1.3.1 The relationship between UPS and Parkinson disease

The ability of the UPS to recognize and selectively degrade misfolded and damaged proteins enable it to protect cells against the toxic effects of protein aggregation. The presence of these

ubiquitin-positive protein aggregates is a common ultra-structural feature of many neurodegenerative diseases like PD (Um et al., 2010). These diseases caused by aggregate-prone proteins are known as proteinopathies (Rubinsztein, 2006). Initial protein aggregation could lead to an accumulation of these aggregates by a chronic imbalance between the generation and clearance of misfolded proteins that could happen if the UPS function is impaired (Bence et al., 2001; Chin et al., 2010). Protein aggregates are thought to impair cell function and viability through a variety of mechanisms, including pore formation, proteasome inhibition and disruption of intracellular transport (Chin et al., 2010). Thus, it is thought that the protein quality control system (composed by the cellular machinery that monitors the quality and levels of the proteins in the cell) plays a critical role in neuronal function and survival, being the UPS one major arm of this quality control (Berke and Paulson, 2003). Also, it is known that proteasome inhibitors increase the frequency of ubiquitin-positive intracellular inclusions in neurodegenerative disorder cell models (Tanaka et al., 2004).

Protein aggregates are oligomeric complexes of non-native conformers originated from non-native interactions between intermediates in protein folding or assembly (Kopito, 2000). Protein misfolding can occur as a result of genetic mutations (causing alterations in primary structure), environmental factors or oxidative stress (causing partial unfolding). When the production of these misfolded proteins, that are often prone to aggregation into oligomers and aggregates, exceeds the capacity of the molecular chaperone system (an additional regulatory mechanism by HSPs that contribute to the removal of misfolded proteins by promoting their refolding or facilitating their degradation, reducing aggregates formation) and of the UPS, aggregated proteins are actively sequestered in a microscopic pericentriolar structure called aggresome which is degraded by autophagy (Chin et al., 2010; Moore et al., 2003). Inclusion bodies also contain proteins that, although not being aggregation-prone, are recruited, concentrated or trapped within inclusions (Berke and Paulson, 2003). These aggressomes are called microtubule-dependent inclusion bodies because the aggregated proteins are specifically delivered to inclusion bodies by dynein-dependent retrograde transport on microtubules (Kopito, 2000). In PD, these aggressomes over time develop to LBs, the pathological hallmark of PD. LBs are cytoplasmatic inclusions consisting of a heterogeneous mixture of protein and lipids. Lipids form the core of the inclusions while the peripheral filamentous elements include proteins like α-synuclein, ubiquitin, synphilin-1, parkin, UCH-L1, proteasomal components, HSPs, other UPS-related proteins and neurofilaments (Moore et al., 2003). The mechanism by which LBs are formed and their role in degeneration remains largely unknown (Imai and Takahashi, 2004). Also, it is unclear if the protein aggregates themselves are pathogenic or are the consequence of an underlying molecular lesion, being possible that a loss of UPS function could be responsible for generating protein aggregates or protein aggregates themselves could impair the protein degradation machinery. Other possibility is that impaired UPS and protein aggregation could participate in a feed-forward cycle where one could affect the other (Betarbet et al., 2005).

Protein inclusions, such as aggressomes, can be experimentally induced by proteasomal inhibition in neuronal and non-neuronal cells. Immunocytochemical analyses have reported that parkin is present in the cellular inclusions after exposure of cells to proteasome inhibitor. However, AR-JP is not accompanied by obvious LBs formation (Imai and Takahashi, 2004). Thus, it was suggested that parkin may promote the formation of LB inclusions being this, one mechanism to detoxify proteins such as α-synuclein or that parkin-mediated neurodegeneration may occur by mechanisms distinct from those that happens in PD with LBs (Dawson and Dawson, 2003; Feany and Pallanck, 2003).

In addition to cytoplasmatic inclusions, further clues that associate a dysfunction of UPS to PD pathogenesis is that, in sporadic PD, levels of 20/26S proteasomes and proteasome activity are reduced in vulnerable regions (Rubinsztein, 2006). But, the major proof is the presence of genetic mutations directly associated with UPS. These occur in parkin and UCH-L1. Since parkin is an E3, the ubiquitin pathway is directly linked to the cause of AR-JP. It is known that mutants of parkin alter the solubility of parkin, increasing its tendency to aggregate (Rogers et al., 2010). In 2008, a study of pathogenic mutations revealed that misfolding and aggregation is characteristic for C-terminal deletion mutants, but alterations in the solubility and formation of parkin aggregates has also been reported for various parkin missense mutations. However, even wild-type parkin is prone to misfolding under severe oxidative stress (Schlehe et al., 2008).

It is thought that a lack of parkin function lead to a toxic accumulation of substrate proteins or parkin itself. Parkin targets a number of substrates that have intrinsic toxic and aggregation properties *in vivo* such as the O-glycosylated form of α-synuclein and α-synucleinP22. Parkin also supresses the toxicity of Pael-R (which when overexpressed elicits a marked ER stress response), of mutated α-synuclein A53T and of a poly(Q)-expanded mutant of ataxin-3 (Khandelwal and Moussa, 2010). Other substrates ubiquitinated by parkin that may exert a direct cytotoxic effect on accumulation includes α/β-tubulins, which in the free, monomeric form are toxic (Kahle and Haass, 2004; Ren et al., 2003), and cyclin E which might force postmitotic neurons into abortive cell cycling, promoting apoptosis. Overexpression of parkin decreases sensitivity to proteasome inhibitors on an E3 ligase activity-dependent manner and also, the knockdown of parkin increases sensitivity to proteasome inhibitors (Petrucelli et al., 2002). Parkin is thus considered a broad neuro-protective agent against a wide range of toxic injuries from proteasomal dysfunction to substrate toxicity (Feany and Pallanck, 2003).

1.3.2   Mitochondrial impairment and oxidative stress in PD

Other mechanisms that could be involved in PD pathogenesis are mitochondrial dysfunction and oxidative stress. Mitochondria are key regulators of cell survival and death and play a central role in ageing, the principal risk factor for PD. This contribution to ageing occurs through the accumulation of mitochondrial DNA (mtDNA) mutations and net production of reactive oxygen species. Also,

mitochondria have been found to interact with many specific proteins implicated in genetic forms of neurodegenerative diseases. They were first implicated in PD because of MPTP whose metabolite, MPP^+, inhibits complex I of the mitochondrial electron-transport chain, causing parkinsonism (Lin and Beal, 2006). Impaired complex I activity leads to free radical stress and makes neurons vulnerable to glutamate excitotoxicity. One proof that mitochondrial impairment may be central to the pathogenesis of PD is the fact that defects in complex I as well as three complex I inhibitors cause dopaminergic cell death and induce the formation of LB-like filamentous inclusions containing α-synuclein (Dawson and Dawson, 2003). The mechanism of toxicity in these complex I inhibition models probably involves oxidative stress. Complex I inhibition and oxidative stress are factors contributing to ageing and were shown to be relevant to PD when complex I deficiency and glutathione depletion were found in the *substantia nigra* of patients with idiopathic or with pre-symptomatic PD (Lin and Beal, 2006). Parkin has been shown to be located, in part, in mitochondria. It is though that this protein acts directly at the mitochondria through its ubiquitination activity, confirmed by a study in 2010 (Fitzgerald and Plun-Favreau, 2008; Lee et al., 2010).

Parkin is thought to be also related to oxidative stress. This protein is up-regulated in response to unfolded protein stress and supresses unfolded protein stress-induced cell death via its E3 activity (Imai et al., 2000). This oxidative stress damages lipids, proteins and DNA and can directly impair protein ubiquitination and degradation systems. Moreover, the toxic products of oxidative damage induce cell-death mechanisms (Fitzgerald and Plun-Favreau, 2008). Parkin mutations lead to oxidative stress, however, wild-type parkin can be associated with the outer mitochondrial membrane and prevent mitochondrial swelling, cytochrome c release and caspase activation (Lin and Beal, 2006). In addition to these mechanisms, induction of protein folding stress in cells, reduced parkin phosphorylation and unphosphorylated parkin had slight but relevantly elevated auto-ubiquitination activity. Thus, regulation of the phosphorylation state of parkin may contribute to the unfolded protein response in stressed cells (Yamamoto et al., 2005). Also, the phosphorylation of parkin by CDK5 (cyclin-dependant kinase 5) may regulate its ubiquitin-ligase activity and so, contribute to the accumulation of toxic parkin substrates and decreased ability of dopaminergic cells to handle with toxic insults in PD (Fitzgerald and Plun-Favreau, 2008).

1.4 Aims

Large *PARK2* deletions account for 50% of the mutations identified in patients with AR-JP of Portuguese origin. Thus, the first aim of this study was to determine the breakpoints of the deletions found in Portuguese patients in order to identify the genomic mechanism underlying these gene rearrangements.

Secondly, through the development of cellular models with point and frameshift mutations, also found in Portuguese families with AR-JP molecular diagnosis, we intended to explore the pathogenic mechanisms of these parkin mutations by assessing the dynamics of formation and degradation of aggregates in AR-JP and the effect of these mutations in the UPS protein degradation capacity. Finally, we aimed to study the role of the UPS in the clearance of parkin aggregates and the effect of UPS impairment in aggregate accumulation.

2 Materials and Methods

2.1 <u>Large deletions breakpoint determination</u>

Large *PARK2* deletions are responsible for about 50% of the Parkinson disease mutations. We have previously characterized a sample of Portuguese patients showing Parkinson disease symptoms regarding *PARK2* mutations and were able to identify several large deletions through multiplex dependent ligation probe amplification (MLPA). *PARK2* gene presents very large introns which makes the determination of deletion breakpoints a hard task. In order to overcome this difficulty several strategies were applied as outlined below.

2.1.1 Subjects

Fifteen patients showed large gene rearrangements and at least eight different deletions were found either in homozygosity (present in the two alelles) or in heterozygosity (only in one allele) as shown in table 2.1.

Table 2.1: List of patients with respective deletions in study.

Patient	Deletion	Homozygozity/Heterozygosity
1	E2	Heterozygozity
2	E3	Heterozygozity
3	E3-E6	Homozygosity
4	E3-E6	Homozygosity
5	E3-E6	Heterozygozity
6	E3-E6	Heterozygozity
7	E3-E6	Heterozygozity
8	E4	Homozygosity
9	E4	Homozygosity
10	E4	Heterozygozity
11	E4	Heterozygozity
12	E4-E7	Homozygosity
13	E5-E6	Homozygosity
14	E7-E9	Heterozygozity
15	E10	Homozygosity

2.1.2   Approach 1: Verification of breakpoints already described
2.1.2.1 Primer design

Some of the deletions identified in Portuguese patients have been already identified in other patient's populations and their breakpoints characterized. In order to verify the presence of these breakpoints among Portuguese patients, primers at approximately 0.5Kb distance of the deletion breakpoints (of the same exons in study) described in three previously published papers (Asakawa et al., 2009; Clarimon et al., 2005; Mitsui et al., 2010) were designed using IDT PrimerQuest (http://eu.idtdna.com/Scitools/Applications/Primerquest/) with the following settings: optimum primer size of 24nt ± 6nt; optimum primer T_M of 60ºC ± 5°C and optimum primer GC% of 50% ± 15%. The list of primers designed is presented in table 2.2.

Table 2.2: List of primers designed for the breakpoints described.

Deletion	Forward	Reverse
E2	TTTGTGGCTGTTTGGTGTGATGGG	AGTTGTGTGACCACAGGAGCATCA
E3_1	AACACACCTGGACACACTGGTGAT	CTCACTTCATCAAACACAGCGGCA
E3_2	AGAGGCTCCACCTCTTCATGCAAT	AGGACACCTTGCTTTGGAGCCTTA
E3_3	AAGAGAGATGGGTGAGGGAACTTG	CATACACAACTGGGAAGGAGCCTA
E3_4	TATGTATGAATGGCAGCCAGCCCA	TGGCAAATGCATTCTCACCATCCC
E3_5	CTGGCCTCTGCTTTCAGGCAATTT	TGCGTCCAAATCCCAGTGAAGAGT
E3_6	TGAATGTAGCCAGCCACCTCACTT	TAGGTGGTGCTAAGTGAAGCCACA
E3_7	AGTTGCTCTTAGCTCTGCCTCGTT	TCACTTCATCAAACACAGCGGCAC
E3_8	ATCTGCTTAAAGCCAGGTGCAGTG	TCCTCTAACCATGTGAGGCAGCAA
E3_9	CGGCCACATCGATTTACTGAGAGA	CCACCACCACTTAACCACAAAGTG
E4_1	ACCTTCAGGTAGAGGTCAAGCACA	ATGTCTGCAGTAGGTGCACACGAA
E4_2	TCAGGCAAGCATCAGATGGAGACA	AGCTCCCTTGGGACCTCTTGAAAT
E4_3	ATGTGGCTTCACTTAGCACCACCT	TACACACACTGCTTTCCAGACCCA
E4_4	AAGAGGTTGGGCTTCTGTTACGGT	ACCTCTCAGCCAAGCCTTACTGTT
E4_5	TCATGCCAGCAGCTCCTTATCAGT	TGCCAGACATGCATTGTGTTCTGC
E4_6	TGGGTCTGGAAAGCAGTGTGTGTA	TGCCTACCAAGCTCTGAAACACCA
E4_7	TTCTGTGTCCATGTGGAGTTCCGT	TTGGAACTGACCAGGAAGGAGCAT
E3-6	ATGCTCAGGACATAGGAGGCGAAT	TCCCACAGTGATACCTGTCATGGA

2.1.2.2 Polymerase chain reaction

Polymerase chain reaction (PCR) amplification was performed with a mix of: 6.25 μL HotStar Master Mix (Qiagen), 1.5 μL of each primer (forward and reverse), 2 μL of DNA sample and 1.25 μL of ddH2O in a final reaction volume of 12.5 μL. PCR amplification parameters are presented in table 2.3 with annealing temperature varying depending on the optimization for each primer pair. All the reactions presented in this work were performed using a Biometra Uno II thermocycler or a Biometra Tgradient thermocycler.

Table 2.3: PCR protocol for fragment amplification.

Cycles	Time	Temperature
1 x	15min	95ºC
35 x	45s	95ºC
	1min 30s	50ºC-60ºC
	1 min	72ºC
1 x	10min	72ºC

After PCR reaction, the products and a blank control were checked for fragment amplification and for the presence of possible contamination, respectively, by electrophoretic separation in a 2% agarose gel in 1x TAE buffer and 0.5 µg/ml Ethidium Bromide. A GeneRuler 100 bp DNA Ladder (Fermentas) was used to define the size of the fragment. Loading dye was added to the DNA samples and gels were run at 120 V.

2.1.3   Approach 2: Range of primers that cover the introns

2.1.3.1 Primer design and PCR amplification

To determine the extension of the deletions present in homozygosity we designed a set of 45 primer pairs covering the two introns surrounding the deleted exons. These primer pairs, which are shown in table 2.4, were designed to amplify a region of between 214 and 632bp and each amplicon was design with approximately 30 Kb of distance from each other.

PCR amplification and fragment analysis was performed as described in 2.1.2.2.

Table 2.4: List of primers designed to cover the relevant introns.

Int	Fw Sequence	Rv Sequence	Product Size
1.1	TCTTTCAGGAAACCGCAGCAAAGC	TTGGCTCAACAACCCTGGAAGAGA	339
1.2	TTGCAGAGGCTCCCTGAACTTGTA	TCTCAAGGTTGGTTGCTCACAGGA	378
1.3	AGTGTCAGTCTCTGTGGCCTTGAT	ATCTTGCACTGGGAGAACAAGGGA	307
1.4	TTTGGGCAGCCTGGGAAATCAAAG	TCCTACTGGGCCAGGATTATGACT	368
1.5	AGGAGCCCTGCATTTCTTGAAGGT	GAAAGCTTAGATTCTCCTGGCGCT	216
1.6	TGTCAGCAGATTCAGGACGGGTTT	GGCTTGGGCTTTATTCTTTGGGCA	408
1.7	ACTTGTTAATGTGGCCTTGGGCAG	AGACCGACAAGCAAGACGCATAGT	632
1.8	AGTCAAAGCCTAGGAGGCTGGTTT	AAATCAGGCAGCAATGAGCCAAGG	497
1.9	AACAAGGCGAATCCCGTCTGTACT	ACAGCTTGCTGGCTCTGTGAGTAA	432
2.1	TTTGTGTACATGTGCTGTCCACGC	ACAAGGTGGGTGATGTGAAATGCC	275
2.2	AAAGGCTCTGTGTGGTCTCCATGA	TCACTTCCAGGCTCCTTTCACACA	569
2.3	ACGTCATGCAGAAGAGCACCACTA	ACTGCCCACCTAGTTGATGGCTAA	533
2.4	TGAGACCCGAAGTCAGATGGTGTT	CTGGAGCTGATAGCCAGTGCAATA	560
2.5	TTTCTCCTGCCCTTGATGATCCCA	TTAAGGCCCAGCCTAATGACCACA	567
3.1	ACCTCCACCACACATTTGGAGCTA	GCACAATGAACACCCACTTGCTGA	415
3.2	TTGCTGCCTCACATGGTTAGAGGA	AAGAAATACTGGACGTGTCCGCCA	214
3.3	AGAATGTGGGGAGTTTGGAGGCTCA	ACCTTGAGTCAGACGGTGGACTTT	527
4.1	TTCAAAGAACAGCGTTGGAGCCAC	ACCAACCCTGGTGATAAGCTCAGT	308

4.2	TATGCTTGCTGTCTCTGACGCTGA	TGCAGCATTTGGTTAATCCCTGGC	396
4.3	TCGTCTTGTTGGCCCGATTACTGA	CACTGGTTGATGCAGCATGTGGTT	264
4.4	TCCACTCACCCACTTGAAGCAGAA	CCAAGGCAGAGCCAGTGTTTGTTT	420
4.5	TGAAAGGGCAGACACAGAAGTGGA	ATCATCCCAGCAAGATGGACCCTT	355
6.1	TTATGCCAACGCCCTCACTAACCA	TACCGTGGACCTGCAATCACTGTT	393
6.2	AACCCATGCCCAGGAGATAACTGT	TGATGTGGTTAAATGCCAGCAGCC	444
6.3	AGACAGCTTGGAAGCGGATCTGAA	TTACATGCCTTGCCTCTGAGTGGA	397
6.4	GAGCTTTGTGCTGTCCAACTGCAA	TGTTACTATTGCCTCAGCCACCCT	240
6.5	TTTGAGAGGCCTCACTTGTGCCTA	TGAGGTGGCATTGGAGATATGCCT	272
6.6	TGCATTGGAGTGTTCCGTCCTACA	TATCGCACACAGGAACAGCACTCA	373
7.1	TCCTCATTGGGTTGAGGGATGTGT	TCTGAAGCAGTTGAGGACGTTGGA	274
7.2	ATAGGGAAAGCCCACCTGTTCCTT	ACCTGTGACTTCCTGCCTCAGTTT	475
7.3	GGGAATGAAAGTGGGCTGCAATGT	TAAAGTTCCCAGTGAGGCACCTGT	416
7.4	TTCCAGCCTGGTCTCCAAACAGAT	TCTGGAAACTGGGAAAGGGTTCCA	264
7.5	AGTCTGTCAACTCAAGCCTGGTCA	GCAGCTGCTTATGCTTAGCTGTGT	224
7.6	ATGCTGTACACAACATGTGCCTGC	AAACCTGGCATTCGGGACAATGTG	378
7.7	CACAAACTTGTGAGCACGGCATGA	AAAGATTCCCGGCAGCATCTCTGA	373
8.1	AGTTCCAGGTGAGCCCTTCAGAAA	ATGCTCTTCTGCCCACTCCCATAA	385
8.2	GGCTTAAACTGTCCATCTGCGCTT	AACCTCTGCAGGGAAGGTGAGAAA	433
9.1	AAGCTGCAGAGAGCTCAGAACAGT	AACCTGGATTGCATGACCCGTACT	514
9.2	AAACTGCCTCCCTGAAACATGCAC	ACTGGGCTTATTGAGAGGCACACA	386
9.3	AAGGCAGCTCTGTGAGGTGCTAAT	TCTGACCATCAGGGACAGGCAAAT	282
9.4	TTACACCTGGGACCTGCTGCATTA	AATGCATGGGTCATGTGGAAACCG	491
9.5	AGCCAGGAGATTGTGAGGGTCATT	ACTGCCAAGTCTATGCCTGTTCCT	271
10.1	AGCAGGATGGTGTGGTAAAGGACA	AAGGAGTCTGCAGTGAGCCAAGAT	275
10.2	AACAGGCAAGAGGGAATCGAAGGA	ACCCATCACAGCTAGGCTGAAACT	588
10.3	CAAGGGTGTTTCCTTTGTGCCCAT	AATCTGGTACACAGCAGGCGATCA	310

2.1.3.2 Long-range PCR

After reducing the possible extent of these deletions, the pair of primers closest to the deletion was used for PCR amplification. As the amplicons were probably greater than 2 Kb, the enzyme used was Expand™ Long Template PCR System (Roche). PCR amplification was performed with a mix of: 0.75 µL of Long polymerase, 5 µL of buffer 3, 1.75 µL of dNTP's (10mM), 6 µL of each primer (forward and reverse), 4 µL of DNA sample and 26.5 µL of ddH2O to make a final reaction volume of 50 µL. PCR amplification parameters are presented in table 2.5, and are different from those used for HotStar Master Mix enzyme for fragments under 2Kb.

Table 2.5: PCR protocol for the amplification of fragments larger than 2 Kb.

Cycles	Time	Temperature
1 x	2 min	94ºC
10 x	10 s	94ºC
	30 s	50ºC-60ºC
	20 min	68ºC
20 x	15 s	94ºC
	30 s	50ºC-60ºC
	20 min + 20 s	68ºC
1 x	7 min	68ºC

DNA fragments and the control blank were checked by electrophoretic separation in a 0.8% agarose gel in 1x TAE buffer and 0.5 µg/ml Ethidium Bromide. Two size markers were used to define the size of the fragment, the 1Kb DNA Extension Ladder (Invitrogen) and the GeneRuler 1kb DNA ladder (Fermentas). 50 µL of DNA samples with loading dye were applied in 200mL gels that run at 120 V.

2.1.3.3 Isolation and purification of DNA fragments from agarose gels

After electrophoretic separation, DNA fragments of interest were excised from the agarose gel on a Transilluminator and purified with the Illustra™ GFX™ PCR DNA and Gel Band Purification Kit (GE Healthcare) according to the manufacturer's instructions.

2.1.3.4 Sequencing

In order to determine the deletion breakpoints at the nucleotide level, isolated and purified fragments were sequenced. When samples were obtained directly from PCR amplification (and not from purified fragments removed from agarose gels), an additional step of purification before sequencing was required. To purify these products, 1 µL of PCR product was added to 0.5 µL of ExoSAP (USB Corporation). The mixture was exposed to a temperature of 37ºC for 15 minutes and then, at 85ºC for 15 minutes, resulting in a maximized enzyme activity followed by its inactivation.

Direct sequencing reactions of both strands were performed with BigDye Terminator v1.1 Cycle Sequencing Kit (Applied Biosystems) using 2 µL of BigDye, 0.5 µL of primer (forward or reverse), 1.5 µL of purified DNA fragment and 6 µL of ddH2O to a final reaction volume of 10 µL. Forward and reverse sequencing are separated reactions. The sequencing reaction parameters are shown in table 2.6.

Table 2.6: Sequencing Protocol.

Cycles	Time	Temperature
1x	5 min	95ºC
35x	10 s	96ºC
	5 s	50ºC
	4 min	60ºC

Sequencing products were purified with the DyeEx Spin Kit (Qiagen) according to the manufacturer's instructions and the fragment sequencing was done by capillary electrophoresis in an ABI-PRISM 3130 XL automatic sequencer (Applied Biosystems).

2.1.4   Approach 3: Single nucleotide polymorphism (SNP) analysis

2.1.4.1 SNP selection

Another approach to narrow the extension of the deletions (in homozygosity and heterozigosity) was the design of a SNP assay. SNP genotype data for parkin gene was obtained through the HapMap Genome Browser (release#24 - phase1&2 full dataset) (Frazer et al., 2007). This data was analyzed with Haploview v4.1 software (Barrett, 2009). 114 SNPs, localized in the introns of interest, were selected taking in account the higher MAF (minor allele frequency) of SNPs and the distance to the previous SNP selected (approximately 10Kb). For each intron several SNPs were selected as shown in table 2.7.

Table 2.7: List of selected SNPs.

Introns	SNPs	Introns	SNPs	Introns	SNPs
Intron 1	rs1893116 rs1893114 rs6934419 rs2846507 rs13206396 rs9365465 rs2846546 rs1893119 rs2846510 rs2803097 rs2803087 rs2023037	Intron 4	rs13191078 rs9295182 rs2156267 rs4412175 rs1893551 rs1954926 rs1954925 rs9347590 rs3892751 rs9347591 rs6455801 rs9365375 rs6904579 rs713054 rs9365377 rs9456748 rs2023078 rs4709579 rs9295184 rs12529283	Intron 7	rs3765474 rs910177 rs9458315 rs12210797 rs1024189 rs10945764 rs12210817 rs9355922 rs9346876 rs13220282 rs1018462 rs11755949 rs9365323 rs10945778
Intron 2	rs7744798 rs11964364 rs4235935 rs952388 rs4709595 rs7771045 rs4708953 rs9347623 rs6935149 rs10945815 rs12205305 rs962900 rs12192200 rs9364652			Intron 9	rs4574609 rs9365285 rs4708909 rs13211741 rs4709526 rs12154057 rs1886237 rs4709531 rs12175609 rs9458289
		Intron 6	rs3016551 rs7739802 rs6455775 rs6913813		

Intron 2	rs4709605	Intron 6	rs6922518	Intron 9	rs577876
	rs6937352		rs12528179		rs517010
	rs2205624		rs2155486		rs12209107
	rs9356016		rs6937081		rs506428
	rs6923741		rs9456721		rs12198566
Intron 3	rs10945803		rs9355368	Intron 10	rs6942109
	rs2023074		rs9355371		rs7766508
	rs4546464		rs9347562		rs6907632
	rs957374		rs9364627		rs9347502
	rs7766877		rs9458419		rs3890730
	rs6935521		rs7746164		
	rs2096982		rs1790022		
	rs1954939		rs1784597		
	rs9365393		rs1626020		
	rs9355994		rs1784588		

2.1.4.2 SNP genotyping

For genotyping we have used the SNaPshot assay (Applied Biosystems), which was applied for the genotyping of the SNPs located in introns 2, 3, 4 and 6. For the remaining introns, and since the number of samples to be tested was small, SNPs were genotyped by PCR amplification and sequencing (as described in 2.1.2.2 and 2.1.3.4).

SNaPshot is a technique specifically used for determining SNP variants and includes a multiplex PCR amplification of the regions containing the SNPs, a purification of the PCR products, a single-base extension (SBE) of the 3'end of unlabeled primers located immediately upstream of the SNPs site, using four fluorescently-labelled dideoxynucleotide triphosphates (ddNTPs) which will emit a specific fluorescence for each ddNTP (Bardien et al., 2009). Finally, the last step is a final purification before products are separated by capillary electrophoresis in an automatic sequencer that records the fluorescence emitted by the ddNTPs.

2.1.4.2.1 Amplification primers and SBE-primer design

Since multiple SNPs can be interrogated in a single SNaPshot reaction, the amplification primers were design for each intron using Primer3 Plus (Untergasser et al., 2007) and then, analyzed with AutoDimer software (Vallone and Butler, 2004) to search for primer-dimers interactions and self-interacting hairpins. The settings used for primer design were: an optimum primer length of 20 bases, an optimum melting temperature of 60ºC and an optimum G/C percentage of 50%. For AutoDimer software, the settings were: minimum score requirement of 6; temperature for dG calculation = 55ºC, Na^+ (Molar) = 0.085 and total strand concentration = 1. All primers with interactions predicted by this

software were excluded and new oligos were designed. Another control was done to the primers by the search in GenomeTester 1.3 (http://bioinfo.ut.ee/genometester/) for primer binding sites, being the settings for exclusion: more than 200 binding sites in the genome and/or more than one amplification product predicted.

SBE-primers were designed as described in literature (Sanchez et al., 2006). To allow a larger separation in fluorescence recording and therefore a better peak profile, primers were modified in order to create a sufficient difference in electrophoretic motility. So, the first primer was 36 bases long and the following primers were created with size intervals of four nucleotides longer. The lengths of the SBE- primers were increased at their 5´end with nucleotides of a "neutral" 40 bp-sequence and with a poly-cytosine tail when more nucleotides were needed. The lengths of the SBE primers were between 35 and 96 nucleotides. When the variants of two SNPs were different (e.g., SNP1: C/T and SNP2: A/G), SBE-primers were designed with the same length to narrow the SBE-primer range, since signal detection would not suffer interference. Amplification primer and SBE-primer sequences for each SNP are presented in appendix 6.1.

2.1.4.2.2   Multiplex PCR and SNaPshot

SNPs from the same intron were simultaneously amplified in a multiplex PCR. All the SNPs located in the four introns were amplified with the same reagents mix consisting of 5 µL of Multiplex PCR Master Mix (Qiagen), 1 µL of an optimized primer mix, 1 µL of DNA samples and 3 µL of ddH2O. Primer mixes consisted of forward and reverse primers of the SNPs which, after an initial trial at a concentration of 2 µM, were altered to the adequate concentrations for amplification. The PCR amplification protocol is presented in table 2.8.

Table 2.8: PCR Multiplex protocol.

Cycles	Time	Temperature
1x	15 min	95ºC
30x	30 s	94ºC
	1min 30s	55ºC
	1min 30s	72ºC
1x	10 min	72ºC

After amplification the PCR products were checked and a control blank was tested using a QIAxcel multicapillary electrophoresis system (Qiagen). Then, products were purified with ExoSAP as described previously.

For single base extension reactions, the mixes used for each assay consist of 1.5 µL of purified product, 1 µL of SNaPshot Multiplex Mix (Applied Biosystems) containing the fluorescent ddNTPs, 1

µL of SBE-primer mix (optimized as in primer mix) and 1.5 µL of ddH2O to a final reaction volume of 5 µL. The SNaPshot reaction was performed with the protocol presented in table 2.9.

Table 2.9: SNaPshot reaction protocol.

Cycles	Time	Temperature
	10 s	96ºC
25x	5 s	50ºC
	30 s	60ºC

After SBE a final product purification was performed with 1 µL of SAP (USB Corporation). In this purification protocol, the products with SAP were subjected to a 37ºC temperature for 1 hour and 30 minutes, followed by a 15 minutes step at 85ºC.

The reactions were then loaded to the ABI-PRISM 3130 XL genetic analyzer (Applied Biosystems) along with 0.15 µL of GeneScan 120 LIZ Size Standard (Applied Biosystems) and 8.85 µL of formamide. The capillary electrophoresis was performed according to the manufacturer's instructions for a SNaPshot assay.

Results are analyzed with the GeneMapper Software Version 4.0 allowing visualization of the peak profiles. One example is presented in figure 2.1. Given the small number of samples, each SNP's genotype was determined manually taking into account both the position (size) of the peak as well as the color of the emitted fluorescence (green for A, blue for G, black for C and red for T). In this work we searched for the SNP missing in the peak profile of the patients with homozygous mutations and in the patients with heterozygous mutations we analyze the presence/absence of heterozygosity of the genotyped SNPs.
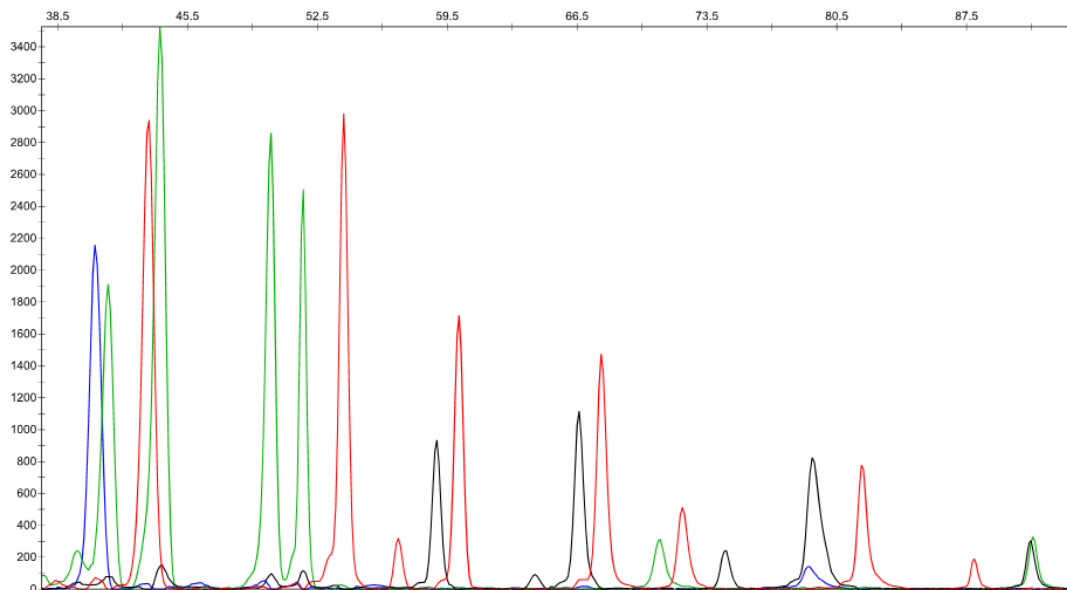
Figure 2.1: Peak profile of a sample from the intron 6 assay generated with GeneMapper Software.

2.1.4.3 PCR Long-range amplification and Sequencing

After SNaPshot analysis, for the deletions in homozygosity, the primers of the SNPs closest to the absent SNaPshot SNPs (forward or reverse according to the desired direction) were used for long range amplification. For the deletions detected in heterozygosity the primers of the first SNPs showing heterozygosity closest to the exon missing (forward or reverse according to the desired direction) were used for PCR amplification. Long range amplification using the Expand Long Template PCR System (Roche) referred above, with the same mix and protocol was used as the amplification product could yet have more than 2 Kb. All steps, from PCR amplification to sequencing were performed as described above in 2.1.3.2 to 2.1.3.4.

2.2 Characterization of point mutations and small scale rearrangements

To explore the pathogenic mechanisms of parkin mutations we selected seven common mutations found in Portuguese Parkinson's patients. These mutations, detailed in table 2.10, are mainly point mutations, resulting in amino acid changes. Also, two small rearrangements were selected, one base pair deletion and an insertion/deletion, both resulting in frameshifts and premature STOP codons. The selected mutations are spread throughout the gene with one mutation in almost every parkin domain (as we can see in fig. 2.2).

Table 2.10: *PARK2* mutations selected.

Region	cDNA	Protein
Exon 2	c.125G>C	p.R42P
Exon 2	c.del155delA	p.N52MfsX29
Exon 7	c.823C>T	p.R275W
Exon 9	c.1072_1073delCT c.1072insA	p.L358RfsX77
Exon 11	c.1204C>T	p.R402C
Exon 11	c.1244C>A	p.T415N
Exon 12	c.1289G>A	p.G430D
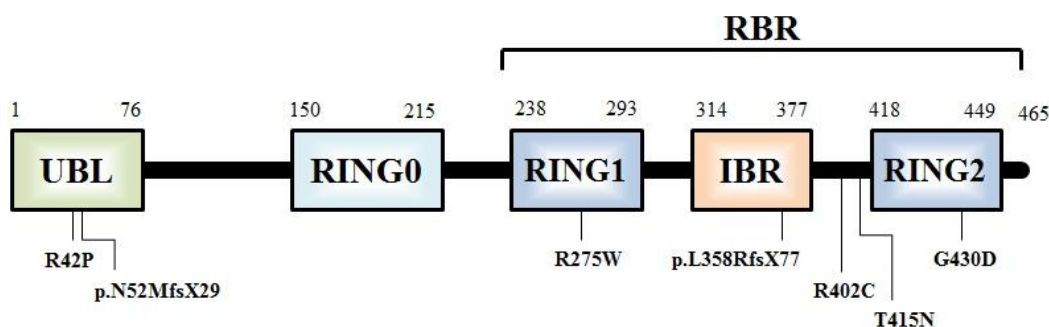
Figure 2.2: Schematic representation of parkin domains with chosen mutations indicated below.

2.2.1 Expression constructs

An N-terminal green fluorescent protein (GFP) tagged wild-type human parkin cDNA cloned in a pEGFP-C1 plasmid was kindly provided by Dr. Sumihiro Kawajiri from Juntendo University School of Medicine, Tokyo, Japan.

This construct was then inserted in DH5α *Escherichia coli* by thermal shock with the following procedure: 25 μL of Library Efficiency DH5α Competent Cells (Invitrogen) were thawed on ice, mixed gently with 1 μL of plasmid DNA (pDNA) and incubated for 30 minutes on ice. After a heat shock at 42°C for 45 seconds, cells were incubated on ice for 2 minutes; 500 μL of S.O.C. medium were added and, incubated for 1 hour at 37°C with shaking. This mix was centrifuged for 5 minutes, the supernatant was discarded and the pellet resuspended in the remaining medium. Then, bacteria were plated on Luria Bertani (LB) agar plates, containing kanamycin to select positive clones, and incubated at 37°C overnight.

To confirm if the construct was correctly inserted and without mutations, the cDNA construct was extracted from bacteria (as described below) and then, confirmed by sequencing with the primers presented in table 2.11. pDNA extracted was directly sequenced with a mix slightly different of that described in 2.1.3.4 but with the same protocol. The mix consists of 2 μL of BigDye Terminator v1.1 Cycle Sequencing Kit (Applied Biosystems), 0.5 μL of primer (forward or reverse), only 1 μL of purified DNA fragment and 6.5 μL of ddH2O.

Table 2.11: Primers designed for cDNA sequencing.

Primer	Sequence
PARK2_F1	CTGGATCAGCAGAGCATTGTTCAC
PARK2_F2	TCCAAACCGGATGAGTGGTGAATG
PARK2_F3	AGTATGGTGCAGAGGAGTGTGT
PARK2_R1	GTCGCCTCCAGTTGCATTCATTTC

2.2.2 DNA extraction

In order to extract pDNA, isolated colonies were grown in liquid LB medium with kanamycin overnight at 37°C with agitation. At this point, it was important to store glycerol stocks for each isolated colony for clone preservation. Liquid cultures were then centrifuged for 10 minutes at 3000 rpm, the supernatant was discarded and the DNA was extracted with the QIAprep Spin Miniprep Kit (QIAGEN) according to the manufacturer's instructions. DNA concentration was determined in a NanoDrop 2000 Spectrophotometer (Thermo Scientific).

2.2.3 Site-directed mutagenesis

For parkin mutant creation, the GFP-tagged wild-type parkin was modified with QuikChange Site-Directed Mutagenesis Kit (Stratagene) according to manufacturer´s instructions. This technique allows substitution, deletion or insertion of single or multiple amino acids in a protein sequence by using two oligonucleotide primers containing the desired mutation. Primer pairs, presented in table 2.12, were design according to the manufacturer's guidelines with QuikChange Primer Design Program (Agilent Technologies).

With site-directed mutagenesis, the oligonucleotide primers, complementary to opposite strands of the vector, were extended during temperature cycling by *Pfu* Turbo DNA polymerase. Then, the mutated plasmid containing staggered nicks was treated with *Dpn* I to digest the parental DNA of *E. coli* strains and to select for mutation-containing synthesized DNA (Weiner and Costa, 1994).

Table 2.12: Primers for site-directed mutagenesis.

Mutation	Forward Sequence	Reverse Sequence
R42P	CGGCTGACCAGTTGCCTGTGATTTTCGCAGG	CCTGCGAAAATCACAGGCAACTGGTCAGCCG
N52MfsX29	GGGAAGGAGCTGAGGATGACTGGACTGTGC	GCACAGTCCAGTCATCCTCAGCTCCTTCCC
R275W	CTGTGTGACAAGACTCAATGATTGGCAGTTTGTTCACG	CGTGAACAAACTGCCAATCATTGAGTCTTGTCACACAG
L358RfsX77	CGAAGGGGGCAATGGCAGGGCTGTGG	CCACAGCCCTGCCATTGCCCCCTTCG
R402C	CGCCGAGCAGGCTTGTTGGGAAGCAGC	GCTGCTTCCCAACAAGCCTGCTCGGCG
T415N	ACCATCAAGAAAACCAACAAGCCCTGTCCCCG	CGGGGACAGGGCTTGTTGGTTTTCTTGATGGT
G430D	CAGTGGAAAAAAATGGAGACTGCATGCACATGAAGTG	CACTTCATGTGCATGCAGTCTCCATTTTTTTCCACTG

After mutagenesis, the DNA vector containing the desired mutations was then transformed into XL1-Blue supercompetent cells following manufacturer´s instructions. The transformation is similar to the transformation of DH5α competent cells described above. Some of the isolated colonies of each mutant that grown on LB agar plates containing kanamycin were picked up, grown in LB liquid medium and after DNA extraction were sequenced for confirmation of the inserted mutation. The entire cDNA was sequenced in order to confirm the absence of additional mutations.

2.2.4   Cell cultures

For parkin mutants characterization, a SH-SY5Y human neuroblastoma cell line (DSMZ –Nr. ACC 209) was used as dopaminergic neurons cell model (Xie et al., 2010).

Cells were maintained in 1:1 DMEM (Dulbecco's Modified Eagle Medium) with Glutamax (Invitrogen) and Ham's F-12 Nutrient Mixture with Glutamax (Invitrogen), 10% of fetal bovine serum (FBS) (Invitrogen) and 1% Antibiotic-Antimycotic (Invitrogen) on 25 or 75 cm^2 tissue culture flasks. Cells were cultured in a humidified 5% CO_2 atmosphere at 37ºC.

Upon confluency, cells were trypsinised and passaged to new flasks until passage 4. Cells from all passages were frozen and stored in vials with DMSO. For transfection, cells were counted and plated at 500 000 cells/well on 12-well plates (used for Western blot, Real-time PCR and Immunocytochemistry), or 39 500 cells in 96-wells plates used for cell viability and proteasome activity assays. All conditions of every test were performed at least three times.

2.2.5   Transfections

SH-SY5Y cells in the adequate concentration were plated in wells 24h before transfection. An initial test using Lipofectamine 2000 (Invitrogen) and FuGENE HD (Roche) showed a better transfection efficiency with FuGENE. So, for transfection, 1.5 µg DNA of each construct (WT, the seven mutants and the vector alone) were mixed with 4.5 µL FuGENE and added to cells in medium without antibiotics according to the manufacturer's protocol. Transfection mixture and cells were incubated for at least 24 hours before proceeding for each specific experiment.

2.2.6 Real-Time quantitative reverse transcription PCR

RNA was extracted from wells at 24h, 48h and 72h after transfection with TRIzol Reagent (Life technologies). TRIzol maintains RNA integrity while disrupt cells and dissolve cells components (Chomczynski, 1993). After homogenization with TRIzol Reagent, chloroform was added and after centrifugation, the supernatant (with the RNA) was removed and precipitated with isopropanol. Precipitated RNA was washed with ethanol and resuspended in DEPC-treated ddH2O. RNA concentrations were determined in a NanoDrop 2000 Spectrophotometer (Thermo Scientific).

After RNA isolation, cDNA was synthesized by reverse transcription of 1 µg total RNA with Oligo(dT) using SuperScript III First-Strand Synthesis System for RT-PCR (Invitrogen) according to manufacturer's instructions. The primers for Real-Time PCR (table 2.13) were designed using Beacon designer (Premier Biosoft), taking into account that each pair of primers amplify through exon-exon junctions assuring that results do not reflect genomic DNA amplification.

Table 2.13: Primers used for real time quantification of *PARK2* and *ACTB* mRNA levels.

Gene	Primer	Sequence	Amplicon Size
PARK2	Fw	5'-CAGCCTCCAAAGAAACCATCAAG-3'	149
	Rv	5'-GTTCCACTCGCAGCCACAG-3'	
ACTB	Fw	5'-GCACTCTTCCAGCCTTCCTTC-3'	176
	Rv	5'-GTGATCTCCTTCTGCATCCTGTC-3'	

Quantitative Real-time PCR was performed to measure *PARK2* and *ACTB* mRNA levels in the transfected cells with 10 µL of iQ SYBR Green Supermix (Bio-Rad), 0.25 µL of primer forward and 0.25 µL of primer Reverse, 1 µL of cDNA at 0.1 µg/ µL (10-fold dilution of the cDNA synthesis reaction) and 8.5 µL of ddH2O to a 20 µL final reaction volume. PCR amplification (parameters shown in table 2.14) was performed in an iQ5 Real-Time PCR detection system (Bio-Rad). The amount of double-stranded PCR product synthesized in each cycle was measured by the SYBR Green I dye, being the fluorescence measured at the end of the annealing step of each cycle to monitor amplification. Real-time PCR amplification of each sample was performed in triplicate. The results were analyzed with the IQ5 Optical System Software (Bio-Rad) where the average threshold cycle of *PARK2* and *ACTB* were determined.

Table 2.14: Real-time PCR amplification parameters.

Cycles	Time	Temperature
1 x	3 min	95ºC
40 x	30 s	94ºC
	30 s	57ºC
	30 s	72ºC

2.2.7 Western blot analysis

For protein expression analysis, cells were collected on ice at 24h, 48h and 72h after transfection and lysed in RIPA buffer (Sigma) with protease inhibitors (complete, EDTA-free tablets, Roche). Samples were then sonicated and centrifuged at 12 000 rpm for 10 min at 4°C. Supernatant and pellet fraction were separated and only supernatants were used.

Protein concentration was determined using a colorimetric assay (DC Protein Assay, Bio-Rad) in microplates according to the manufacturer's instructions.

Lysates were resuspended in Laemmli loading buffer with β-mercaptoethanol (responsible for the reduction of disulfide bonds) and denatured at 95ºC for 5 minutes. Samples were loaded on a 10% sodium dodecyl sulfate-polyacrylamide gel electrophoresis (SDS-PAGE) gel (Bio-Rad), being the proteins separated according to their molecular weight, and then transferred to a polyvinylidene fluoride (PVDF) membrane (Millipore). After blotting, PVDF-membranes were blocked with 3% non-fat dry milk in PBS containing 1% Tween-20 (PBS-T) for 1 h with agitation. Membranes were probed with the primary antibody mouse monoclonal anti-GFP (Abcam and Rockland) or mouse monoclonal anti-parkin antibody (Cell Signaling) in blocking solution overnight with agitation at 4°C. As a loading control we have used β-actin and thus membranes were also incubated with monoclonal anti β-actin antibody (Sigma) for one hour with agitation at 4ºC. After washing with PBS-T, membranes were incubated with anti-mouse (Santa Cruz) secondary antibody. After three washes with PBS-T, the proteins were detected with FemtoMax Chemiluminescent Substrate Kit (Rockland) for western blotting.

2.2.8 Fluorescence microscopy assays

To detect aggregates, SH-SY5Y cells were grown on glass coverslips washed and coated with collagen (Stemcell) and transfected 24 hours after seeding with the wild-type parkin, the parkin mutants or the GFP tagged vector.

After 24h, 48h or 72h of expression, cells were fixed in 4% paraformaldehyde/sucrose in PBS for 20 minutes at room temperature. Nuclei were stained with 100 μL Hoechst 33258 (Invitrogen) at 1μg/μL and finally, cells were embedded in 5 μL Prolong Gold (Invitrogen) mounting medium and sealed with nail polish. Images were obtained on a Zeiss Axio Imager Z1 with a coupled device camera, using 20X or 100X (oil) objectives. Images were acquired in the AxioVision release 4.8. The presence and quantification of aggregates was analyzed using open source ImageJ in at least 20 cells per experiment in three different glass coverslips.

2.2.9   Proteasome inhibition

To assess the UPS in the presence of parkin overexpression, cells were incubated with 5µM MG132 (N-CBZ-Leu-Leu-Leu-Al) (Calbiochem), a proteasome inhibitor, diluted in dimethyl sulfoxide (DMSO). MG132 was added to the cells cultured in glass coverslips 24h after transfection. Cells were incubated 12h with the proteasome inhibitor before fixation, nuclei coloration, mounting and aggregate analysis were performed as described in 5.2.8. A control with cells incubated 12h with only DMSO was included in all tests in which MG132 was used.

2.2.10   Proteasome activity assay

To the measure of proteasome activity the Proteasome-Glo Chymotrypsin-Like, Trypsin-Like and Caspase-Like Cell-Based Assays (Promega) were used. These luminescent assays measure the three major proteolytic activities, described as chymotrypsin-like, trypsin-like and post-glutamyl peptide hydrolytic or caspase-like, which are contained in the 20S core. Each assay contains a specific luminogenic proteasome substrate in a buffer optimized for cell permeabilization, proteasome activity and luciferase activity. These fluorogenic substrates are Suc-LLVY-aminoluciferin (Succinyl-leucine-leucine-valine-tyrosine-aminoluciferin), Z-LRR-aminoluciferin (Z-leucine-arginine-arginine-aminoluciferin), and Z-nLPnLD-aminoluciferin (Z-norleucin-proline-norleucine-aspartate-aminoluciferin) for the chymotrypsin-like, trypsin-like and caspase-like activities. In this assay, proteasome cleavage of each substrate result in the generation of a luminescent signal produced by a luciferase reaction, that is proportional to the amount of proteasome activity in cells. This luminescence was read, 10 minutes after adding the substrate, in a Synergy 2 SL luminescence Microplate Reader (Biotek) at 175nm. These assays were performed in 96-well plates (one plate for assay) and in addition to the samples transfected with the different constructs, several controls were also included: transfected samples incubated for 12h (24h after transfection) with the proteasome inhibitor MG132, transfected samples incubated for the same time with DMSO, cells without transfection and wells with medium only. These assays were read 36h after transfection of all samples. All tests were done in duplicate in each plate, in a total of three plates for assay.

2.2.11 Viability assays

As for assessing proteasome activity, the measure of the cell viability in the presence of the different constructs was performed with a luminescent assay from Promega, the CellTiter-Glo Luminescent Cell Viability Assay. This assay allows the determination of the number of viable cells in culture by the quantification of the luminescent signal proportional to the amount of ATP present (indicating the presence of metabolically active cells). In this assay it is only needed the addition of a single reagent (CellTiter-Glo Reagent) directly to the cells in DMEM/FBS medium. The luminescence was also read, 10 minutes after adding the reagent, in a Synergy 2 SL luminescence Microplate Reader (Biotek) at 175 nm.

Two different tests were done, one to analyze cell viability in the presence of the different constructs at 24h, 48h or 72h after transfection. In this test only transfected samples and the controls (non-transfected cells and medium only) were tested. In a second assay were tested samples expressing the different constructs for 24h and after 12h with the proteasome inhibitor MG132, as well as, the controls: transfected samples incubated for the same time with DMSO, cells without transfection and wells with medium only. These assays were read 36h after transfection of all samples. All tests were done in duplicate in each plate, in a total of three plates for each assay.

2.2.12 Statistical analysis

All experiments were performed in triplicates (N=3) and in some tests duplicates or triplicates were performed for each experiment. Cell viability, proteasome activity, RNA expression and aggregate quantification data are expressed as mean ± standard error (SE). Comparison of MG132 effect on the studied mutants was done using one-way ANOVA with a Bonferroni post-hoc test for multiple comparisons. Number of cells with and without aggregates between wild type and mutant cells was compared by χ^2 test. Nonparametric tests were used when homogeneity of the variances was not observed. Differences were considered to be significant when $p<0.05$. Statistical analysis was performed using PASW Statistics 18.

3   Results

During this project we have developed an efficient strategy to narrow the intronic position of the large *PARK2* deletions frequently identified in patients with Parkinson disease. Also we have created and characterized cellular models overexpressing mutant parkin with seven different mutations found in patients with juvenile Parkinson disease. We have selected mutations located in different parkin domains in order to have a broader insight into the effect of the diverse mutations. We were able to demonstrate the existence of two different groups of GFP-positive cells showing high and low parkin expression. Our data show that the different studied mutations do not have an impact on cell viability, although resulted in differences in the number of cells showing parkin aggregates and in the number of aggregates present in each cell. We were also able to show that inhibition of proteasome activity by incubation with MG132 has an impact both in cell viability and in aggregate formation, resulting in decreased viability and increased aggregate formation in cells with inhibited proteasome function. Finally, during this thesis project we have created SH-SY5Y transgenic cell lines permanently expressing wild-type and mutant parkin that will allow further exploring the mechanisms involved in Parkinson disease pathogenesis.

3.1 Large *PARK2* deletion breakpoint determination

The mapping of the large deletions identified in Portuguese patients proved to be an extremely difficult task probably due to the large size of the introns in which the deletions under study are located. In fact, the first two approaches applied in the context of this project failed in the determination of the deletion breakpoints. In the first approach no amplification product was obtained probably meaning that the deletion breakpoints present in the Portuguese patients are different from the previously described.

In the second approach, some amplification fragments were obtained as expected, however, the breakpoint detection at the nucleotide level, by sequencing, was not achieved. A possible explanation for this is the reduced amount of amplification product isolated from the agarose gel to be afterwards used in the sequencing reaction. Also, additional optimization of the PCR reactions with these sets of primers was not possible due to the presence of several unspecific fragments.

In order to overcome these difficulties we proceeded to the SNP approach to narrow the region where the different deletions are located, allowing to reduce the size of the fragments to be amplified and sequenced.

After SNaPshot and sequencing analysis, the SNPs closest to the breakpoint sites (table 3.1) were determined. With this approach we were able to narrow the position for all the studied deletions. The forward primers of the SNPs upstream and the reverse primers of the SNPs downstream to the narrowed breakpoint were used for amplify the fragments. When none of the SNPs within introns in study were present (in patients with homozygous deletions) or when all of SNPs were in homozygosity (in patients with heterozygous deletions), it was necessary to use the primers of the closest exons.

Table 3.1: List of the SNPs/exons closest to the breakpoint of each patient.

Patient	Deletion	upstream SNP	downstream SNP
1	2	rs9365465	rs6935149
2	3	rs4235935	rs957374
3	3-6	rs962900	rs9347562
4	3-6	rs962900	rs9347562
5	3-6	E2	rs9355371
6	3-6	rs4235935	rs9364627
7	3-6	rs4235935	rs9364627
8	4	rs2023074	rs9456748
9	4	rs6935521	rs2023078
10	4	rs9355994	rs713054
11	4	rs9355994	rs713054
12	4-7	rs957374	rs13220282
13	5-6	E4	rs9458419
14	7-9	rs6937081	rs9458289
15	10	rs9365285	rs3890730

These primer pairs combinations were used for PCR amplification with the Expand^{TM} Long Template PCR System (Roche) and the obtained fragments are presented in figure 3.1.
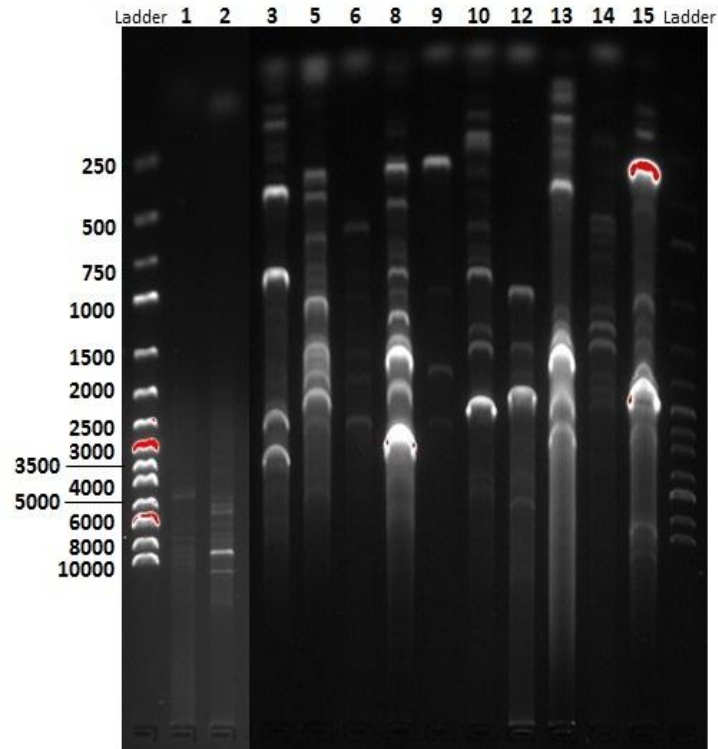
Figure 3.1: Image of an agarose gel showing the fragments amplified with the primer combinations presented in table 3.1. Note that in this experiment, patients 4, 7 and 11 were not tested since it is probable that these patients have the same deletion breakpoint as patients 3, 6 and 10.

Further optimization of the PCR conditions allowed the almost complete reduction of unspecific fragments in the samples of patients 3, 9, 13 and 15 as we can see in figure 3.2. These fragments will now be sequenced in order to confirm the presence of the deletion breakpoint. For the remaining deletions the changes introduced in the PCR conditions resulted in no amplification as can be seen by the presence of genomic DNA smear, and further optimization is required.
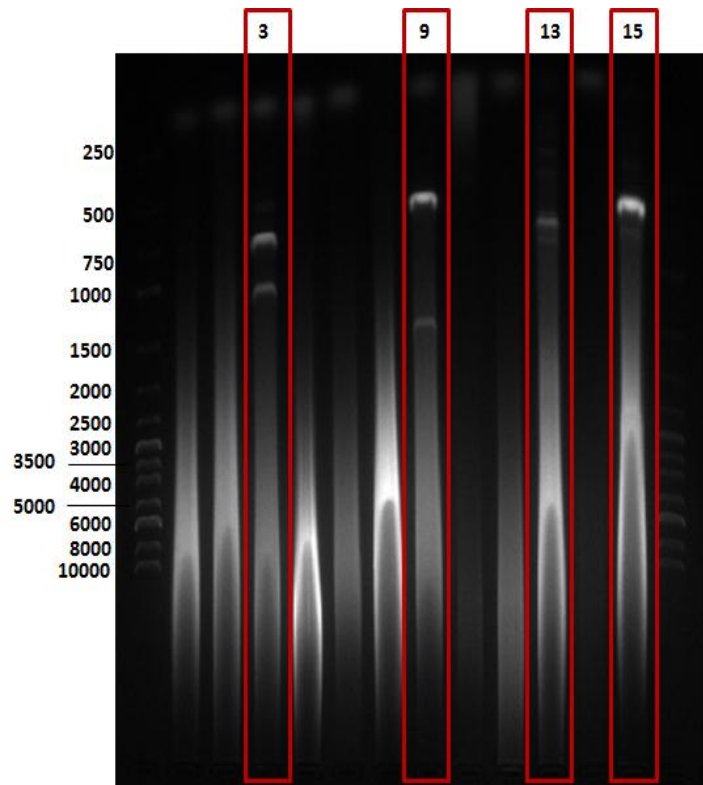
Figure 3.2: Image of the agarose gel after further optimization of fragments obtained for patients 3, 9, 13 and 15.

3.2 Functional characterization of *PARK2* point mutations and small rearrangements

In order to perform a full characterization of the obtained cell lines, parkin expression was assessed at the protein level through florescence microscopy and western-blot, and at the RNA level through real-time PCR. The impact of wild-type and mutant parkin expression on cell survival was also assessed as well as aggregate formation characterization. Proteasome activity in the presence of wild-type and mutant parkin was also assessed.

3.2.1   Parkin expression in SH-SY5Y cells

Neuroblastoma cells have proved to be a difficult cell line to transfect, nonetheless, we have optimized the transfection protocol up to an estimated transfection efficiency of 50%.
Analysis of transfected cells under an optic fluorescent microscope allowed us to observe in our GPF positive cells two different cell populations: cells with low GFP expression and cells with high GFP

expression (e.g. figure 3.3 and figure 3.4), in which the high expression population is estimatted to account for 10% of the GFP positive cells.
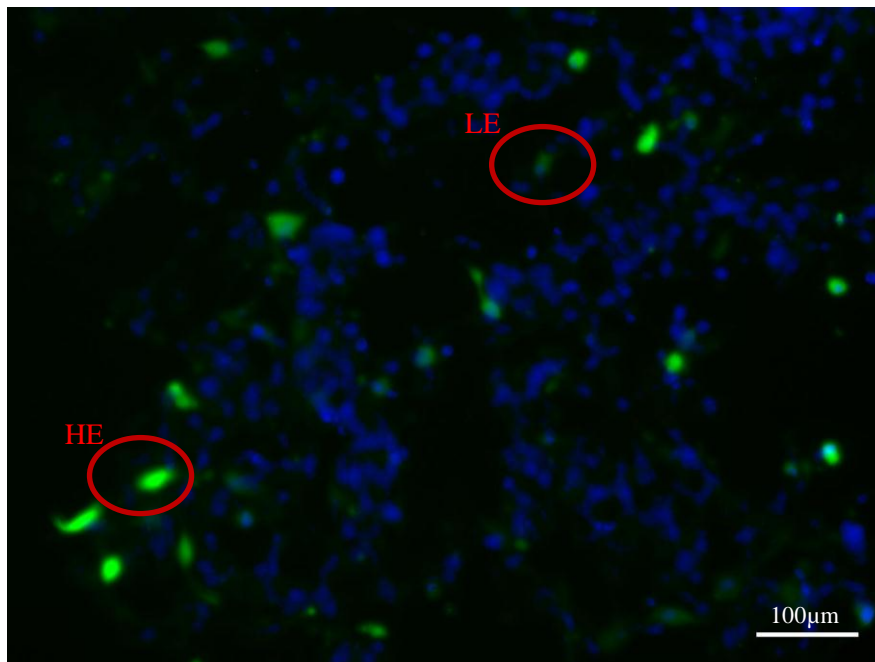
Figure 3.3: Representative image obtained with a 20X objective on a Zeiss Axio Imager Z1 of the pEGFP wild-type protein 48h after transfection. Note that we can see two different GFP positive cell population: high (HE) or low (LE) GFP expression.
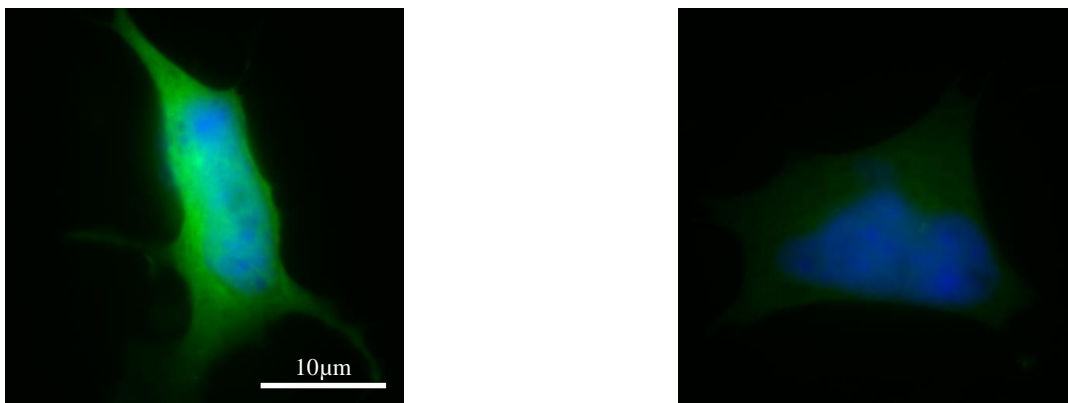
Figure 3.4: Images obtained with a 100X oil objective on a Zeiss Axio Imager Z1 of the WT parkin at 72h after transfection. It is notable the difference in GFP expression between this two cells.

Quantitative analysis of GFP-parkin protein levels, by western-blot, in SH-SY5Y cells has been also a challenging task. Western blot was performed with two different anti-GFP antibodies but

despite the many attempts, and the easy detection of the housekeeping gene β-actin (*ACTB*), GFP-parkin could not be observed.

Recently we have performed an additional attempt using an anti-parkin antibody and were able to detect parkin by this method. However, the epitope of this monoclonal antibody is located in the carboxy terminus of the protein, thus not allowing the detection of the mutants resulting from frameshift mutations where this part of the protein is not present due to a premature STOP codon (figure 3.5).
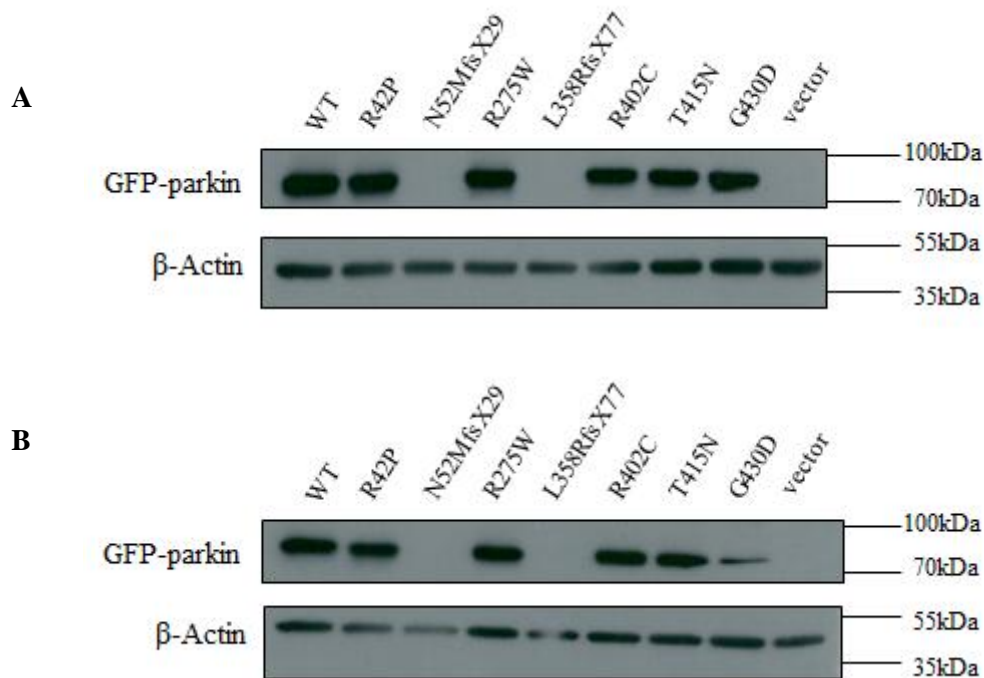
Figure 3.5: Immunoblotting of the soluble fraction of SH-SY5Y cells extracted 48h (A) and 72h (B) after transfection, probed with antibodies against parkin and β-actin. Both GFP-parkin fusion protein (with approximately 79 kDa) and β-actin (with approximately 42 kDa) are at the correct weight. The proteins resulting from the expression of the constructs harboring the frameshift mutations, N52MfsX29 and L358RfsX77 were not detected by the anti-parkin antibody.

The expression levels from wild-type and the different parkin mutants still need to be quantified in order to assess possible differences in the amount of soluble protein. Also, a new anti-EGFP antibody will be used in order to observe and quantify the protein levels for all mutants.

Quantitative analysis of parkin expression in our model system was performed, and *PARK2* mRNA expression was normalized towards *ACTB* levels. Total mRNA was extracted at 24h, 48h and 72h after transfection, cDNA was synthesized and real-time PCR was optimized to 100% efficiency. The mRNA expression results of three independent experiments are represented in figure 3.6, showing that relative expression of normal and all mutant parkin do not significantly differ at each time point.

Thus, we can infer that transfection efficiency of the different construct does not present significant variation allowing us to proceed with mutants' characterization and comparison.
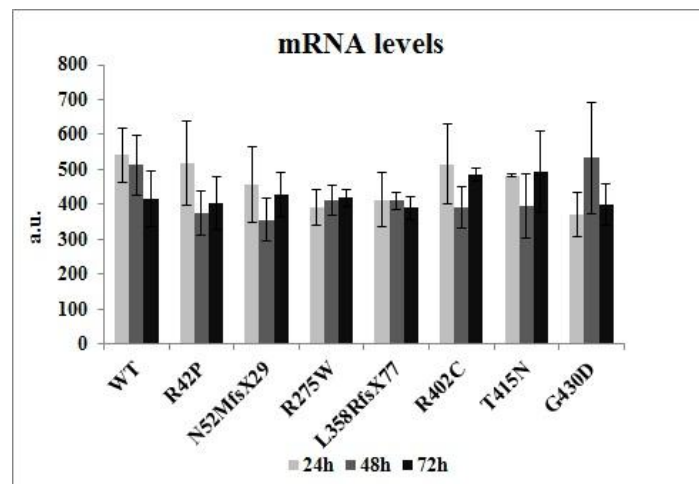
Figure 3.6: Quantitative analysis of parkin mRNA levels at 24h, 48h and 72h after transfection. Data is expressed as arbitrary units (a.u.) ± SE. Note that the empty vector is not represented in this chart due to its low level, coming up with more than 15 CTs of difference from *PARK2*.

3.2.2 Wild-type and mutant parkin aggregate formation

Mutant protein aggregation is a common hallmark in several neurodegenerative disorders. Parkin aggregate formation was characterized by analyzing the images obtained by fluorescence microscopy of the coverslips. All images were analyzed with ImageJ for aggregate quantification. Representative images of parkin are displayed in figure 3.7, randomly selected from each condition at a given time point.

	24h	48h	72h

WT

R42P

N52MfsX29

R275W

L358RfsX77

10μm
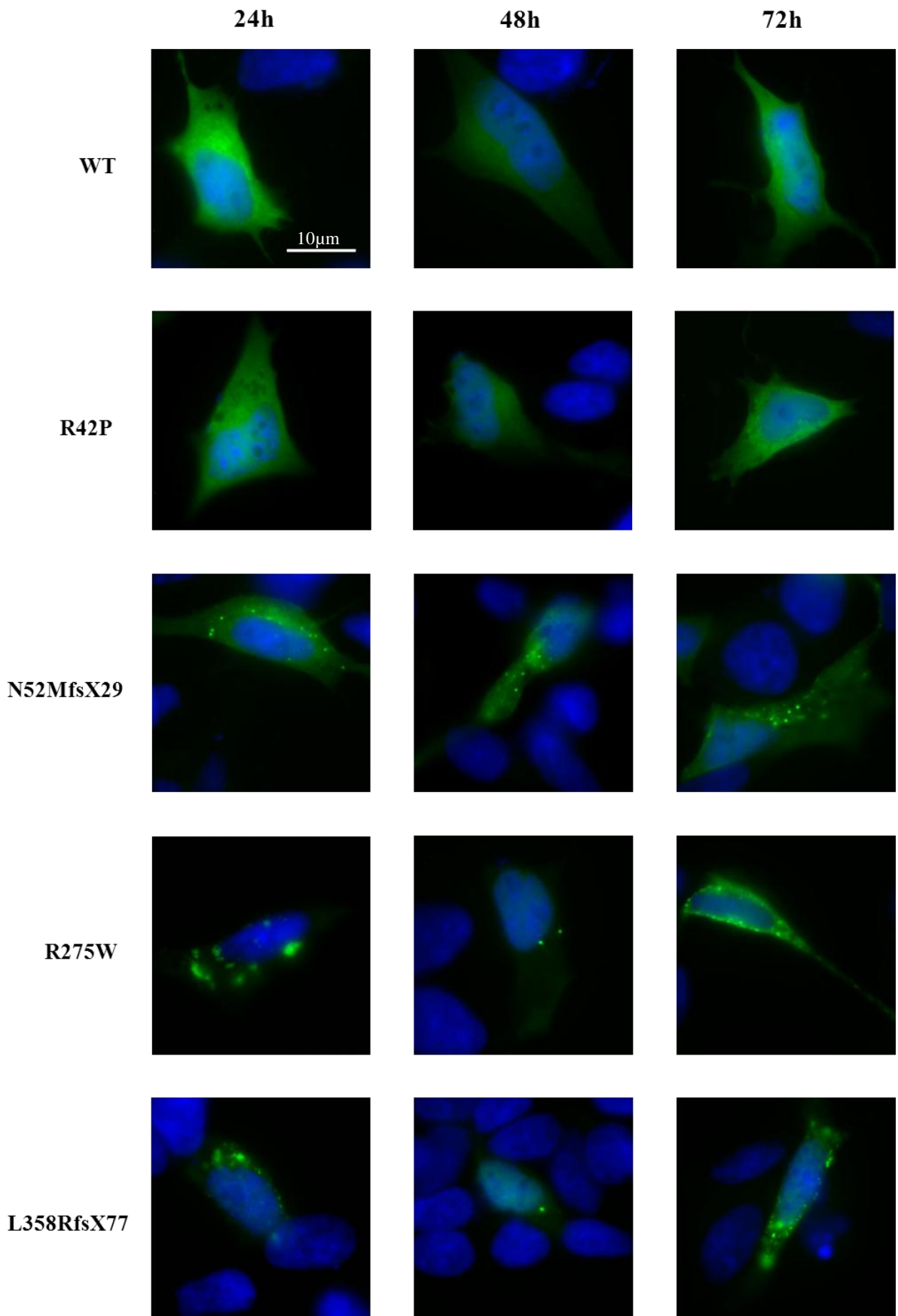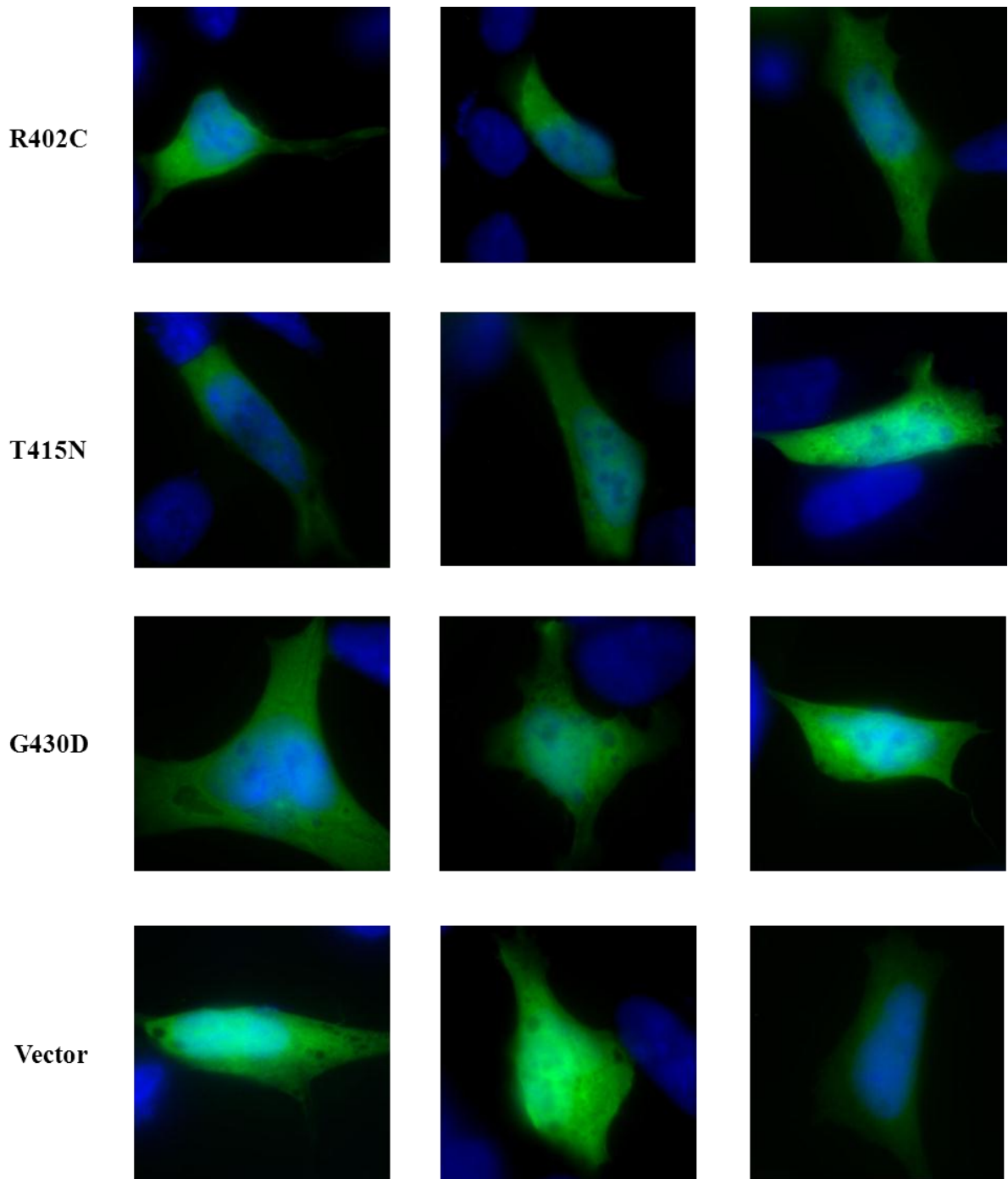
Figure 3.7: Representative images of wild-type and mutant GFP-parkin aggregation in SH-SY5Y cells at 24h, 48h and 72 hours after transfection. Aggregate formation was mostly noticed in the frameshift parkin mutants (N52MfsX29 and L358RfsX77) and in the R275W mutant. The cells' nucleus were counterstained with Hoescht (blue). These images were obtained with 100X oil objectives on a Zeiss Axio Imager Z1. Note that we can see two different aggregate types: small dot-like inclusions (e.g. image N52MfsX29/24h) and larger massive aggregates (e.g. image R275W/24h).

The number of transfected cells with or without aggregates was quantified for two separate experiments and for the three different time points (24h, 48h and 72h). At least 20 cells were analyzed for each condition in each separate experiment and the relative number of cells with or without aggregates is shown (fig. 3.8). Results indicate a significant difference in the number of cells with aggregates at 24h transfection for the N52MfsX29 ($P < 0.001$), R275W ($P = 0.003$) and L358RfsX77 ($P < 0.001$) mutants; at 48h for the R42P ($P = 0.003$), N52MfsX29 ($P < 0.001$), R275W ($P = 0.001$), L358RfsX77 ($P < 0.001$) and G430D ($P = 0.048$) mutants; and at 72h for only the frameshift mutants N52MfsX29 ($P < 0.001$) and L358RfsX77 ($P = 0.003$).
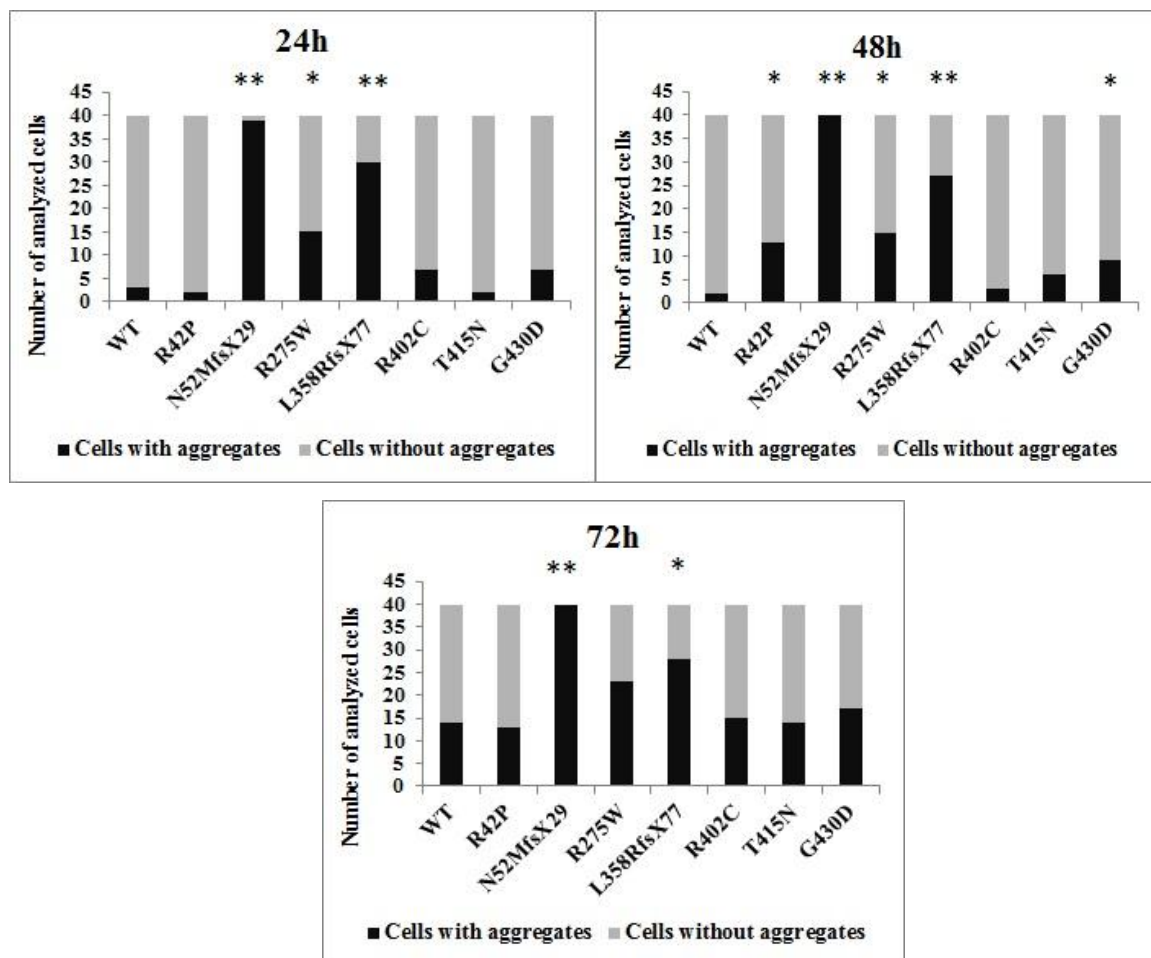
Figure 3.8: Quantitative analysis of aggregate formation of wild-type and mutant parkin at 24h, 48h and 72h after transfection. These results correspond to the analysis of 20 cells per condition in each independent experiment. P-values are as follows: * $P < 0.05$ and ** $P < 0.001$.

Regarding the average number of aggregates per cell with parkin aggregates at 24h, 48h and 72h after transfection (represented in figure 3.9), statistical analysis indicates that the distribution of aggregate number at the three transfection time points is different when comparing wild-type with

mutant parkin. Once again, the observed differences are probably caused by an increase in the mean number of aggregate in cells expressing N52MfsX29, R275W and L358RfsX77 mutants.
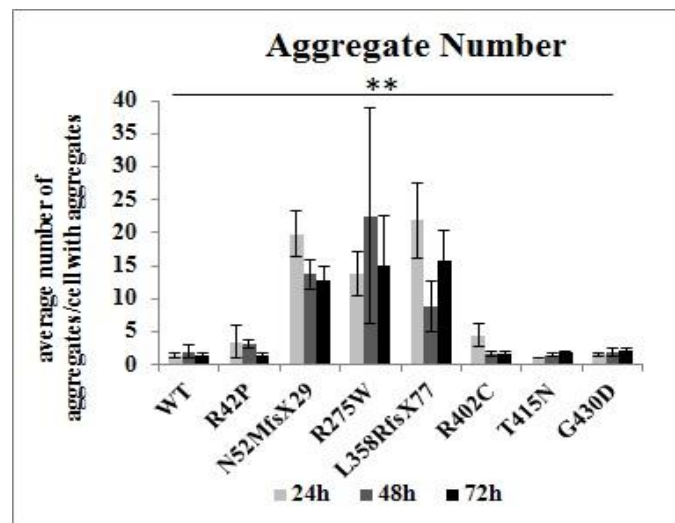
Figure 3.9: Mean number of aggregates per cell with parkin aggregates. Results are presented as mean ± SE. These results correspond to the analysis of 20 cells per condition in each independent experiment. P-value is ** $P < 0.001$.

We still need to determine the influence of the different expression levels in aggregate formation since apparently, cells with higher expression present more aggregates than cells with lower expression (figure 3.10).
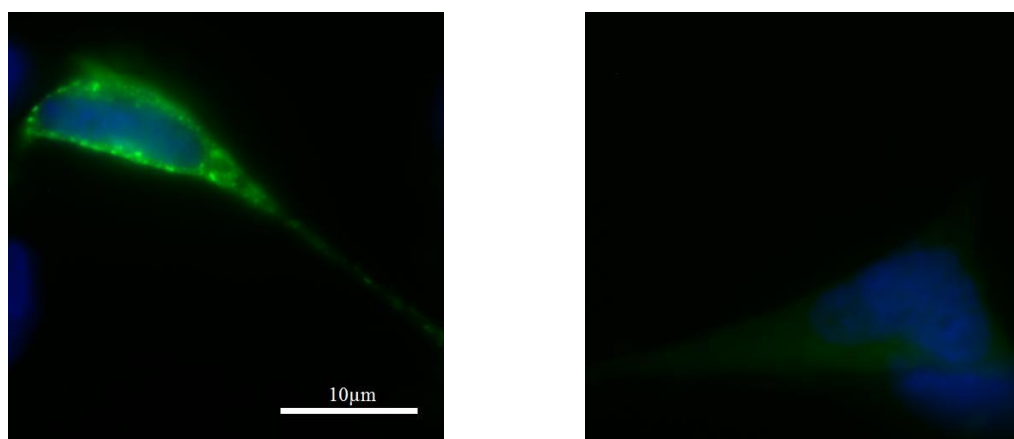
Figure 3.10: Images obtained with a 100X oil objective on a Zeiss Axio Imager Z1 of the R275W mutant at 72h after transfection. It is remarkable the difference in aggregate formation between this two cell populations.

3.2.3 Cell survival in wild-type and mutant parkin cell lines

In order to assess cell viability in the presence of wild-type and mutant parkin over-expression, we have used the CellTiter-Glo kit that correlates total ATP with the amount of viable cells. In figure 3.11 we present the results of three independent experiments regarding cell survival at 24h, 48h and 72h after tranfection. Our results show that the different parkin mutants do not have a significant impact on cell viability at each time point.
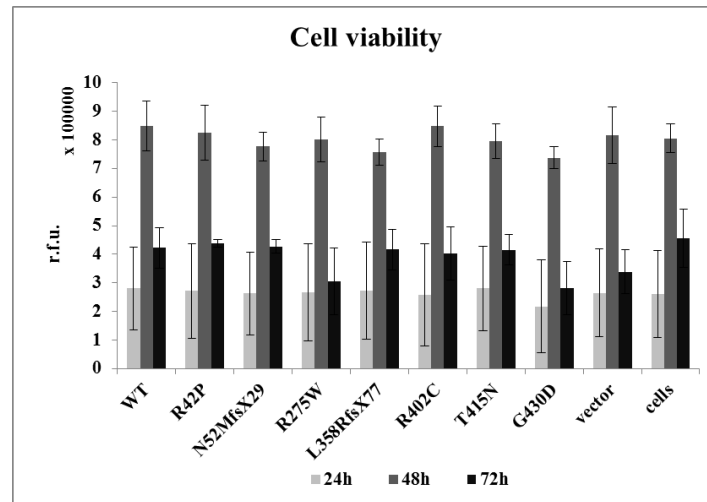
Figure 3.11: Levels of cell viability at the three transfection time points in cells transfected with wild-type and the different parkin mutants, as well as, with the empty vector. Results are expressed in relative fluorescence units (r.f.u.) and correspond to the analysis of 3 independent experiments. A control for cells without transfection was also included in the assay.

3.2.4 Ubiquitin proteasome system and parkin aggregate formation

In order to assess the role of the UPS in parkin aggregation we induced UPS impairment by treating with MG132, a proteasome inhibitor, to the cell culture medium 24h after cell transfection. The cells, growing in coverslips, were incubated for 12h with this inhibitor at 5μM before fixation and preparation for fluorescence microscopy analysis (figure 3.12).
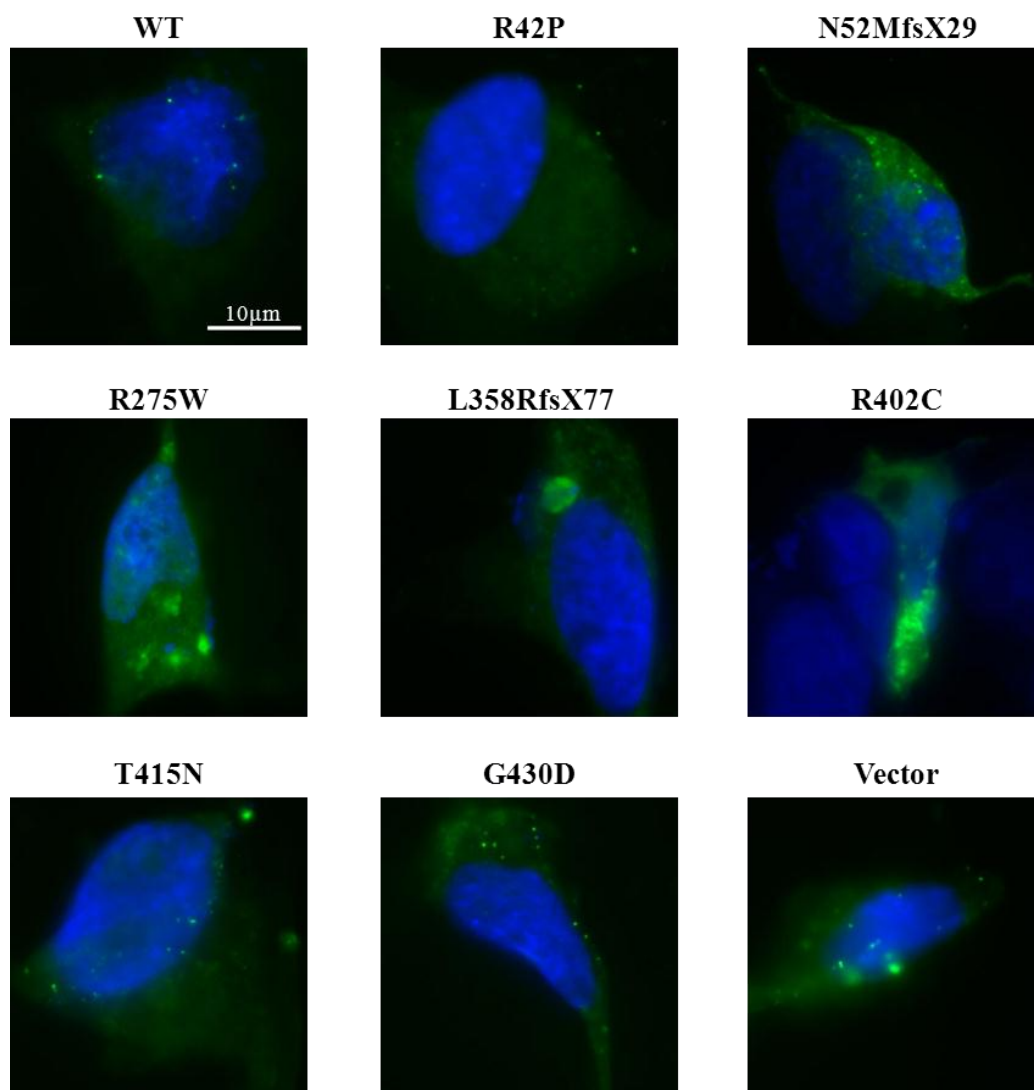
Figure 3.12: Representative images of wild-type and mutant GFP-parkin aggregation in SH-SY5Y cells after UPS inhibition. Aggregate formation was identified in all transfected cells after 12h incubation with 5μM of MG132. These images were obtained with 100X oil objectives on a Zeiss Axio Imager Z1. Note that we can see two different aggregate types: small dot-like inclusions (e.g. image G430D) and larger massive aggregates (e.g. image R275W).

The number of transfected cells with or without aggregates was quantified for one experiment after proteasome inhibition. The number of cells with aggregates (figure 3.13) are presented, as well as the mean number of aggregates per cells with aggregates (figure 3.14). No statistically significant results were found in aggregate formation between wild-type and parkin mutants. Analysis of the mean number of aggregates per cell indicates that the distribution of aggregate number is different between wild-type and parkin mutants, probably due to the impact of two particular mutants, N52MfsX29 and R275W.
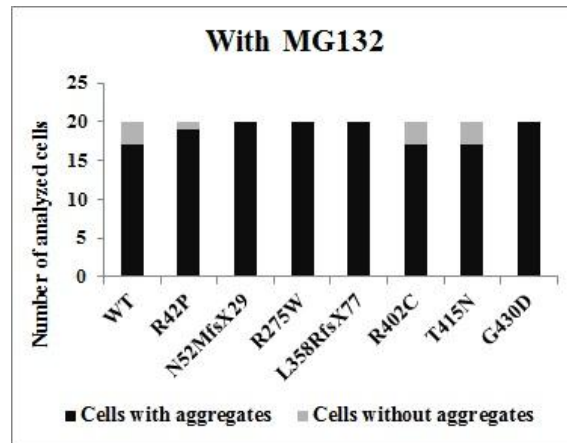
Figure 3.13: Quantitative analysis of aggregate formation of wild-type and mutant parkin after 12 hours of proteasome inhibition with 5µM of MG132. These results correspond to the analysis of 20 cells per condition in one experiment.
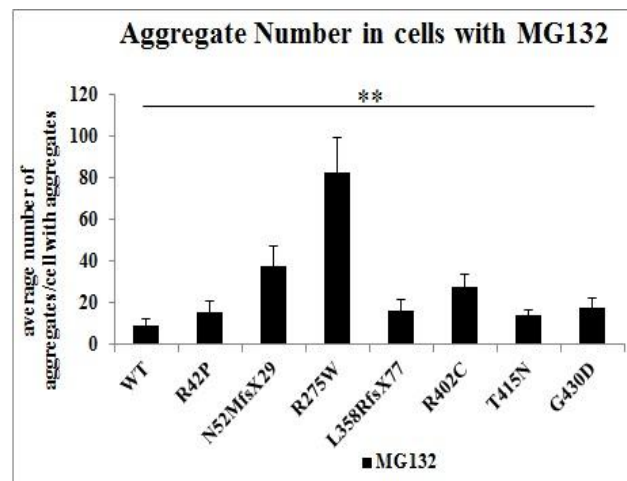
Figure 3.14: Mean number of aggregates per cell with parkin aggregates parkin after 12 hours of proteasome inhibition with 5µM of MG132. Results are presented as mean ± SE. These results correspond to the analysis of 20 cells per condition in one experiment. P-value is ** $P < 0.001$.

3.2.5   Proteasome activity under parkin overexpression

In order to characterize the effect of the studied mutations in the proteasome degradation capacity, all three proteasome activities (caspase-like, trypsin-like and chymotrypsin-like) were measured. However, our results show that none of the mutants has a direct impact in any of the proteasome activities (figure 3.15). Nevertheless, proteasome inhibition with 5µM of MG132 for 12h resulted in a significant decrease in all proteasome activities.
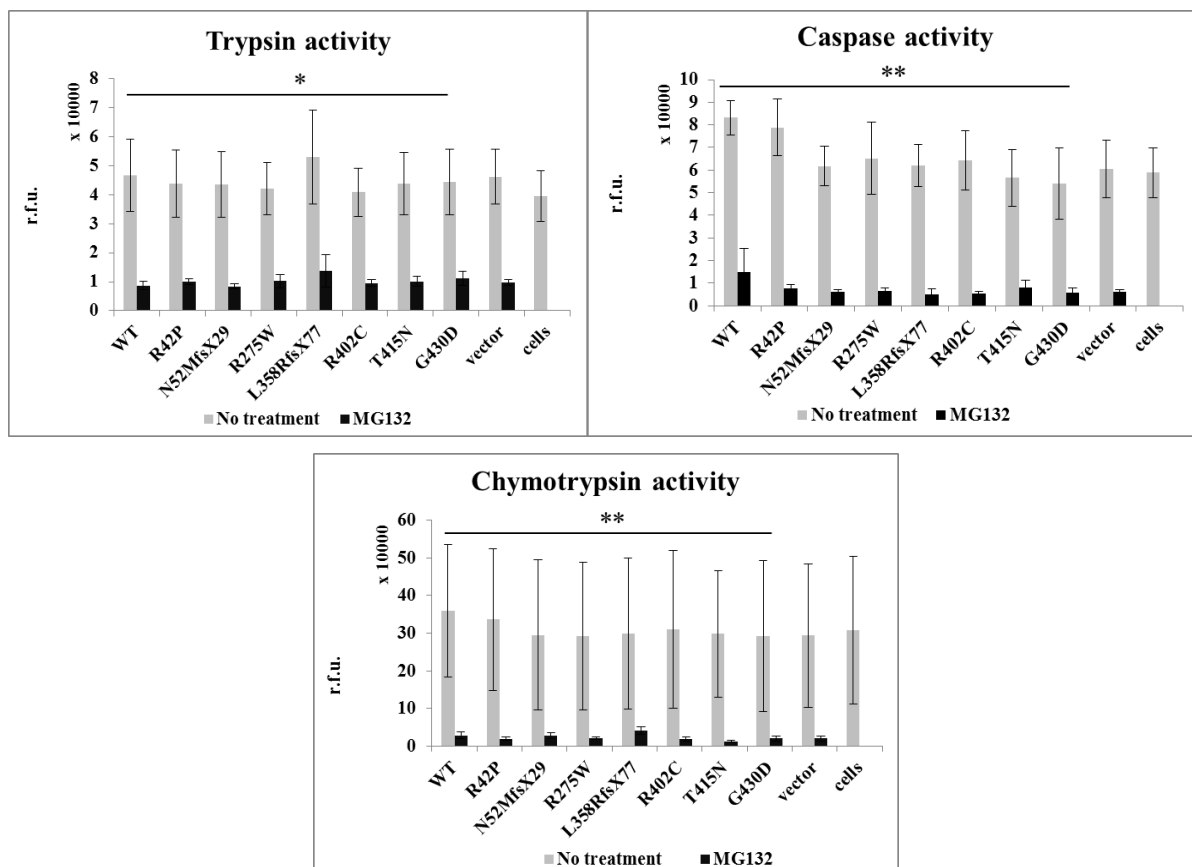
Figure 3.15: Proteasome activity quantification. Representation of all proteasome activities: caspase, trypsin, chymotrypsin in cells transfected with wild-type, parkin mutants or GFP empty vector in the presence or absence of 5μM MG132 (12h incubation). Results are expressed in relative fluorescence units (r.f.u.), and correspond to the analysis of three independent experiments for each proteasomal activity. Note that a control comprising untransfected cells was also used. * $P < 0.05$ and ** $P < 0.001$.

3.2.6 Impact of proteasome inhibition on cell viability

Cell viability of each mutant was also evaluated after proteasome inhibition through a 12h incubation with MG132 (figure 3.16). In line with what we have seen before regarding the mutant behavior versus wild-type parkin, proteasome inhibition did not affect the mutant viability when compared to normal parkin. However, very significant results were obtained regarding proteasome inhibition in general, with a decrease in cell viability after 12h incubation with 5μM of MG132.
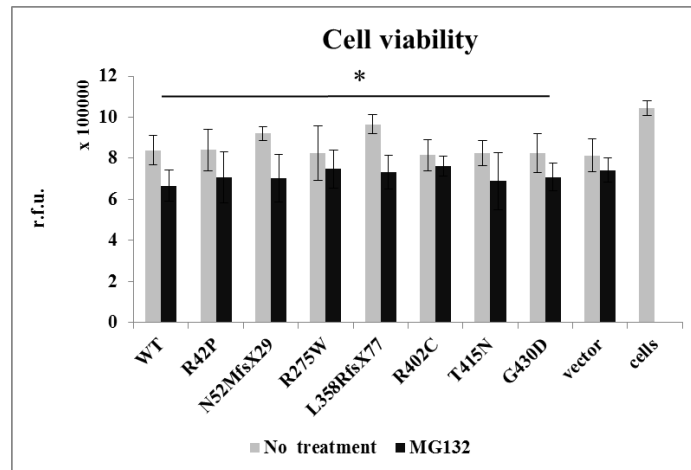
Figure 3.16: Representation of cell viability in cells transfected with wild-type, parkin mutants or empty GFP vector, with and without 12h incubation with MG132 (5µM). Results are expressed in relative fluorescence units (r.f.u.), corresponding to the analysis of three independent experiments. Note that a control comprising untransfected cells was also used.

4 Discussion

Parkinson disease is the second most common progressive neurodegenerative disorder that affects almost 2% of population above 65 years old. Aging and increased lifespan transformed neurodegenerative diseases in an ever-growing social and economic burden for society (Nuytemans et al., 2010). Mutations in the parkin encoding gene are the main cause of monogenic forms of recessive PD (Wang et al., 2005) with a 50% frequency in familial patients (Nuytemans et al., 2009). The study of these mutations is therefore of the most importance for understanding the pathogenesis of this disease.

4.1 *PARK2* deletion breakpoint determination

Gross deletions account for 50 to 60% of causative germline mutations found in *PARK2* (Mitsui et al., 2010). The high frequency of this type of mutation may be explained, in part, by the extremely large introns present in this gene (with intron 1, 2, 6 and 7 representing > 180Kb in size) (Hedrich et al., 2004) spanning a total of 1.4Mb (Mitsui et al., 2010). Another possible explanation is the genomic context of *PARK2*. This gene is located within the third largest observed human fragile site, FRA6E, which spans for approximately 3.6Mb and contains eight different genes (Clarimon et al., 2005). Common fragile sites, like FRA6E, are chromosomal regions sensitive to certain forms of replication stress that replicate late during the S phase. These regions are susceptible to form gaps, breaks and rearrangements in tumors and in cells exposed to particular culture conditions, like when exposed to a DNA replication inhibitor. Interestingly, the majority of deletions and duplications documented in *PARK2* are located between exons 3 and 8, which comprise the FRA6E center, of which the most unstable regions are exons 3 and 4 representing deletion hotspots (Clarimon et al., 2005; Mitsui et al., 2010). This high frequency of repetitive elements and instability allows for repeated and independent deletion events to occur, especially in the large *PARK2* introns where this propensity is higher (Hedrich et al., 2004).

Due to the giant introns of the *PARK2* gene, the determination of the exact breakpoint sites for the different deletions proved to be an extremely laborious and hard task, mainly when we applied conventional methods, such as PCR-based genome walking. After this attempt, we used a SNP approach, a powerful technique for identifying genome rearrangements, deletions and duplications (Bayrakli et al., 2007) that allowed us to narrow the extension of the deletions. However, it was not yet possible to determine the precise positions of breakpoints, as it is still necessary to analyze the junction-sequences in detail to explore its causative mechanism. It remains unclear if the same exon deletion is a consequence of a similar rearrangement or if these are the result of different mechanisms, produced by independent events. The current hypothesis is that rearrangements are independent and

recurrent events (Periquet et al., 2001). This theory is supported by the results that rearrangements reoccurring in the same breakpoint are less frequent that non-reocurring rearrangements (Mitsui et al., 2010). To date, only a small number of breakpoints in *PARK2* have been determined. The largest study of these breakpoints used a custom-designed high-density array for comparative genomic hybridization (array CGH) system (Mitsui et al., 2010), a successful, although expensive method.

To identify the mechanisms that originate breakpoints, we will first need to analyze the sequences flanking the breakpoints to search for junction-sequence signatures such as the presence of microhomologies. There are various mechanisms of genomic rearrangements, to which microhomology regions often contribute to, and therefore we can expect to find them at the identified junctions, such as happens for non-homologous end joining (NHEJ). The NHEJ is the major pathway for repairing double-strand breaks in chromosomal DNA, which has the potential to fuse any double-strand break end, without the requirement of an extended homology (Asakawa et al., 2009; Mitsui et al., 2010). The NHEJ is thus a highly flexible process that results in diverse breakpoint junctions, either showing short microhomologies (generally 1-4 bp) or inserted sequences without homology. It was also shown that the formation of key components of the NHEJ pathway occurs during replication stress conditions (Mitsui et al., 2010). This reparation mechanism has already been involved in parkin deletions in a previous study (Asakawa et al., 2009). Another mechanism, possibly implicated in *PARK2* deletion formation, is the association of breakpoints with interspersed repetitive sequences, such as *Alu* elements, which are transposable sequences involved in recombination events (Periquet et al., 2001). These elements are commonly associated with breakpoints, and are reported to originate genomic deletions by promoting recombinational instability (de Smith et al., 2008). Transposable elements are abundant in the genome, although *Alu* element density in the first 130 Kb of intron 2 of parkin gene is of 1 *Alu* per 2.5 Kb. This could help explain the high frequency of deletions of exons 2 and 3 (Periquet et al., 2001).

4.2 Functional characterization of *PARK2* point mutations and small rearrangements

4.2.1 Parkin aggregate formation and cell viability in SH-SY5Y cells

Different types of mutations spreading throughout the entire *PARK2* gene have been found. This large spectrum of parkin mutations, differ in their predicted consequences on the function of the protein, depending on the type of sequence variation found within the gene. Also, it is thought that the different location of the mutations within the gene result in different phenotypes. In 2003, a study showed that mutations in functional domains resulted in onset of the disease approximately 9 years earlier than mutations in domains not known to be essential for parkin function (Lohmann et al., 2003).

In this project and in order to further characterize the pathophysiological mechanisms leading to parkin dysfunction, we have selected seven mutations, missense and frameshift mutations (caused by a small deletion or by a novel indel mutation) found in Portuguese patients that are scattered along the protein, covering almost all parkin domains.

The identification of parkin's role in the ubiquitin proteasome system as an E3 ubiquitin ligase suggests that proteasome dysfunction is central to neuronal loss in AR-JP. Also, there are evidences linking UPS dysfunction with neurodegenerative diseases, including PD (Ciechanover and Brundin, 2003). Many neurodegenerative diseases, also called proteinopathies, are characterized by the presence of intra or extracellular inclusions resulting from conformational changes of specific proteins (aggregation-prone proteins) that acquire an misfolded conformation (with an increase in β sheet conformation that tend to self-aggregate), accumulate and aggregate into insoluble fibrils (Vekrellis and Stefanis, 2006). Several links between protein aggregation and UPS have already been found, and it has been shown that one can influence the other. Some studies support that protein aggregation can lead to UPS dysfunction (Vekrellis and Stefanis, 2006) and others that UPS impairment leads to further protein aggregation and inclusion formation in neuronal cells (Ardley et al., 2003; Rideout and Stefanis, 2002). It is also known that in the apoptosis process, resulting in neuronal death, UPS function is compromised, probably due to caspase cleavage of proteasomal subunits (Canu et al., 2000). A reciprocal complicated relationship between UPS dysfunction, protein aggregation and neuronal death exists, as UPS dysfunction leads to neuronal death (Lang-Rollin and Stefanis, 2006) and protein aggregation also has this same ability by other UPS dysfunction independent mechanisms (Lansbury and Lashuel, 2006).

However, and despite the importance of parkin in this system, few studies exist concerning the effects of mutant parkin in UPS function and neuronal death.

In this thesis context we aimed at exploring aggregate formation mediated by a wide range of parkin mutations and explored the mutations effects in parkin clearance by the 26S proteasome and the effect of UPS impairment in aggregate accumulation. In order to accomplish this we used an N-terminal GFP-tag to visualize wild-type and mutant protein in cells, allowing us to monitor the protein aggregation process without the need for immunostaining (Shen et al., 2011) in an dopaminergic neuronal-like cell line, SH-SY5Y.

It is known that parkin is prone to misfolding. In 2003, a study by Winklhofer and colleagues showed that in physiological conditions parkin was found almost exclusively in the detergent-soluble fraction, and that the majority of wild-type parkin is converted into a detergent-insoluble conformation upon oxidative or thermal stress (although not aggregating in general). Nigral dopaminergic neurons are particularly exposed to oxidative-stress since the metabolism of dopamine produces various reactive oxygen and nitrogen species (Winklhofer et al., 2003). Interestingly, parkin seems to be uniquely sensitive to dopamine-induced inactivation when compared with other RBR proteins (Wong et al., 2007).

Our results show that wild-type parkin is homogenously expressed in the cytoplasm of SH-SY5Y cells and that occasional parkin aggregates are found, as previously described (Cookson et al., 2003; Henn et al., 2005; Sriram et al., 2005).

Regarding the mutants we studied, the R42P mutation shows a distribution similar to wild-type parkin, with a predominantly homogenous cytosolic distribution corroborating previous results (Henn et al., 2005), and rarely showing some aggregates. Although we have a statistically significant result regarding aggregate formation at 48h after transfection, consistent with what has been described in other studies at this time point (Kyratzi et al., 2007; Sriram et al., 2005; Wang et al., 2005) we believe that this is not a highly aggregate prone mutant and as we increase the analyzed samples, we will lose the significant value. This, may be the result of a particular low number of aggregates found for wild-type parkin at this time point. These results are in agreement with other studies that described this mutant as behaving similarly to normal parkin, only rarely forming aggregates in transfected cells (Ardley et al., 2003; Hampe et al., 2006; Schlehe et al., 2008). Nevertheless, previously published data regarding this mutant are contraditory. It is known that the R42P mutation is located within the binding site of Rpn10 subunit of the 26 proteasome, that includes position 42 of the parkin UBL domain (figure 4.1) (Sakata et al., 2003). This mutation is described by an NMR study to alter the position of the β3 strand and completely unfold the UBL domain, probably impairing its interaction with the 26S proteasome. These poorly folded protein structures are sensitive to degradation and/or aggregation (Safadi et al., 2011; Safadi and Shaw, 2007), which was confirmed by Henn and collaborators, by showing that this mutation decreases parkin stability, being rapidly degraded by the proteasome. This mutation, was found not to affect parkin membrane association, contrary to what has been described for C-terminal deletion mutants (Henn et al., 2005).
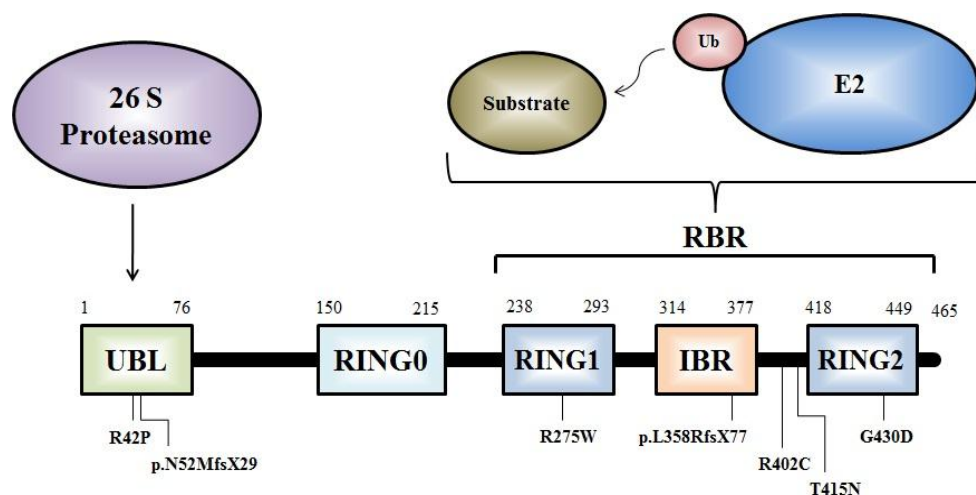
Figure 4.1: Schematic representation of parkin domains with analyzed mutations indicated below. Proteins that have been shown to interact with parkin are depicted above: the 26S proteasome binds to the Ubl domain; and both substrate and E2 enzymes have been shown to interact with many locations within the RBR domain.

Interestingly, the majority of missense mutations are located in the C-terminal RBR domain (Mata et al., 2004), which has been implicated in the binding of parkin substrates and the recruitment of E2 ubiquitin-conjugating enzymes. These three domains together represent the critical zone of the E3 ubiquitin-ligase activity of the parkin protein (Sironi et al., 2008).

In this study we found that the two frameshift mutations are highly prone to aggregation at all studied time points. Also, we can propose that the mutant N52MfsX29 might have a more pathogenic effect probably due to massive aggregation, present in almost all cells. This makes sense because this mutation causes a deletion of the entire RBR domain. These results are in agreement with several studies where it has been described that C-terminal deletion mutants are inactivated by rapid parkin misfolding and formation of protein aggregates. This leads to a significantly altered cellular localization from a homogenous cytosolic distribution, in the case of the wild-type protein, to scattered aggregates (Kyratzi et al., 2007; Sriram et al., 2005; Wang et al., 2005; Winklhofer et al., 2003). In a study of Henn and collaborators it is also described that these mutations fail to interact with cellular membranes, probably due to parkin sequestration in aggregates, leading to the absence of parkin at other membrane compartments (Henn et al., 2005).

Interestingly, we have found that the R275W mutation, located in the RING1 domain, also shows a different cellular localization, forming intracellular inclusions, according to what has been described (Cookson et al., 2003; Hampe et al., 2006; Sriram et al., 2005; Wang et al., 2005) indicating that aggregation is not restricted to C-terminal deletion mutants. Also, we did not observe a statistically significant result for aggregation of this mutant 72h after transfection, which we believe, may partially result from cell death and to the marked presence of low GFP expressing cells found that we will further discuss below.

A patient with a compound heterozygous mutation in parkin gene (a R275W mutation and a deletion of 40bp in exon 3) has been found to present Lewy body pathology (Farrer et al., 2001). Also, patients carrying the R275W mutation tend for an earlier age at onset than those with two truncating mutations (Lohmann et al., 2003). Furthermore, this mutation has been proposed to be responsible for Parkinson disease in the heterozygous state. This suggests that the R275W mutation may have a unique effect, such as a dominant negative, that distinguishes it from other parkin mutations.

Regarding the remaining mutations analyzed in our study, R402C, T415N and G430D, all showed a similar homogenous cellular localization, similar to wild-type parkin, occasionally presenting aggregates, in a small population of transfected cells. Although the R402C mutant has not been characterized before, the other two behave as already described (Sriram et al., 2005; Wang et al., 2005). The pathogenic mechanism of the T415N mutant is probably related to its inability to bind E2 ligases, as this mutation along with T240R, has been described by Zhang and colleages as responsible for abolishing UbcH7 and UbcH8 binding (Zhang et al., 2000).

Other mutations were also found to be aggregation-prone such as T240R (Kyratzi et al., 2007), R256C and C431F (Sriram et al., 2005), C289G, C418R and C441R (Gu et al., 2003; Hampe et al., 2006), and all are located in RING domains. Nevertheless, the G430D mutant within the RING2 domain is apparently not prone to aggregation. However, these differences between the formation of aggregates could be due to the relative importance of the mutated residues, since the majority we describe above target cysteines. These residues define the structure and function of the RING finger domains and mutations in these residues are thought to alter the RING conformation (Zheng et al., 2000). The high cysteine content found in the RBR domain seems to predispose parkin to oxidative stress-induced inactivation and misfolding (Wong et al., 2007).

These findings suggest that only C-terminal mutations, in RING domains, replacing essential amino acids, like the highly conserved cysteines, are critical for the maintenance of the native structure of parkin; or truncating mutations that lead to C-terminal deletions are prone to aggregation. Wang and collaborators, however, described that many mutations that do not reside within parkin RING fingers produce alterations in protein solubility and result in aggregation (Wang et al., 2005). Still, analyzing the mutants described by them that have a tendency to form inclusions, we observe that besides the R42P mutation, that has contradictory results, only two mutations are not located within RING domains. Concerning these mutations, one is in the IBR domain (R334C) that is also important for parkin function, and the other (C212Y) is within the new RING0 domain that has a similar structure to other RING domains. Additionally, it was shown that truncating mutations exceeding three amino acids produced insoluble parkin (Rankin et al., 2011).

Several parkin mutants have been found to have a detergent-insoluble conformation, with a higher propensity to be sequestered into aggressome-like structures (Sriram et al., 2005) Mainly, the mutants found with a detergent-insoluble conformation tended to form visible aggregates when overexpressed (such as R275W, several C-terminal deletion mutants and point mutations in RING domains), but mutations like R42P need to be further characterized as contradictory results have been found. This could be due to differences in the cell types used or different epitope tags. However, all results in literature highlight the importance of RING and Ubl domains for the correct folding of parkin.

Additionally, we have found statistically significant differences in the number of aggregates present in cells expressing mutant parkin, when compared to wild-type. These differences are due to the two frameshift mutations and the R275W point mutation. However, these results could be slanted because we observe that in some cases, mostly in R275W transfected cells, aggregates tend to concentrate in a single massive aggregate. This could be similar to the masses described by Wang et al., that appear to resemble aggressomes, a centriole-associated structure, where it was found that these major perinuclear aggregates colocalized with γ-tubulin (a centrosome marker) and were also enriched in ubiquitin (Wang et al., 2005). This mutation is also described by Cookson et al. as being able to form aggressome-like structures, that in many cells accumulate in a single, large perinuclear aggregate

(Cookson et al., 2003). This structure could be a precursor of LB, thus explaining the presence of Lewy bodies in a patient with this mutation. In addition, we observed that in the N52MfsX29 mutant that causes deletion of the entire RBR domain, the aggregates were so many and scattered throughout the cytoplasm that ended up being too close together and could not be analyzed as separate entities. Another interesting finding is that our cells grown in coverslips showed two different populations of GFP expressing cells: cells with low GFP expression and cells with high GFP expression. We observed that possibly, different levels of expression are related to differences in the presence and number of aggregates, which can skew the results. This phenomenon may be responsible, for example, for the absence of a statistically significant result for the R275W mutant at 72 h after transfection.

We have also found that cells with low expression tend to survive longer; the R275W mutant, at 72h after transfection, showed increased cell death, and we could almost only find cells with low expression. This means that, although the images obtained and subsequently analyzed are mostly of cells with high expression, in cases with high levels of cell death, it was difficult to gather enough cells with high expression and thus some cells with low expression levels, which show fewer aggregates, were also analyzed.

Regarding cell viability we did not find an effect of the expression of the different parkin mutants with the assay applied. These results are not consistent with our observations by fluorescence microscopy or with the results published by Kyratzi et al. where it was shown that apoptotic death occurred with mutant parkin overexpression. This study described that both R42P mutation and C-terminal deletions induced apoptosis and showed that there is a correlation between the ability of these mutants to induce death and their ability to aggregate (Kyratzi et al., 2007).

These negative results could be due to the presence of epithelial cells and non-transfected cells in our samples or due to the assay used, which measures the ATP present in the sample. It was shown that cells die with increased cytosolic ATP levels, as ATP is a requisite to the apoptotic cell death process (Zamaraeva et al., 2005), which may have influenced our results. So, we need to test neuronal death of mutants by other methods such the counting of transfected cells with apoptotic nuclei that was used by Kyratzi et al. in order to confirm the cell death results.

4.2.2 Proteasome Activity in parkin expressing cells

To analyse the effect of mutants on the proteasome degradation capacity, we assessed the three types of proteasome activity in order to evaluate the state of the proteasome in the presence of the parkin mutants. Our results show that mutant parkin expression does not result in a significant impairment of any of the proteasomal activities. Although in the chymotrypsin assay, considered representative of the activity of the proteasome, we have observed highly discordant results between

experiments as shown by the large standard error, which will be repeated for confirmation. There were no outcome indicators of the effect of any particular mutant in these activities. We noticed however a small decrease in two proteasome activities of cells with mutant parkin relative to wild-type: caspase and chymotrypsin-like. So, it is likely that the mutants do not affect the ability of the proteasome to bind substrates, however, mutant parkin substrates no longer can be degraded by this pathway, aggravating the pool of proteins susceptible to aggregation, thus justifying the observation of no statistically significant results between mutants.

These results contradict the findings of Kyratzi where significant results were found for the R42P mutant and a C-terminal deletion mutant. Also, analysis of GFPu (an artificial proteasome substrate) accumulation in cells showed a small decrease in all mutants as well as in wild-type parkin (Kyratzi et al., 2007). This difference can be due to the presence of epithelial cells and non-transfected neuroblastomas in our samples. It would therefore be interesting to repeat this experiment in cells permanently and stably expressing these constructs, which we already created.

4.2.3 Effect of ubiquitin proteasome system inhibition in parkin expressing cells

In order to assess the effect of proteasome inhibition in cells expressing wild-type and mutant parkin we have incubated cells with MG132, a peptide aldehyde that can enter the cell and selectively inhibit the degradative pathway of the proteasome, since it is a substrate analogue and a potent transition-state inhibitor primarily of the chymiotrypsin-like activity of the proteasome (Lee and Goldberg, 1998). Our results show that proteasome inhibition resulted in an increase in aggregate formation in cells expressing wild-type, as well as, for all the mutants. This similar high levels of aggregate presence observed in all mutant and wild-type parkin cells reinforces the importance of UPS in the clearing of protein and preventing aggregation, which is probably related to the amount of cell death that we observed in these cells. These results are consistent with those seen in several studies that show that even wild-type parkin can accumulate into aggregates (with aggressome-like properties) under conditions where proteasome activity is diminished (Ardley et al., 2003; Junn et al., 2002). Also consistent with previous descriptions, we found that aggregates are located preferentially at the nuclear periphery rather than within the nuclei. Ardley et al. found that addition of MG132 increased the amount of monomeric and high-molecular-weight species of insoluble parkin, that probably represent ubiquitinated parkin (Ardley et al., 2003).

Nevertheless and despite the number of cells with aggregates being similar in all parkin expressing cells, a statistically significant difference was found in the number of aggregates between transfected cells. This was probably due to the large number of aggregates found in the R275W mutant, which could indicate a major pathogenic effect for this mutation.

In addition, we observed massive cell death on the coverslips after a 12h incubation period with 5µM MG132. This vulnerability of dopaminergic neurons to the toxicity of proteasome inhibitors was also confirmed by other studies (Biasini et al., 2004; Nakaso et al., 2004). As expected, all proteasome activities showed a huge reduction with the addition of the proteasome inhibitor MG132.

4.2.4 Parkin mutants and pathogenic mechanism

The great diversity and number of mutations found in parkin suggests that some should share a dysfunction mechanism. In this search for pathogenic mechanisms, some studies focused in the characterization of the ubiquitination properties of parkin mutants and its effect when interacting with substrates. Less ubiquitinated proteins were found in cell lysates in the presence of some mutants, which could indicate a reduced E3 ligase activity (Henn et al., 2005).

As evidence indicates, misfolding and aggregation of parkin are probably the major mechanisms of parkin inactivation. Aggregation of parkin or its mutants, spontaneously or under stress conditions, leads to mislocalization and/or dysfunction of the protein. These aggregates could also be responsible for the compartmentalization of parkin away from its normal cytoplasmic distribution, probably depleting it from essential sites of action, leading to an apparent loss of function (Hampe et al., 2006; Sriram et al., 2005). Besides, aggregation-prone parkin mutants could be responsible for the UPS impairment, by "clogging" the system, where these proteins are targeted for degradation and, because of their conformation, are poorly degraded by the proteasome, inhibiting the access of other substrates or recruiting the proteasome during an attempt to degrade the misfolded proteins, which ultimately leads to depletion of proteasomal units and other UPS components from their usual sites of action (Bence et al., 2001; Vekrellis and Stefanis, 2006) culminating in the accumulation of substrates. Even a slowing down of the degradation process can lead to significant effects on the accumulation of UPS substrates. Note that it is not the inclusions, but the less mature forms of aggregates (low order oligomers) that are associated with UPS impairment, because well-defined inclusions are unlikely to interact with the proteasome as substrates (Vekrellis and Stefanis, 2006).

It is also probable, that a correlation between agreggate formation, proteasomal activity and neuronal death exists.

The role of aggregates in cells is still a matter of debate regarding their role as protective or damaging. These aggregates probably result from a detoxification protecting mechanism, which attempts to clear intermediate species by storing them in an inert form. However, a toxic effect could appear if these aggregates would act as a physical barrier to normal intracellular traffic, which becomes increasingly important when we look at this in a neuronal context, as blockage of axonal and vesicular transport or sequestration of vital cellular components such as ubiquitin, ubiquitin-binding

proteins, HSPs or even the proteasome itself (leading to UPS dysfunction) could severely impair cellular homeostasis (Vekrellis and Stefanis, 2006). Despite this many possibilities, it remains to be clarified if it is UPS dysfunction that causes aggregate formation or vice-versa. Although, by the evidence, we think that it is probable that protein misfolding and aggregation are the primary event. However the mechanisms responsible for the pathogenic effects of mutants that seem to have a preserved stability, subcellular distribution, protein interactions and parkin enzymatic activity remain to be elucidated. One possibility is that these mutants could have an increased predisposition to stress-induced alterations as described in a 2005 study, where two soluble Parkin mutants are more prone to rotenone-induced changes in solubility than wild-type parkin (Wang et al., 2005a).

As functional parkin has been shown to have multiple neuroprotective effects, such as protecting cells against damage induced by mutant α-synuclein and other agents (Feany and Pallanck, 2003; Petrucelli et al., 2002), its cellular depletion, as a result of aggregation or loss of its E3 function, would probably lead to an increased predisposition to apoptosis under stress conditions, causing neuronal cell loss. Furthermore, parkin is a tumor suppressor gene, that has already been linked to cancer, autism, type II diabetes and Alzheimer disease (Cesari et al., 2003; Kay et al., 2010).

4.3   Conclusions

The main aims proposed at the beginning of this thesis' work were accomplished. Despite the large size of the *PARK2* introns we were able to develop an efficient strategy to narrow down the location of the breakpoints for the deletions found in Portuguese patients and are now close to the determination, at the nucleotide level, of these breakpoints. Also, a cellular model for juvenile Parkinson disease (*PARK2*) was successfully created, through efficient transient expression of both wild-type and mutant parkin, and validated through mRNA expression and fluorescence microscopy. Stable expression of these constructs was also achieved, providing a good platform for future confirmation of some of the obtained results and to further explore the mechanisms involved in parkin aggregate formation and clearance.

We have described, for the first time the aggregation-prone characteristics of N52MfsX29 and L358RfsX77 mutants, as well as for the R275W mutant, reinforcing the role of protein aggregation in Parkinson disease associated neuronal dysfunction. However, for the other four mutations studied no aggregation was found and the mechanisms of action of these mutants still need to be further explored. In this study we have also proposed to characterize the mutants interaction with the ubiquitin-proteasome system through the biochemical characterization of a representative subset of parkin mutations, observing its effects on proteasome activity, cell viability and also in aggregate formation. We were able to show that proteasome inhibition, confirmed by the quantification of all three

proteasome activities, has an impact in aggregate formation, resulting in increased aggregation and in a reduction of cell viability, although no major differences were found between the studied mutants.

Our results show that different parkin disease-causing mutations have diverse impacts in the cell and it is therefore very important to search for the different pathogenic mechanisms resulting in neurodegeneration as a starting point to find a way to treat or perhaps reverse the effect of these mutations in patients with AR-JP. This can only be possible by the knowledge of the biochemical processes that occur in these mutant cells. Characterization of large deletions in this gene is also an important for the understanding of the genomic mechanisms involved in deletion formation.

4.4   Future Perspectives

In light of the results obtained until now it is important to pursue some lines of research. First, in the near future we would like to determine the deletion breakpoints for the large *PARK2* rearrangements that will provide insight into the genomic mechanisms responsible for its origin.

Parkin protein levels quantification by western-blot, with an anti-Parkin antibody will allow to characterize the protein levels of different mutants in the soluble and insoluble fraction.

SH-SY5Y cells expressing mutant parkin did not show differences from wild-type in the assay used to infer cell viability, however, cell death was observed by fluorescence microscopy, and therefore, other methodology will have to be used in order to clarify mutant parkin impact in cell survival.

Also, it will be important to confirm the effect of the different parkin mutations in the proteasome activities, either by repeating the experiments performed in order to reduce variability or applying a different assay.

Finally, it would be important to expand the study of the UPS in parkin expressing cells, by assessing the effect of a proteasome activator (PA28γ) in aggregate formation and cell viability, in order to explore if enhancing proteasome activity could be a potential therapeutic target for Parkinson disease.

5 References

Ardley, H.C., Scott, G.B., Rose, S.A., Tan, N.G., Markham, A.F., and Robinson, P.A. (2003). Inhibition of proteasomal activity causes inclusion formation in neuronal and non-neuronal cells overexpressing Parkin. Mol Biol Cell *14*, 4541-4556.

Asakawa, S., Hattori, N., Shimizu, A., Shimizu, Y., Minoshima, S., Mizuno, Y., and Shimizu, N. (2009). Analysis of eighteen deletion breakpoints in the parkin gene. Biochem Biophys Res Commun *389*, 181-186.

Bardien, S., Human, H., Harris, T., Hefke, G., Veikondis, R., Schaaf, H.S., van der Merwe, L., Greinwald, J.H., Fagan, J., and de Jong, G. (2009). A rapid method for detection of five known mutations associated with aminoglycoside-induced deafness. BMC Med Genet *10*, 2.

Barrett, J.C. (2009). Haploview: Visualization and analysis of SNP genotype data. Cold Spring Harb Protoc *2009*, pdb ip71.

Bayrakli, F., Bilguvar, K., Mason, C.E., DiLuna, M.L., Bayri, Y., Gungor, L., Terzi, M., Mane, S.M., Lifton, R.P., State, M.W.*, et al.* (2007). Rapid identification of disease-causing mutations using copy number analysis within linkage intervals. Hum Mutat *28*, 1236-1240.

Bence, N.F., Sampat, R.M., and Kopito, R.R. (2001). Impairment of the ubiquitin-proteasome system by protein aggregation. Science *292*, 1552-1555.

Berke, S.J., and Paulson, H.L. (2003). Protein aggregation and the ubiquitin proteasome pathway: gaining the UPPer hand on neurodegeneration. Curr Opin Genet Dev *13*, 253-261.

Betarbet, R., Sherer, T.B., and Greenamyre, J.T. (2005). Ubiquitin-proteasome system and Parkinson's diseases. Exp Neurol *191 Suppl 1*, S17-27.

Biasini, E., Fioriti, L., Ceglia, I., Invernizzi, R., Bertoli, A., Chiesa, R., and Forloni, G. (2004). Proteasome inhibition and aggregation in Parkinson's disease: a comparative study in untransfected and transfected cells. J Neurochem *88*, 545-553.

Bossy-Wetzel, E., Schwarzenbacher, R., and Lipton, S.A. (2004). Molecular pathways to neurodegeneration. Nat Med *10 Suppl*, S2-9.

Canu, N., Barbato, C., Ciotti, M.T., Serafino, A., Dus, L., and Calissano, P. (2000). Proteasome involvement and accumulation of ubiquitinated proteins in cerebellar granule neurons undergoing apoptosis. J Neurosci *20*, 589-599.

Chaugule, V.K., Burchell, L., Barber, K.R., Sidhu, A., Leslie, S.J., Shaw, G.S., and Walden, H. (2011). Autoregulation of Parkin activity through its ubiquitin-like domain. EMBO J.

Chin, L.S., Olzmann, J.A., and Li, L. (2010). Parkin-mediated ubiquitin signalling in aggresome formation and autophagy. Biochem Soc Trans *38*, 144-149.

Choi, P., Ostrerova-Golts, N., Sparkman, D., Cochran, E., Lee, J.M., and Wolozin, B. (2000). Parkin is metabolized by the ubiquitin/proteosome system. Neuroreport *11*, 2635-2638.

Chomczynski, P. (1993). A reagent for the single-step simultaneous isolation of RNA, DNA and proteins from cell and tissue samples. Biotechniques *15*, 532-534, 536-537.

Ciechanover, A., and Brundin, P. (2003). The ubiquitin proteasome system in neurodegenerative diseases: sometimes the chicken, sometimes the egg. Neuron *40*, 427-446.

Clarimon, J., Johnson, J., Dogu, O., Horta, W., Khan, N., Lees, A.J., Hardy, J., and Singleton, A. (2005). Defining the ends of Parkin exon 4 deletions in two different families with Parkinson's disease. Am J Med Genet B Neuropsychiatr Genet *133B*, 120-123.

Cookson, M.R., Lockhart, P.J., McLendon, C., O'Farrell, C., Schlossmacher, M., and Farrer, M.J. (2003). RING finger 1 mutations in Parkin produce altered localization of the protein. Hum Mol Genet *12*, 2957-2965.

Crosiers, D., Theuns, J., Cras, P., and Van Broeckhoven, C. (2011). Parkinson disease: Insights in clinical, genetic and pathological features of monogenic disease subtypes. J Chem Neuroanat.

Dawson, T.M. (2006). Parkin and defective ubiquitination in Parkinson's disease. J Neural Transm Suppl, 209-213.

Dawson, T.M., and Dawson, V.L. (2003). Molecular pathways of neurodegeneration in Parkinson's disease. Science *302*, 819-822.

de Lau, L.M., and Breteler, M.M. (2006). Epidemiology of Parkinson's disease. Lancet Neurol *5*, 525-535.

de Smith, A.J., Walters, R.G., Coin, L.J., Steinfeld, I., Yakhini, Z., Sladek, R., Froguel, P., and Blakemore, A.I. (2008). Small deletion variants have stable breakpoints commonly associated with alu elements. PLoS One *3*, e3104.

Dev, K.K., van der Putten, H., Sommer, B., and Rovelli, G. (2003). Part I: parkin-associated proteins and Parkinson's disease. Neuropharmacology *45*, 1-13.

Farrer, M., Chan, P., Chen, R., Tan, L., Lincoln, S., Hernandez, D., Forno, L., Gwinn-Hardy, K., Petrucelli, L., Hussey, J.*, et al.* (2001). Lewy bodies and parkinsonism in families with parkin mutations. Ann Neurol *50*, 293-300.

Feany, M.B., and Pallanck, L.J. (2003). Parkin: a multipurpose neuroprotective agent? Neuron *38*, 13-16.

Finley, D. (2009). Recognition and processing of ubiquitin-protein conjugates by the proteasome. Annu Rev Biochem *78*, 477-513.

Fitzgerald, J.C., and Plun-Favreau, H. (2008). Emerging pathways in genetic Parkinson's disease: autosomal-recessive genes in Parkinson's disease--a common pathway? FEBS J *275*, 5758-5766.

Frazer, K.A., Ballinger, D.G., Cox, D.R., Hinds, D.A., Stuve, L.L., Gibbs, R.A., Belmont, J.W., Boudreau, A., Hardenbol, P., Leal, S.M.*, et al.* (2007). A second generation human haplotype map of over 3.1 million SNPs. Nature *449*, 851-861.

Gasser, T. (2009). Mendelian forms of Parkinson's disease. Biochim Biophys Acta *1792*, 587-596.

Glickman, M.H., and Ciechanover, A. (2002). The ubiquitin-proteasome proteolytic pathway: destruction for the sake of construction. Physiol Rev *82*, 373-428.

Gu, W.J., Corti, O., Araujo, F., Hampe, C., Jacquier, S., Lucking, C.B., Abbas, N., Duyckaerts, C., Rooney, T., Pradier, L.*, et al.* (2003). The C289G and C418R missense mutations cause rapid sequestration of human Parkin into insoluble aggregates. Neurobiol Dis *14*, 357-364.

Hampe, C., Ardila-Osorio, H., Fournier, M., Brice, A., and Corti, O. (2006). Biochemical analysis of Parkinson's disease-causing variants of Parkin, an E3 ubiquitin-protein ligase with monoubiquitylation capacity. Hum Mol Genet *15*, 2059-2075.

Hedrich, K., Eskelson, C., Wilmot, B., Marder, K., Harris, J., Garrels, J., Meija-Santana, H., Vieregge, P., Jacobs, H., Bressman, S.B.*, et al.* (2004). Distribution, type, and origin of Parkin mutations: review and case studies. Mov Disord *19*, 1146-1157.

Hedrich, K., Kann, M., Lanthaler, A.J., Dalski, A., Eskelson, C., Landt, O., Schwinger, E., Vieregge, P., Lang, A.E., Breakefield, X.O.*, et al.* (2001). The importance of gene dosage studies: mutational analysis of the parkin gene in early-onset parkinsonism. Hum Mol Genet *10*, 1649-1656.

Henn, I.H., Gostner, J.M., Lackner, P., Tatzelt, J., and Winklhofer, K.F. (2005). Pathogenic mutations inactivate parkin by distinct mechanisms. J Neurochem *92*, 114-122.

Imai, Y., Soda, M., and Takahashi, R. (2000). Parkin suppresses unfolded protein stress-induced cell death through its E3 ubiquitin-protein ligase activity. J Biol Chem *275*, 35661-35664.

Imai, Y., and Takahashi, R. (2004). How do Parkin mutations result in neurodegeneration? Curr Opin Neurobiol *14*, 384-389.

Junn, E., Lee, S.S., Suhr, U.T., and Mouradian, M.M. (2002). Parkin accumulation in aggresomes due to proteasome impairment. J Biol Chem *277*, 47870-47877.

Kahle, P.J., and Haass, C. (2004). How does parkin ligate ubiquitin to Parkinson's disease? EMBO Rep *5*, 681-685.

Khandelwal, P.J., and Moussa, C.E. (2010). The Relationship between Parkin and Protein Aggregation in Neurodegenerative Diseases. Front Psychiatry *1*, 15.

Kitada, T., Asakawa, S., Hattori, N., Matsumine, H., Yamamura, Y., Minoshima, S., Yokochi, M., Mizuno, Y., and Shimizu, N. (1998). Mutations in the parkin gene cause autosomal recessive juvenile parkinsonism. Nature *392*, 605-608.

Klein, C., Lohmann-Hedrich, K., Rogaeva, E., Schlossmacher, M.G., and Lang, A.E. (2007). Deciphering the role of heterozygous mutations in genes associated with parkinsonism. Lancet Neurol *6*, 652-662.

Koegl, M., Hoppe, T., Schlenker, S., Ulrich, H.D., Mayer, T.U., and Jentsch, S. (1999). A novel ubiquitination factor, E4, is involved in multiubiquitin chain assembly. Cell *96*, 635-644.

Kopito, R.R. (2000). Aggresomes, inclusion bodies and protein aggregation. Trends Cell Biol *10*, 524-530.

Kyratzi, E., Pavlaki, M., Kontostavlaki, D., Rideout, H.J., and Stefanis, L. (2007). Differential effects of Parkin and its mutants on protein aggregation, the ubiquitin-proteasome system, and neuronal cell death in human neuroblastoma cells. J Neurochem *102*, 1292-1303.

Lang-Rollin, I., and Stefanis, L. (2006). Pathways of neuronal cell death induced by proteasomal inhibition. In The proteasome in neurodegeneration, L. Stefanis, and J.N. Keller, eds. (New York, Springer), pp. 39-55.

Lansbury, P.T., and Lashuel, H.A. (2006). A century-old debate on protein aggregation and neurodegeneration enters the clinic. Nature *443*, 774-779.

Lee, D.H., and Goldberg, A.L. (1998). Proteasome inhibitors: valuable new tools for cell biologists. Trends Cell Biol *8*, 397-403.

Lee, J.Y., Nagano, Y., Taylor, J.P., Lim, K.L., and Yao, T.P. (2010). Disease-causing mutations in parkin impair mitochondrial ubiquitination, aggregation, and HDAC6-dependent mitophagy. J Cell Biol *189*, 671-679.

Lin, M.T., and Beal, M.F. (2006). Mitochondrial dysfunction and oxidative stress in neurodegenerative diseases. Nature *443*, 787-795.

Lohmann, E., Periquet, M., Bonifati, V., Wood, N.W., De Michele, G., Bonnet, A.M., Fraix, V., Broussolle, E., Horstink, M.W., Vidailhet, M.*, et al.* (2003). How much phenotypic variation can be attributed to parkin genotype? Ann Neurol *54*, 176-185.

Lucking, C.B., Durr, A., Bonifati, V., Vaughan, J., De Michele, G., Gasser, T., Harhangi, B.S., Meco, G., Denefle, P., Wood, N.W.*, et al.* (2000). Association between early-onset Parkinson's disease and mutations in the parkin gene. N Engl J Med *342*, 1560-1567.

Marin, I., Lucas, J.I., Gradilla, A.C., and Ferrus, A. (2004). Parkin and relatives: the RBR family of ubiquitin ligases. Physiol Genomics *17*, 253-263.

Mata, I.F., Lockhart, P.J., and Farrer, M.J. (2004). Parkin genetics: one model for Parkinson's disease. Hum Mol Genet *13 Spec No 1*, R127-133.

Matsumine, H., Saito, M., Shimoda-Matsubayashi, S., Tanaka, H., Ishikawa, A., Nakagawa-Hattori, Y., Yokochi, M., Kobayashi, T., Igarashi, S., Takano, H.*, et al.* (1997). Localization of a gene for an autosomal recessive form of juvenile Parkinsonism to chromosome 6q25.2-27. Am J Hum Genet *60*, 588-596.

Mitsui, J., Takahashi, Y., Goto, J., Tomiyama, H., Ishikawa, S., Yoshino, H., Minami, N., Smith, D.I., Lesage, S., Aburatani, H.*, et al.* (2010). Mechanisms of genomic instabilities underlying two common fragile-site-associated loci, PARK2 and DMD, in germ cell and cancer cell lines. Am J Hum Genet *87*, 75-89.

Mo, X., Liu, D., Li, W., Hu, Z., Hu, Y., Li, J., Guo, J., Tang, B., Zhang, Z., Bai, Y.*, et al.* (2010). Genetic screening for mutations in the Nrdp1 gene in Parkinson disease patients in a Chinese population. Parkinsonism Relat Disord *16*, 222-224.

Moore, D.J., Dawson, V.L., and Dawson, T.M. (2003). Role for the ubiquitin-proteasome system in Parkinson's disease and other neurodegenerative brain amyloidoses. Neuromolecular Med *4*, 95-108.

Moore, D.J., West, A.B., Dawson, V.L., and Dawson, T.M. (2005). Molecular pathophysiology of Parkinson's disease. Annu Rev Neurosci *28*, 57-87.

Nakaso, K., Yoshimoto, Y., Yano, H., Takeshima, T., and Nakashima, K. (2004). p53-mediated mitochondrial dysfunction by proteasome inhibition in dopaminergic SH-SY5Y cells. Neurosci Lett *354*, 213-216.

Nuytemans, K., Meeus, B., Crosiers, D., Brouwers, N., Goossens, D., Engelborghs, S., Pals, P., Pickut, B., Van den Broeck, M., Corsmit, E.*, et al.* (2009). Relative contribution of simple mutations vs. copy number variations in five Parkinson disease genes in the Belgian population. Hum Mutat *30*, 1054-1061.

Nuytemans, K., Theuns, J., Cruts, M., and Van Broeckhoven, C. (2010). Genetic etiology of Parkinson disease associated with mutations in the SNCA, PARK2, PINK1, PARK7, and LRRK2 genes: a mutation update. Hum Mutat *31*, 763-780.

Olanow, C.W., and McNaught, K.S. (2006). Ubiquitin-proteasome system and Parkinson's disease. Mov Disord *21*, 1806-1823.

Periquet, M., Lucking, C., Vaughan, J., Bonifati, V., Durr, A., De Michele, G., Horstink, M., Farrer, M., Illarioshkin, S.N., Pollak, P.*, et al.* (2001). Origin of the mutations in the parkin gene in Europe:

exon rearrangements are independent recurrent events, whereas point mutations may result from Founder effects. Am J Hum Genet *68*, 617-626.

Petrucelli, L., O'Farrell, C., Lockhart, P.J., Baptista, M., Kehoe, K., Vink, L., Choi, P., Wolozin, B., Farrer, M., Hardy, J.*, et al.* (2002). Parkin protects against the toxicity associated with mutant alpha-synuclein: proteasome dysfunction selectively affects catecholaminergic neurons. Neuron *36*, 1007-1019.

Pickart, C.M. (2001). Mechanisms underlying ubiquitination. Annu Rev Biochem *70*, 503-533.

Przedborski, S., Vila, M., and Jackson-Lewis, V. (2003). Neurodegeneration: what is it and where are we? J Clin Invest *111*, 3-10.

Rankin, C.A., Roy, A., Zhang, Y., and Richter, M. (2011). Parkin, A Top Level Manager in the Cell's Sanitation Department. Open Biochem J *5*, 9-26.

Ren, Y., Zhao, J., and Feng, J. (2003). Parkin binds to alpha/beta tubulin and increases their ubiquitination and degradation. J Neurosci *23*, 3316-3324.

Rideout, H.J., and Stefanis, L. (2002). Proteasomal inhibition-induced inclusion formation and death in cortical neurons require transcription and ubiquitination. Mol Cell Neurosci *21*, 223-238.

Rodriguez-Oroz, M.C., Jahanshahi, M., Krack, P., Litvan, I., Macias, R., Bezard, E., and Obeso, J.A. (2009). Initial clinical manifestations of Parkinson's disease: features and pathophysiological mechanisms. Lancet Neurol *8*, 1128-1139.

Rogers, N., Paine, S., Bedford, L., and Layfield, R. (2010). Review: the ubiquitin-proteasome system: contributions to cell death or survival in neurodegeneration. Neuropathol Appl Neurobiol *36*, 113-124.

Ross, C.A., and Poirier, M.A. (2004). Protein aggregation and neurodegenerative disease. Nat Med *10 Suppl*, S10-17.

Rubinsztein, D.C. (2006). The roles of intracellular protein-degradation pathways in neurodegeneration. Nature *443*, 780-786.

Safadi, S.S., Barber, K.R., and Shaw, G.S. (2011). Impact of autosomal recessive juvenile Parkinson's disease mutations on the structure and interactions of the parkin ubiquitin-like domain. Biochemistry *50*, 2603-2610.

Safadi, S.S., and Shaw, G.S. (2007). A disease state mutation unfolds the parkin ubiquitin-like domain. Biochemistry *46*, 14162-14169.

Sakata, E., Yamaguchi, Y., Kurimoto, E., Kikuchi, J., Yokoyama, S., Yamada, S., Kawahara, H., Yokosawa, H., Hattori, N., Mizuno, Y.*, et al.* (2003). Parkin binds the Rpn10 subunit of 26S proteasomes through its ubiquitin-like domain. EMBO Rep *4*, 301-306.

Sanchez, J.J., Phillips, C., Borsting, C., Balogh, K., Bogus, M., Fondevila, M., Harrison, C.D., Musgrave-Brown, E., Salas, A., Syndercombe-Court, D., *et al.* (2006). A multiplex assay with 52 single nucleotide polymorphisms for human identification. Electrophoresis *27*, 1713-1724.

Schlehe, J.S., Lutz, A.K., Pilsl, A., Lammermann, K., Grgur, K., Henn, I.H., Tatzelt, J., and Winklhofer, K.F. (2008). Aberrant folding of pathogenic Parkin mutants: aggregation versus degradation. J Biol Chem *283*, 13771-13779.

Shen, D., Coleman, J., Chan, E., Nicholson, T.P., Dai, L., Sheppard, P.W., and Patton, W.F. (2011). Novel cell- and tissue-based assays for detecting misfolded and aggregated protein accumulation within aggresomes and inclusion bodies. Cell Biochem Biophys *60*, 173-185.

Shimura, H., Hattori, N., Kubo, S., Mizuno, Y., Asakawa, S., Minoshima, S., Shimizu, N., Iwai, K., Chiba, T., Tanaka, K., *et al.* (2000). Familial Parkinson disease gene product, parkin, is a ubiquitin-protein ligase. Nat Genet *25*, 302-305.

Shimura, H., Hattori, N., Kubo, S., Yoshikawa, M., Kitada, T., Matsumine, H., Asakawa, S., Minoshima, S., Yamamura, Y., Shimizu, N., *et al.* (1999). Immunohistochemical and subcellular localization of Parkin protein: absence of protein in autosomal recessive juvenile parkinsonism patients. Ann Neurol *45*, 668-672.

Shulman, J.M., De Jager, P.L., and Feany, M.B. (2011). Parkinson's disease: genetics and pathogenesis. Annu Rev Pathol *6*, 193-222.

Sironi, F., Primignani, P., Zini, M., Tunesi, S., Ruffmann, C., Ricca, S., Brambilla, T., Antonini, A., Tesei, S., Canesi, M., *et al.* (2008). Parkin analysis in early onset Parkinson's disease. Parkinsonism Relat Disord *14*, 326-333.

Skovronsky, D.M., Lee, V.M., and Trojanowski, J.Q. (2006). Neurodegenerative diseases: new concepts of pathogenesis and their therapeutic implications. Annu Rev Pathol *1*, 151-170.

Sriram, S.R., Li, X., Ko, H.S., Chung, K.K., Wong, E., Lim, K.L., Dawson, V.L., and Dawson, T.M. (2005). Familial-associated mutations differentially disrupt the solubility, localization, binding and ubiquitination properties of parkin. Hum Mol Genet *14*, 2571-2586.

Tan, J.M., Wong, E.S., Kirkpatrick, D.S., Pletnikova, O., Ko, H.S., Tay, S.P., Ho, M.W., Troncoso, J., Gygi, S.P., Lee, M.K., *et al.* (2008). Lysine 63-linked ubiquitination promotes the formation and autophagic clearance of protein inclusions associated with neurodegenerative diseases. Hum Mol Genet *17*, 431-439.

Tanaka, K., Suzuki, T., Hattori, N., and Mizuno, Y. (2004). Ubiquitin, proteasome and parkin. Biochim Biophys Acta *1695*, 235-247.

Um, J.W., Im, E., Lee, H.J., Min, B., Yoo, L., Yoo, J., Lubbert, H., Stichel-Gunkel, C., Cho, H.S., Yoon, J.B.*, et al.* (2010). Parkin directly modulates 26S proteasome activity. J Neurosci *30*, 11805-11814.

Untergasser, A., Nijveen, H., Rao, X., Bisseling, T., Geurts, R., and Leunissen, J.A. (2007). Primer3Plus, an enhanced web interface to Primer3. Nucleic Acids Res *35*, W71-74.

Vallone, P.M., and Butler, J.M. (2004). AutoDimer: a screening tool for primer-dimer and hairpin structures. Biotechniques *37*, 226-231.

Vekrellis, K., and Stefanis, L. (2006). Protein Aggregation and the UPS: a two-way street. In The proteasome in neurodegeneration, L. Stefanis, and J.N. Keller, eds. (New York, Springer), pp. pp39-55.

von Coelln, R., Dawson, V.L., and Dawson, T.M. (2004). Parkin-associated Parkinson's disease. Cell Tissue Res *318*, 175-184.

Wang, C., Tan, J.M., Ho, M.W., Zaiden, N., Wong, S.H., Chew, C.L., Eng, P.W., Lim, T.M., Dawson, T.M., and Lim, K.L. (2005). Alterations in the solubility and intracellular localization of parkin by several familial Parkinson's disease-linked point mutations. J Neurochem *93*, 422-431.

Weiner, M.P., and Costa, G.L. (1994). Rapid PCR site-directed mutagenesis. PCR Methods Appl *4*, S131-136.

Winklhofer, K.F., Henn, I.H., Kay-Jackson, P.C., Heller, U., and Tatzelt, J. (2003). Inactivation of parkin by oxidative stress and C-terminal truncations: a protective role of molecular chaperones. J Biol Chem *278*, 47199-47208.

Wong, E.S., Tan, J.M., Wang, C., Zhang, Z., Tay, S.P., Zaiden, N., Ko, H.S., Dawson, V.L., Dawson, T.M., and Lim, K.L. (2007). Relative sensitivity of parkin and other cysteine-containing enzymes to stress-induced solubility alterations. J Biol Chem *282*, 12310-12318.

Xie, H.R., Hu, L.S., and Li, G.Y. (2010). SH-SY5Y human neuroblastoma cell line: in vitro cell model of dopaminergic neurons in Parkinson's disease. Chin Med J (Engl) *123*, 1086-1092.

Yamamoto, A., Friedlein, A., Imai, Y., Takahashi, R., Kahle, P.J., and Haass, C. (2005). Parkin phosphorylation and modulation of its E3 ubiquitin ligase activity. J Biol Chem *280*, 3390-3399.

Yu, F., and Zhou, J. (2008). Parkin is ubiquitinated by Nrdp1 and abrogates Nrdp1-induced oxidative stress. Neurosci Lett *440*, 4-8.

Zamaraeva, M.V., Sabirov, R.Z., Maeno, E., Ando-Akatsuka, Y., Bessonova, S.V., and Okada, Y. (2005). Cells die with increased cytosolic ATP during apoptosis: a bioluminescence study with intracellular luciferase. Cell Death Differ *12*, 1390-1397.

Zhang, Y., Gao, J., Chung, K.K., Huang, H., Dawson, V.L., and Dawson, T.M. (2000). Parkin functions as an E2-dependent ubiquitin- protein ligase and promotes the degradation of the synaptic vesicle-associated protein, CDCrel-1. Proc Natl Acad Sci U S A *97*, 13354-13359.

Zheng, N., Wang, P., Jeffrey, P.D., and Pavletich, N.P. (2000). Structure of a c-Cbl-UbcH7 complex: RING domain function in ubiquitin-protein ligases. Cell *102*, 533-539.

6 Appendices

6.1 Tables with the amplification primers and SBE-primers designed

Table 6.1: List of amplification primers designed for the SNPs selected.

Intron	SNP	Fw Sequence	Rv Sequence
1	rs1893119	TGGCATGTGCATTGCATCAG	TCAGCAGTATACCTGCTATG
	rs2023037	TCTAGGAGGAGTGGATTCAG	TGGTGATGAGCAAAGTGTGG
	rs9365465	CATGCCTTCAGCTACAAAAC	CTGATTATTAATCCCCTGGC
	rs13206396	AAAGGGTATCCTCCACAGGA	CCTAATAACCCTCCGAATGC
	rs6934419	AAGGCTGCCCCATCTTATAG	GCTAGGTCCAGTGAAATGTG
	rs2803097	TGCAGAAACAAGCCTCCAAC	GTGGAAGACCCTCCATATTG
	rs1893114	TTAAACCACGTGTGGCATCC	TCCTTTGAGGTCAGAAGTAG
	rs1893116	AAAGGTCAGGGCAGTCTTTG	AGTTCCTGACACTGTCTATC
	rs2846510	CATCAAAGCTCTGCCTGAAG	ATCCCAGTGCTTTCTCCAAG
	rs2846507	GCTTAGCGATTTAACCGATG	ATTAAATGCAGCCCCACGAG
	rs2846546	CATGAATTGAGATCCATTGG	ACCCCTTTGGAAGAGTAGTC
	rs2803087	AGATCGCACCACTGCATTCT	GCATGTGTTTACTTGTCATC
2	rs12192200	GGCTGTTTCATCTACACTGA	GCCAAGACCTGATTCAGACA
	rs4235935	AGTTCATTGGCATCGTCTAC	AAAGTGGCATGATTCCTGCG
	rs4709605	TCCATAAAGTCCTGGTGGTG	GCCACCACATCGGCTAATTT
	rs4708953	CTTTATTAGTGCTAGAGCCC	AAGAAAGCATTTGGCAACCC
	rs9364652	AGAAGAACTGAAGGCCCTTG	GCTGGGCGATTCTTGATTTG
	rs6937352	GCACAGAACTTACTGCTCCA	CACCTGTAGACAATGATGCC
	rs7744798	GCTGATCCAGGTCACAATTC	TGTCTACCGTGTGTAGTGTG
	rs952388	GTGTCCACTTAGGGCCAAAA	GGCCAGGTAATACTTCCGTT
	rs7771045	TGTCCCCATCCAAATCTCAC	TCTTACATGGAGACAGGCAG
	rs2205624	ACTCCCTGTCATTGTGTGTG	AATACAGTTGGCCTTCCTCC
	rs962900	TTATTCACACAAGGGTGCGG	TCCTCTTCAGCTCTTCATTC
	rs10945815	AACATTCATCTCAGGGACCC	GGACCAACAAGACTCCTGTA
	rs6935149	AAAGCTAGCCAGGTGTGATG	TACATGATCTCAGTAGATGC
	rs6923741	TTGTGTACTCTGACCCAGGA	TAGAGACCCGTCCTTTGTTG
	rs9347623	CTTCAGCATTTGTACTTCCC	TTAGGAAAACTGGCCTCCAC
	rs4709595	CTGATCGATGAAATGCAGCC	CCCTGCAAGCATTGAATACC
	rs9356016	AACAGGTAAACTGAGGAAGC	GGGTCTGTGTGTTTGCATTC
	rs12205305	CACCCCAATAGAAACTTGCC	TTATAGAGGCGGGGTTTCTC
	rs11964364	ACCATCTGTACCCCAATAAC	TGCCAAGATTGTTCAGCACA
3	rs2023074	AGTGTAGAGTCTCCTTAGAG	CTTCACTCCAAACCTTGTCC
	rs7766877	AGAGAGACGTGTTTCAACTG	TACGTGTGGTTGACCAACTG
	rs4546464	TGAGAATGCTGCAGAGTCAC	GCCATCTAGGTGTGTGTAAG
	rs957374	AAAAGGAGATACCCTGGGTC	GTTGCTTTCAGCTCCTTGAG
	rs9355994	GCCAGATGCACTAGGAAATG	GGAGACCTATCTACTAGTTC
	rs9365393	AAAGAGCTAGACCCTGCTTC	AGAGCACGTATCCCATTCAC
	rs6935521	GGAGATACGAATGGACATGC	CTATGATTCTGAGCTGCATC

3	rs2096982	TGCCGGTTGGGATTATTGAC	GTTGGCTTCAGTCTGTGTTC
	rs1954939	ACATTTCACACAACGGAGGC	AAATCATATGCCCACTGGGG
	rs10945803	ATCACAGTTTGCTGGGCTTC	TGGTGTTTGCCTAGGTAGAG
4	rs713054	GGACAACAACAGTGAAAAGG	TTCACCTGAGACGAATCCTG
	rs4709579	AACGGGACAAGGGAAGGTAA	TCTTTCCCTGATTCTCCCCA
	rs13191078	ATTGACAGAGCTTCCAGGAG	ATCTGCTACAAAGTGCCAGG
	rs2156267	GCCCCCATGATTCTATTACC	TGTTTCAGTTTAGGTACGTG
	rs9365377	CAGTGGTGCAATGTTAGCTC	TCTGCTGATGCTCAAGTTCC
	rs9295184	CTGGTCCTACTTAAGAGCAC	TTCCTAGGGCTTTCCTTCTG
	rs12529283	AAGAAAATGGCAGTAGCAGC	CCAAAAGAGCCAGGTTAAGG
	rs9456748	ATGTACACCCACAGACATGC	TTGGACACTTGAGTGTTTGG
	rs9347591	TGAGAAGGAAAAGGCAGACG	CCCACTTTCTAAGACTTCCC
	rs3892751	CACACAAGGCTGTTTGAAGG	ATGACAGAGCAAGACCCTAC
	rs1893551	GAAGAGCTGCTAGCATTCTC	CAACAGATAAACCCACAGCC
	rs6904579	AGCCTTGTAGATTCTGTGCC	ACGAGGGTCAAACTCATCAG
	rs6455801	CAACTGGGAATAACACAGAG	AGACCCAGTCTGTAAAAGCC
	rs1954926	TACCAAACCATTCCTGCACC	GCTTGGAGCTGACTAGAATG
	rs1954925	TCTGTGCTGCCACAGTATTG	ACCAAGCAGTTGAAATAACC
	rs4412175	ATTCCATAAACCTTTGGGTC	GGGATACAACTGAACAAGTG
	rs9365375	TCAGAGGGTTGCCAAATGAC	TACAGTCTTCCTGTGCTACC
	rs9347590	CTCAGAGAACTGATTCACCG	AATTGTAGCCTCTGCTCAGC
	rs9295182	GAGATAGGTCTTGACAGAGG	AGATCAACGTGTGTCAGCAG
	rs2023078	GCTCCCATACATTAGGTAGG	CGGAGACCTTGATAATCGAC
6	rs3016551	TCTGACACCTCCCACTTTTG	TGACTGATCCCCTCTACCAT
	rs7739802	TTAGCTTGTGGGAGGAAGTG	GAAGGAGAAGGAAACTCAGC
	rs6455775	GCCAGTGACATAAACGtACC	GAGTGAACCCATTTTGCCAG
	rs6913813	AGGCTGCAGTCAATAGGAAG	CCAGCTCAATCAGAAAAGGG
	rs6922518	GACAGTTTCAGCGGATTGAG	AATACAGTAGCAGGCTGTCC
	rs12528179	ATGGGCTCTGATAGAATGTG	TATTGAAACTGTAGCCGCAC
	rs2155486	GATGATGGTGTTACTGACCG	CTTCTGTGAAGCACCTCCAT
	rs6937081	TTGCATATGGGACACACCAC	AAGTCGCTGCTCAGTGAAGA
	rs9456721	GATACTCTGAAAACACACTG	TGGCATGCTGTTGCTAAGTG
	rs9355368	GACACAGAGCTTCCCAAGAT	AGCATCCACCTTTTCTCCAG
	rs9355371	CAGGTGAGATGTGAACGTGT	CAGGCTCATGTGTTATTGGC
	rs9347562	TCTTTTCTCTGCCCTTATGG	ACCCTTGACGATTTTGCCTT
	rs9364627	CTGCTGTTAACCACAATGGG	ATATGTATGTCCTCCCCACC
	rs9458419	GATCACACCCTGCCTCAATA	GGCACTAAACAATTAGGGGG
	rs7746164	CTGCCTACAGAGCAGAGATT	TGGTGATTTTCCAGGGCCAT
	rs1790022	GTTTCTCCTCTCCTACAG	AACAGCCCTTTTTCTCAGCC
	rs1784597	ATGTGAACTCCTGGCCTTTC	CTCTGTACAACCAGACTCAG
	rs1626020	AGACCCTTGCTAGAACTTTG	CACTAAAAAGTGTCCCAGCA
	rs1784588	CTGCTCTAGTTCTGATCTGG	GTTTCACATTGTTCTCTCAC
7	rs12210817	AACTCTTTCCTTCTCCCTCC	AAAGCCAACCCAAGCCACTC
	rs9458315	TGTTGCATAGGGCCTGTTAG	GAGCAATCACTTGATGCTGG
	rs1018462	CTCTCTTTACTCTTTTGGAG	ACAGTTTCCTAACCAGGATG

7	rs11755949	GCCTGGACTTGGTTTCTATC	GTTATCAGAGTGAGGCCTTC
	rs13220282	CATGGTCCAAATTCTGATAG	CTAGATGGTATAATATCCCC
	rs12210797	TCTAATGCTGAGCCCAGTTC	AAAGTAAGACACGAGTGCGG
	rs910177	ACAGAAGCCCTCTTTTGCAG	ACTCCAGGGACAAGAAATTC
	rs9346876	GAGTGTTGGGTGAGTCAAAC	CCACAAATCGGCAAACTCAG
	rs9355922	GGCAAAAAGTAGAAAAGCTC	ATCTTATGGGCCTGTGGTTC
	rs3765474	TCTCCCAGAATCCTGAAGTG	TTCAGGTACACGTCTGTGTC
	rs9365323	AGCATTACCTTCAACGCCTG	TGGAAGTCAGATGCTGGAAG
	rs10945778	ACTAGGCTTTTCTGAGGTGC	ACAGGCTAGGGTATGAGATG
	rs1024189	CTGCTCTCTGACATTGGTGC	GACTGTAGAAAGTATCTGGG
	rs10945764	AATAGCATCTCGTCGACAGG	AATTGACTGAGCTGTGGTGG
9	rs9365285	TATGCTCTCGGTCCCTAATC	TCCTACCTTAGCCTTTGGGA
	rs13211741	TTCAGGGAGAGATGGTGTAG	GGTGATGAGGCACCTTTATC
	rs4574609	AAGAAATGGGTGGCTATGGG	TAGAGGGCATTGGTTCCTTG
	rs12175609	TGTGAGCCAAGGCAAGGAAG	GGTCTACAAAATGGTGAAGG
	rs4708909	AAGAGGAGACTGTGGAAAGG	AAATGACACCAGTACCCTGC
	rs577876	GCCATGTGAGAAGGAATACC	TAAGCATGTGCAGTGCATGG
	rs12198566	TGTTCTTTCTGATGTCTCCC	GGACCTTGGAAAGAGAAAAC
	rs9458289	GCTATGGCTCATAGTTGTCC	GTTTACATCTCAGGTGCCAG
	rs4709526	TGCCATTATCCCAGGCTAAC	CCTTGGAGAGGATGTTGTTC
	rs517010	GCAACTAGGATCTCAGGAAC	AAAGAGTCCTTGCCCAGTTG
	rs4709531	CTAAATCGTTCTGTATGCCG	AGGATACATACCCACACTTG
	rs12209107	AAGCCCAGTGACATCGTATC	TACAGGCTAGTGTTAGGAGG
	rs12154057	TTAGAGGAACTGGGAGATGC	CTCAGCCATCACAAACATCC
	rs1886237	CCCTCCTTGATTTTGGACAG	AAGTTTCAGTCCATGGGAAC
	rs506428	TCGCAAGTTTTAGGGTTCAC	AGACTCAGACACACACACTC
10	rs9347502	ATAAGGCCCTTCATTTCCTG	TTGAGACCTACAGGGATGAG
	rs3890730	GGAAAAGCTGATTGGGACTC	TCAGCCCTCTTCACACTTTC
	rs69421090	GCTTTGTTCTGTCCAGGAAG	GTTACATCCAGAGCCGTTTG
	rs77665080	AATGGGGGAAATGGAACAAC	AAAAGGTAGGCTCTGTGGTC
	rs69076320	ATCTCCCAATACTGGGACTG	AGAGTTACAGTCCAGGAGAG

Table 6.2: List of SBE-primers designed for the SNPs selected.

Intron	SNP	Sequence
2	rs12192200	AACTGACTAAACTAGGGATGGCTTCTCTCCTTCAAC
	rs6937352	AACTGACTAAACCAATGATGCCTTGTCCTAACAGCC
	rs9364652	AACTGACTAAACTAGGTGTTAAGTCTTCAGATGAATGTAG
	rs952388	AACTGACTAAACTAGAGATCGAATTTATTCACACACATGC
	rs7744798	AACTGACTAAACTAGGTGCGAAATGCGAGATAGAGTTTAACTTG
	rs7771045	AACTGACTAAACTAGGTCACCTTGAATTGTAATAATCCTCTCAC
	rs962900	AACTGACTAAACTAGGTGCCGAGGCAAATCCTGTTGTCACTGCCTCCT
	rs6923741	AACTGACTAAACTAGGTCGTTTCGTCTTTCTTGCATTCACAAAGAATA
	rs9347623	AACTGACTAAACTAGGTGCCTTAAGGTTCTGGAAGAATAAATTCCAACTATT
	rs9356016	AACTGACTAAACTAGGTGCCACGTCGTGAAAGACTTCAGAACCTGCTAAAGT
	rs12205305	AACTGACTAAACTAGGTGCCACGTCGTGAAAGGTTTCTTTGATCATACCTATAAAG
	rs11964364	AACTGACTAAACTAGGTGCCACGTCGTGATTTTTATTTGGATTTTTAATAGACTAC
	rs4709605	AACTGACTAAACTAGGTGCCACGTCGTGAAAGTCTGACGTAGGTCTTCCCTATCCTAA TA
	rs2205624	AACTGACTAAACTAGGTGCCACGTCGTGAAAGCCTTCCCTTTTCCTCTTTCATTTTTTA T
	rs4235935	CCCCAACTGACTAAACTAGGTGCCACGTCGTGAAAGTCTGACAAGAGGCTTGTTCCAG GCAATC
	rs4709595	AACTGACTAAACTAGGTGCCACGTCGTGAAATTGAATACCTCTTCATCAATCTTTTATT CCAAC
	rs4708953	CCCCCCAACTGACTAAACTAGGTGCCACGTCGTGAAAGTCTGACAATAACCAGCCAA ATGGAGTGTTA
	rs10945815	CCCAACTGACTAAACTAGGTGCCACGTCGTGAAAGTCTGACAAATAATTTACATTTGA GTTTTTGTCAAATA
	rs6935149	CCCCCCAACTGACTAAACTAGGTGCCACGTCGTGAAAGTCTGACAAAAACGTATCAA ACTAGAAATAGAGGACTTT
3	rs7766877	AACTGACTAAACTAGTCATAAGGGCTGTGGAATTG
	rs4546464	AACTGACTAAACTAGTCACAGGCCGGCATGTATTC
	rs957374	AACTGACTAAACTAGGTAGATCTTGTGGAAACGAAGATA
	rs6935521	AACTGACTAAACTAAAAAATAAATATGTGATTTTGACAC
	rs2023074	AACTGACTAAACTAGGTGCCACGAACTGCCTGTTCCATGCTTT
	rs2096982	AACTGACTAAACTAGGTGTGTTCACAAGTTATCTTCCTAATAT
	rs9355994	AACTGACTAAACTAGGTGCCACGTGAATCCTGTTGTGTACATATTCA
	rs9365393	AACTGACTAAACTAGGTGCCACGTCGGACCTAATCACCTCCAAATTTCTTA
	rs1954939	AACTGACTAAACTAGGTGCCACGTCGTGAAGAAGATAGAGAATCACAAAAATGTA
	rs10945803	AACTGACTAAACTAGGTGCCACGTCGTGAAAGTCTGCACATAGCTGCTTGGTCTCTGA A
4	rs713054	AACTGACTAAACTAGGAAGGCCCCCAAACTCAGACA
	rs2023078	AACTGACTAAACTATTGTTCTAGTCTATCAGTTTCC
	rs9365377	AACTGACTAAACTAGGTAAATTGTATTAGGTAATCCAGAG
	rs9295184	AACTGACTAAACTAGTCCCTTTTTAATGCTTGAATCGTAA
	rs4709579	AACTGACTAAACTAGGTGCCACGTTGGACAAATATTGATACAGT
	rs9347591	AACTGACTAAACTAGGcAAGTAACCTTCGGGACCATCCATGTTT
	rs3892751	AACTGACTAAACTAGGTGCCGTAACATTTTGGATGTTATTTTCTGCAA
	rs9347590	AACTGACTAAACTAGGTGCCACGTCGTGGTTACATGAGGCACAGCTTC
	rs9365375	AACTGACTAAACTAGGTGCCACGTCGTGAAAGAATATTCCTGACCCAATCCA
	rs9295182	AACTGACTAAACTAGGTGCCACGTCGTGAAAGTCTTTTCACATGGCCTTTCGTCTG

4	rs13191078	AACTGACTAAACTAGGTGCCACGTCGTGAAAGTCTGACcgGAGTCCTAACCTTCTGCCTT
	rs2156267	CAACTGACTAAACTAGGTGCCACGTCGTGAAAGTCTGACAAATATTTGAACACTTCCTTGGAGT
	rs12529283	CCAACTGACTAAACTAGGTGCCACGTCGTGAAAGTCTGACAAcATGGTTTCGATCAACCGTCTTTAAG
	rs9456748	CCCCCCAACTGACTAAACTAGGTGCCACGTCGTGAAAGTCTGACAAaAGGATATAAAATTTAGGAATCTGGC
	rs1893551	CCCCCCCAACTGACTAAACTAGGTGCCACGTCGTGAAAGTCTGACAAGTCCTTTTCAACCTGCTCAACCACATTTT
	rs6904579	CCCCCCCCCAACTGACTAAACTAGGTGCCACGTCGTGAAAGTCTGACAAAGCACATTCTCTACTTATAGATAAATTTTT
	rs6455801	CCCCCCCCCCCCCAACTGACTAAACTAGGTGCCACGTCGTGAAAGTCTGACAAATTTTTAGGGAATAATAAAATATTAGTTTT
	rs1954926	CCCCCCCCCCCCCCAACTGACTAAACTAGGTGCCACGTCGTGAAAGTCTGACAAGTAATAATGTAATGAATTTTATATTTTTACATCT
	rs1954925	CCCCCCCCCCCCCCCAACTGACTAAACTAGGTGCCACGTCGTGAAAGTCTGACAATAGATACTTCTTCATTTTACTTAGGAGGAGAGCAGCA
	rs4412175	CCCCCCCCCCCCCCCAACTGACTAAACTAGGTGCCACGTCGTGAAAGTCTGACAACCATAAACCTTTGGGTCTTTTATGTTAACAGCTCAAACTGGC
6	rs7739802	AACTGACTAAACTAGGTGAGTCCCCCTTTGCCCAAC
	rs12528179	AACTGACTAAAATTGAAACTGTAGCCGCACTAGTCC
	rs3016551	AACTGACTAAACTAGGTGCGTCACTCCCCTGTTGAAGATA
	rs9355368	AACTGACTAAACTATCCACCTTTTCTCCAGCATTCCCCCA
	rs6913813	AACTGACTAAACTAGGTGCCACGACCATCTCTTAGAGCGGGCTC
	rs9355371	AACTGACTAAACTAGGAGCAGCAGCATCAGGAAACAAGACATGG
	rs9364627	AACTGACTAAACTAGGTGCCACGTCGGCTTCGCTGATCATGTCACCCT
	rs9347562	AACTGACTAAACTAGAACAGTGAAGTTTCTTGTAAACCAGTGAAATTC
	rs1784588	AACTGACTAAACTAGGTGCCACGTCGTGAAAGAAGCCAGTGAGAAATTCTTG
	rs6937081	AACTGACTAAACTAGGTGCCACGTCGTGAAAGTCTGCACGAGGACGTGAACGGCTC
	rs9458419	AACTGACTAAACTAGGTGCCACGTCGTGAAAGTCTGAGTATTGTTATTGTTGCTATGTAG
	rs6922518	AACTGACTAAACTAGGTGCCACGTCGTGAAAGTCTGACAGATCGCCTGTCATACATAGCACTCC
	rs2155486	CCAACTGACTAAACTAGGTGCCACGTCGTGAAAGTCTGACAAGGGCTGTGATGAGGCAACGGTGTCCA
	rs6455775	CCCCCAACTGACTAAACTAGGTGCCACGTCGTGAAAGTCTGACAAGAGTGAACCCATTTTGCCAGAGCTAAC
	rs1790022	CCCCCCCAACTGACTAAACTAGGTGCCACGTCGTGAAAGTCTGACAAGTTAACTTTTACTGTATCACAGTGGCCTA
	rs1784597	CCCCCCCCCCCAACTGACTAAACTAGGTGCCACGTCGTGAAAGTCTGACAAAAGGAAGGAAGAAAAACTGGCTGAGCCAA
	rs7746164	CCCCCCCCCCCCCAACTGACTAAACTAGGTGCCACGTCGTGAAAGTCTGACAATTATGCTTGTATTTTAAATATATGTTGTTAC
	rs9456721	CCCCCCCCCCCCCCCAACTGACTAAACTAGGTGCCACGTCGTGAAAGTCTGACAAAGTGTATTTTAAAGCTTTTCTTTTTTGTTTCAG
	rs1626020	CCCCCCCCCCCCCCCCAACTGACTAAACTAGGTGCCACGTCGTGAAAGTCTGACAATTCTAATGGCAATTTTATCCTTATAATTAGCAATTTG

6.2 Communications

6.2.1 Posters in conferences

S. Morais, J. Pinto-Basto, J. Sequeiros, I. Alonso. Large gene rearrangements are the most common parkin mutations in Portuguese Patients with Juvenile Parkinson Disease.14ª Reunião da Sociedade Portuguesa de Genética Humana, 18-20 Novembro, Coimbra, 2010.

S. Morais, J. Pinto-Basto, J. Sequeiros, I. Alonso. Parkin mutations and Juvenile Parkinson disease in Portuguese patients. 60th Annual Meeting ASHG, November 2-6, Washington, 2010.

S. Morais, E. Cruz, J. Pinto-Basto, J. Sequeiros, I. Alonso. Juvenile Parkinson disease and parkin mutations in Portuguese patients. Congresso de Neurologia, 5-7 Novembro, Lisboa, 2009.